Silicate injection for IOR.

Master thesis conducted by Kevin Jarleiv Hardy
For the University of Stavanger, Petroleum Reservoir

Abstract

This thesis is a literature study of sodium silicate as an enhanced oil recovery method. We will follow the steps from experiments conducted, simulations, and then actual field operations conducted in the Snorre field, Norway. The objective of the sodium silicate is to plug high permeable zones in the reservoir (in – depth); in order to divert the following injected fluids to improving the reservoir sweep efficiency. Sodium silicate has only been previously used to plug near the injection well, but comprehensive qualification program revealed that the onset of gelation can be controlled. This thesis will highlight key design, response measurement plan and operational experiences.

The updated status is that the large scale interwell operation is still on – going, meaning that not all the tracers have reached the producer (officially at least). This implies that more time is needed to be certain on whether or not this operation were truly successful.

Acknowledgments

I would like to give my sincere gratitude to both my mentors,
Steinar Evje and Pål Andersen.
They have given me good advices and motivation throughout the semester.

Also want to give my thanks to
Kjetil Skrettingland and Dag Chun Standnes
Who took the time to answer questions and provide professional guidance.

Nomenclature

A = Gelation time tuning parameter, 2.6E-5
a = Exponent
B = Tuning parameter
d = Diameter, m
E_a = Activation energy, 50.6 kJ/mol
F = Permeability x height ratio
H = Height, m
I = Injectivity Index, m^3/bar/day
I_r = Relative Injectivity Index, m^3/day/bar
K = Longitudinal dispersion coefficient, ft^2/hr
k = Permeability, D
l = Length, m
n = SiO_2 to Na_2O molar ratio
N_{pe} = Peclet number
P = Pressure, bar
PV = Pore volume
q = Injection rate, l/min
R = Gas constant, 8.31 J $K^{-1}mol^{-1}$
r_e = External radius, m
r_f = Front position of slug, m
RF = Resistance Factor, mobility reduction
RRF = Residual Resistance factor, permeability reduction
r_t = Tail position of slug, m
r_w = Effective wellbore radius, m
T = Absolute temperature, K
t = Turbidity, NTU
tg = Gelation time, day
Δx = Length of mixing zone, x_{10}-x_{90}, m
α = Silicate dependent exponent, -0.6/ wt%
β = Acid dependent exponent, -0.7/wt% 2 M HCl
ϕ = Porosity in porous media
γ = Calcium dependent exponent, -0.11/$ppm^{1/2}$

Contents

1 Introduction

One of the growing challenges we face today is discovering new untouched oil reserves. This forces us to get more out of the more mature oil reservoirs in order to sustain the level of production needed. Improving the oil recovery while also maintaining low expenses is always difficult, but this again is very important in the development of making improvements of the today's technology and the understanding we have for enhanced oil recovery (EOR). As a field becomes more mature, the amount of water produced increases (water – cut). Enhanced oil recovery techniques such as gas and water injection, also contribute to undesirable fluid production, such as the injected fluids and formation water. Too much water and gas production cause several issues related to production, such as decreased oil production, increased cost, and environmental problems (D. Hatzignatiou et al. 2014).

A not so uncommon scenario we may encounter in the Norwegian continental shelf is heterogeneous oil reservoirs, which can for instance be caused by lots of faults caused by continental rifts. Heterogeneous reservoirs are layers/zones with large variations in permeability, horizontally and/or vertically. The problem we often encounter with heterogeneous reservoirs when injecting water is poor sweep efficiency and high water cuts. This occurs because water will always take the "easiest" pathway to the producer, so the area with lower permeability will not be mobilized. There are different ways of accommodating this issue, such as drilling new wells into unswept zones or by conformance control (D. Hatzignatiou et al. 2014). Another approach that could be less time consuming and cheaper way of dealing with this is to block the higher permeable layers with gels, consisting of sodium silicate, so that the injected water will be forced to divert into non-swept zones of the reservoir (K. Skrettingland et al. 2014).

Diverting water with sodium silicate is not a new phenomenon in itself, it has earlier been used in the oil industry for near-well treatments to combat unwanted water production (Lund and Kristensen 1993 and Rolfsvåg et al. 1996). This technology could for instance also be used for mitigating unwanted supercritical carbon dioxide (CO^2) leakage out of the storage formation and/or diverting injected CO^2 within the reservoir to enhance storage mechanisms and reduce leakage risks (D. Hatzignatiou et al. 2014). Near –well treatment is considered to be a fairly simple task, and can be obtained either by mechanical isolation or by low volume chemical treatments in order to block the higher permeable layers. But with reservoirs where the different layers are not isolated, when the higher permeable layers are extended from the injector closer to the producer, then near – well treatment will not affect the fractional oil flow. In these situations deep in - depth chemical treatment is a possibility in order to force the injected water to divert into non - swept zones, see Figure 1 for in – depth gelation illustration (Stavland et al. 2011a).

It exists several types of chemicals that could be used to block high permeable zones in the formation, such as BrightWater and cross linked polymer gels. The similarity with these chemicals is the idea of permeability reduction that is delayed to a desirable distance from the injector, so that the fluid injectivity prior to plugging is good. To ensure decent injectivity, the viscosity of the injected chemicals must be low (Stavland, A. et al. 2011). How sodium silicate reduces permeability will be further discussed in more detail later on.

The reason for using sodium silicate compared to other chemicals is that it's easily available, and much more environmentally friendly than most of the techniques used for diversion. Environmentally it is considered as a green chemical by PLONOR (Pose Little Or No Risk to the Marine Environment). Silicate is a natural product, which has many different applications such as purifying fresh water, agriculture and even found in hieroglyphs that helps conserve them. Also, it is much cheaper than other methods, like using polymer to increase the injected water viscosity for instance. This requires large chemical volumes over a long period of time, which is a costly operation (K. Skrettingland et al. 2012). BrightWater does not need to be injected in large volumes, but it is very expensive and not environmentally friendly. Since silicate is cheaper, bigger volumes can be injected, and it is more likely to block the higher permeable zones, and less precision of the gelation is needed compared to BrightWater (quote K. Skrettingland).

In order to initiate the sodium silicate gelation at a desired stage of the process, activators can be added. Activators are basically acids used to reduce the pH in the sodium silicate solution. Increasing amount of acid will decrease gelation time (Krumrine and Boyce 1985). But because of the complex chemical reactions, pH is not constant and will not be the best method to control the gelation time. The initiation of the gelation is also controlled by other factors like salt and temperature. If one uses distilled water instead of brine as injection fluid, the gelation process will be significantly slower. As for most chemical gel reactions, the kinetics is controlled by temperature and the Arrhenius equation can be applied. To clarify, salt and acid makes the sodium silicate solution more sensitive, but it is the temperature which initiates the actual gelation (Stavland et al. 2011a).

There are chemical challenges when injecting alkaline sodium silicate offshore, because mixing silicate with sea water or formation water will result in precipitations (Stavland et al. 2011a). If the assignment was near well treatment this could actually benefit plugging of the wanted region, since precipitation will create more solids that will assist the silicate in blocking the porous media. But with deep in – depth gel plugging it will become a problem, the precipitation before the designated area of blockage will not be possible to control and will plug undesired zones. Precipitation concerns was actually one of the main arguments for not using silicate in deep in-depth situations, but after core flooding experiments done its proven possible to have both delayed gelation and minimal precipitation without damaging the formation (Skrettingland et al. 2011). This method and the process will be further clarified later.

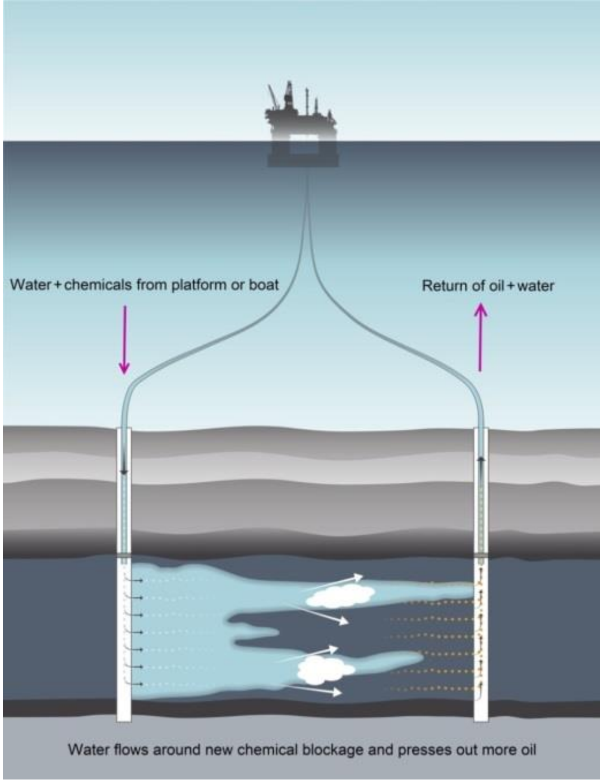

Figure 1; Illustration of in-depth water diversion

In Figure 1, those white “clouds” represents sodium silicate that has congealed into gel which blocks the thief zones and diverts future injected fluids.

1.1 Objectives

This thesis will be a literature study on different aspects of sodium silicate as an enhanced oil recovery method; we will follow the steps from experiments conducted, simulations based on the experimental results, and then actual field operations conducted based on the conclusions and knowledge gained.

Field operations will be divided into two different operations conducted.
1. Single Well Injection Pilot
2. Large Scale Interwell Field Pilot

These field operations use the same experimental results, yet the field simulations are of course not the same.

Some additional subtopics that will be answered:
- Check if experimental results are comparable with the outcomes from the simulations.
- Defining limitations with both the operational work and the modeling part.
- Discuss how to further improve results especially with the modelling part.
- Check if experimental, simulation and actual field operations outcome is comparable.
- In the field operation conducted, were there actually any EOR improvements?
- After field operations were conducted, what would have been different if it was done again?

1.2 Laboratory Experiments

In this thesis it will be focused on experiments conducted by Stavland, A., Jonsbråten, H.C., Vikane, O., Skrettingland, K. and Fischer 2011a, 2011b and 2011.

These experiments are all conducted in laboratories, in core scale size. Engineers use small scale models (core scale) to test the likely performance of a particular design at an early stage of development without incurring the full expense of a full-sized prototype, or to better understand the bigger picture behind natural development of nature (Bak, Tang and Wiesenfeld, 1987).

The leading purpose of the experiments is to find out if sodium silicate gel actually is applicable as an in – depth plugging material. For instance, a good understanding of the bulk gel kinetics is important in order to control the placement of the plugging gel. Bulk gel kinetics is a collective term for everything that affects the gelation process in some way. But also the strength of the gel is examined, since it should withstand high pressures and temperatures in the reservoir over time.

This might sound like a “straightforward” process, but it is quite complexed due to all the involving parameters that must be taken into consideration.

1.2.1 Introduction To Experiments Conducted With Sodium Silicate

Sodium silicate is diluted in low salinity water and is an alkaline fluid which has nearly water like viscosity in the beginning, and the chemical form for sodium silicate is $Na_2O(SiO_2)_x$. It's produced with different SiO_2:Na_2O weight ratios, *n*. Typically *n* systems is ranged from 2.00 to 3.22, and both the alkalinity and the density increases as *n* decreases. Overview of sodium silicate chemistry can be found in Iler (1979); illustration of how pH and salt influences the gelation for instance, is shown in Figure 2.

The experiments were conducted with sodium silicate systems from BIM Norway, Krystazil K40, with SiO_2:Na_2O = 3.2. The sodium silicate had an initial SiO_2 concentration of 27.4 wt%, and pH of approximately 11.04. The acidic activator used was HCl, with the concentration of 2.0 M. The sodium silicate solutions had turbidity close to 1 and low viscosity of approximately 1.3 mPas at 20°C, when diluted to 4 wt% SiO_2 in water (Stavland et al. 2011a).

The core flood experiments were performed in three different porous media; Bentheim sandstone, Berea sandstone and quartz sand.

- Bentheim cores with length 25 cm and diameter 3.8 cm, with permeability 2 Darcy and porosity 0.22 – 0.30.
- Berea cores with length 7 cm and diameter 3.81 cm, with permeability 500 mD and porosity 0.22 – 0.30.
- Quartz sand with 30 cm long sand columns with diameter 2.8 cm, with permeability 9 or 2 Darcy and porosity 0.22.

The core was placed into an oven while the silicate solution was placed at 20°C outside the oven and injected at a constant rate by Quizix pumps. The differential pressures were monitored by Honeywell smart transmitters. The salinity of the formation water has been varied, but in most of the experiments 0.5 wt% KCl was used. Bulk gelation times were measured by visual inspection using a gel code ranging from 0 to 3. Turbidity was measured on a Hach 2100P Turbidimeter.

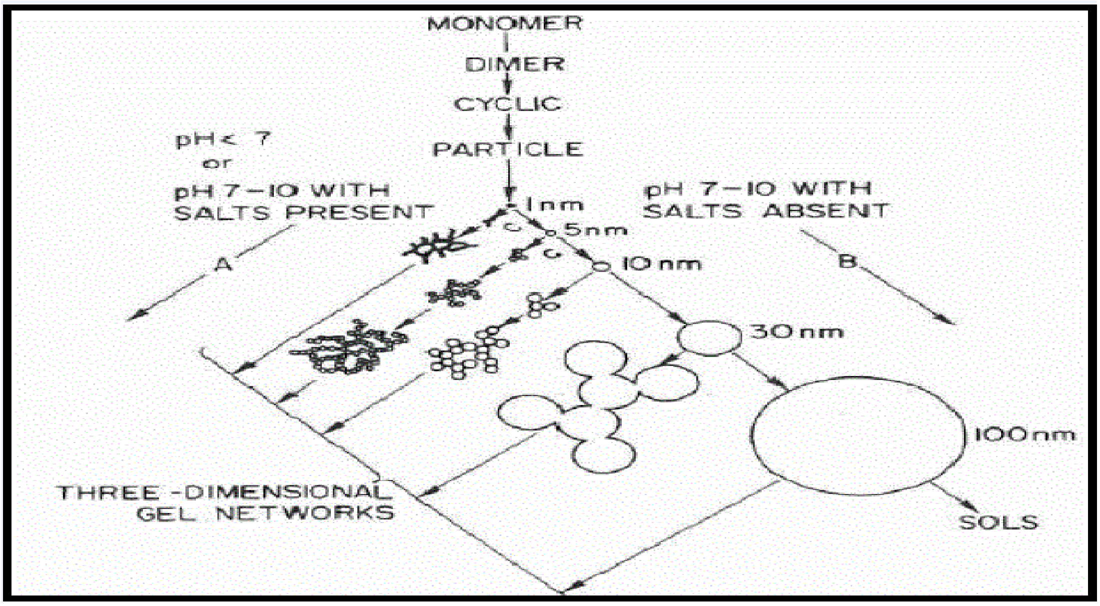

Figure 2; Schematical illustration of polymerization of silica, from Iler (1979).

1.2.2 Filterability Experiments

Before the silicate gelation process starts, the solution is clear and the viscosity is almost like fresh water, then because of aggregate formation it begins to get cloudier and the viscosity gradually increases until rigid gels are formed. Also what Figure 2 illustrates, sequential steps in polymerization from monomer (nano – size particles) to large particles and gel (Iler 1979). The system found by Stavland et al. (2011a) ranging gel development from 0 to 3, where 3 is fully developed rigid gel, is a simple and reliable quantification method to measure both gelation time and where in the development the gel is. Turbidity is one method of measuring gelation time, during the gelation process the turbidity will increase, and for 4 wt% SiO_2 solutions the turbidity is measured to be 170 NTU (Nephelometric Turbidity Unit). Turbidity is the phenomenon that occurs when a certain amount of light is passed through a liquid based sample and this light again is reflected in various directions by the particles in the liquid that is not dissolved; the more gel in the solution, the less light is recorded by the receiver (see paper; ISO 7027). Another method used in addition is filtering the solution; with for instance 3μm filter is plugged by the gel in a 4 wt% SiO_2 solution, this coincides with turbidity measurements of 170 NTU.

Filterability is the ability the solution has to pass through the filter it is filtered through, referring to particles small enough to pass the filter of a particular pore diameter (J.C. Segen 1992), with sodium silicate the filterability in a porous media can be related to the turbidity (Stavland et al. 2011b). Sodium silicate core flood experiments were conducted in 500 mD Berea sandstones with the dimensions; Length 7 cm and Diameter 3.81 cm, the silicate was diluted to 4 wt% in reverse osmosis brine with salinity of 100 ppm NaCl. Reverse osmosis (RO) is a water purification technology that uses a semipermeable membrane to remove larger particles from the liquid, which in this case is salt from the seawater. In reverse osmosis, an applied pressure is used to overcome osmotic pressure that is driven by chemical potential, a thermodynamic parameter. Reverse osmosis can remove many types of molecules and ions from solutions, including bacteria, and is used both in industrial processes and the production of potable water (J. Glater 1998). This solution of sodium silicate was injected at a rate of 2 ml/min at 20°C and displaced 5000 ppm KCl brine, which was pre-injected into the core. The total injected sodium silicate was 100 pore volumes, followed by additional KCl brine.

Experiments with non-filtered sodium silicate revealed that front core will most likely be plugged, but not the second core, since the particle sizes is too large. In order to control front core plugging and improve filterability so that plugging appears later, then the silicate solution must go through a pre-filtration process. Non-filtered and filtered tests were conducted and compared (see Figure 3 for demonstration). Pre-filtration with 25 μm diameter filters did not improve the filterability, but with 5 μm filter the mobility reduction (RF) in the front core was stable. Similar experiments with non-filtered silicate in 2 Darcy Bentheim sandstone core did not show an increased RF. Also, some pressure increase was revealed with Berea sandstone core as can be seen in Figure 3.

Core flooding experiments were also executed in Berea cores at residual oil saturation, $k_w(S_{or})$ = 20 mD. As can be seen in Figure 4, RF increased when the silicate solution was filtered through a 5 μm filter, while a stable RF was observed if the filter size was 1.2 μm. The low mobility reduction in this experiment may be explained by the incremental oil produced from the oil saturated cores.

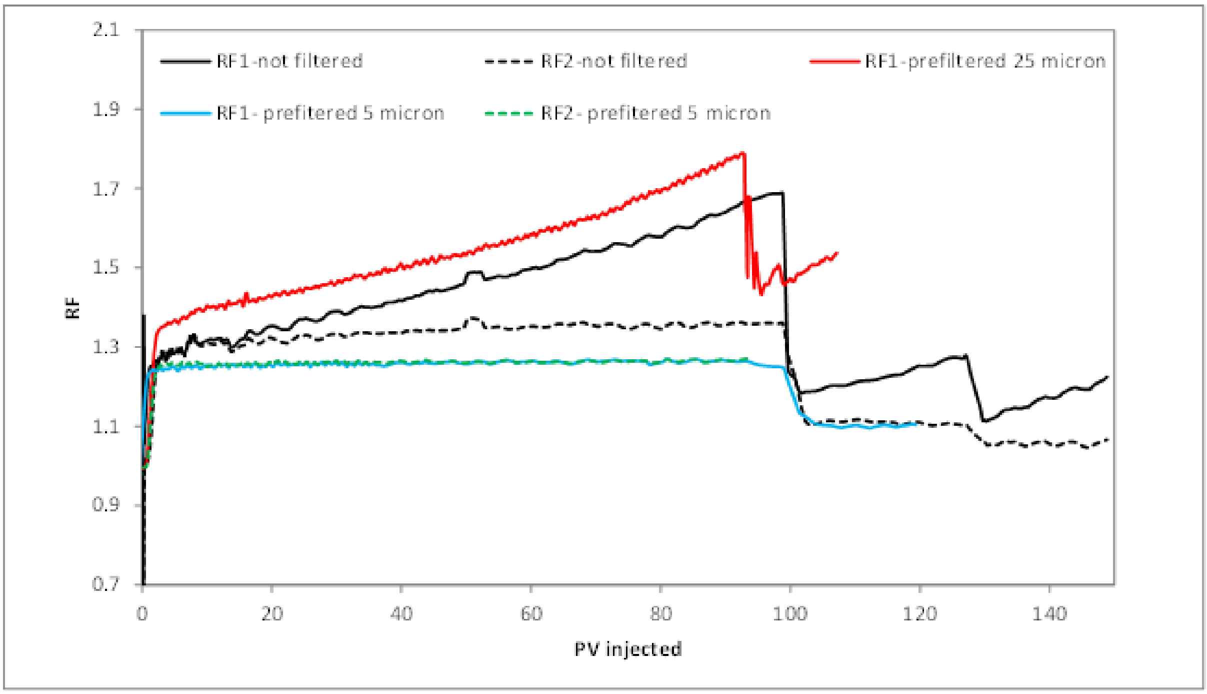

Figure 3; Effect of filter size on the mobility reduction, RF, when 4 wt% silicate solutions were injected through water saturated 500 md Berea cores at injection rate of 2 ml/min at 20°C.

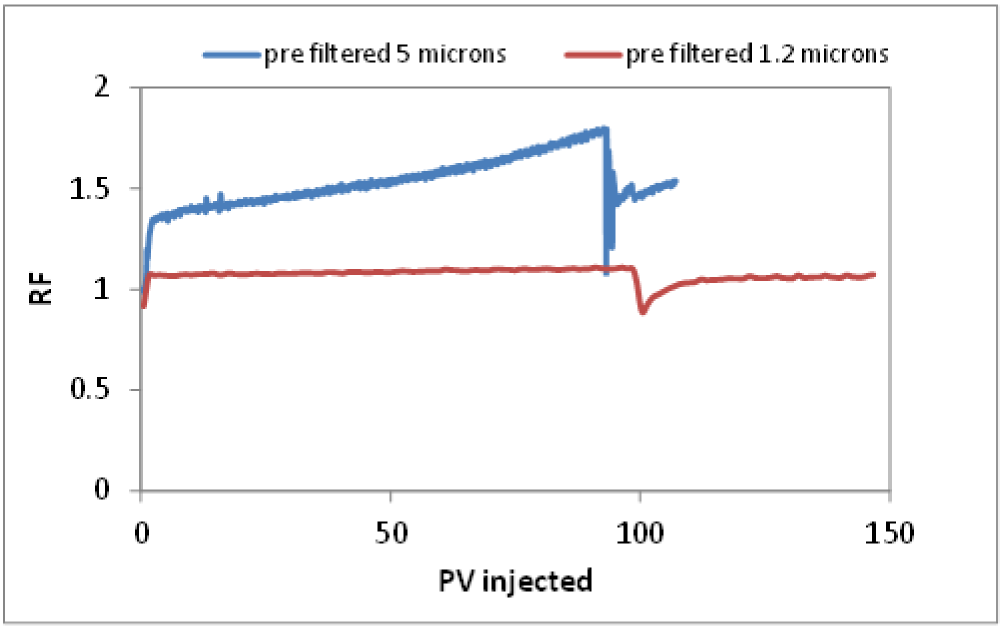

Figure 4; Effect of filter size on the mobility reduction, RF, when 4 wt% silicate solutions were injected through water saturated 500 md Berea cores at residual oil saturation at injection rate of 2 ml/min at 20°C.

It was assumed that the effective pore size could be characterized as a capillary tube model, $r=(8k/\varphi)^{0.5}$, where r is the pore radius, k is the permeability and φ is the porosity. For the 2 Darcy Bentheim, the pore radius is 9 µm, and the pore radius for the 500 mD Berea is 4.4 µm. From Figure 3 and 4 it can be concluded that plugging will not occur in a porous media with pore size larger than approximately 10 µm, and for cores with low permeability early plugging can be avoided by filtrating the silicate solution with a filter size which is equivalent to the reservoir pore size.

1.2.3 Mixture Of Sodium Silicate And Formation Water Experiments

Mixing injected seawater with formation water may generate insoluble materials (solids); this is called precipitation. Main forces that activates the chemical reactions is pH and temperature, since under normal circumstances seawater contains ions like Mg^{2+}, Ba^{2+}, Sr^{2+} and Ca^{2+}. Standard practice to prevent precipitation can be to adjust pH, adding a scale inhibitor or removing the undesirable ions prior to a planned injection operation (S. S. Zumdahl 2005).

Alkaline fluids are not miscible with seawater or magnesium-rich formation water. This means that precipitation will occur as for example magnesium hydroxide, $Mg(OH)_2$. Since the solubility product of $Mg(OH)_2$ is so low, $k_{Mg(OH)2}$ = 1xE-11, one can say it is almost insoluble, so when this solid is created there is “no turning back”. Precipitation of magnesium hydroxide will occur if pH is greater than 10, but not only that. 97% of all magnesium ions from the seawater will react and create $Mg(OH)_2$ precipitations. Another precipitation that could occur when injecting silicate is $Ca(OH)_2$, with solubility product; $k_{Ca(OH)2} = 4x10^{-6}$ which is soluble at pH up to 12 (Stavland et al. 2011a). Also the sodium silicate will react with Mg^{2+} and Ca^{2+} and form Mg-Ca-silicate complexes that may lead to precipitation but also premature activation of the gel.

But as revealed later in this thesis, seawater fractions (seawater fractions is the percentage of metals present in the seawater, for instance magnesium and calcium) up to 10-15% will actually become miscible in sodium silicate solutions, even at pH above 11. This will lower the effective divalent cation concentration in the solution and reduce the effects of precipitations; divalent cation is a common term for positive charged ions with valence of 2, for example Mg^{2+}, Ba^{2+}, Sr^{2+} and Ca^{2+}. Even though this ‘softening’ of the diluted sodium silicate water is vital, it is not sufficient. Further experiments also revealed that a pre-flush of KCl to displace formation water to avoid as much interaction between formation water and sodium silicate was essential for this to work. However, even with enormous amounts of pre-flush volumes, interactions between them will occur. Even so, the more volumes of pre-flush KCl injected, the further sodium silicate is able to reach into the formation, because it will lead to less interaction between them. This method will be further discussed later on.

A number of flood experiments were conducted to examine the effects when different concentrations of sodium silicate and formation water were mixed. The sodium silicate concentrations varied from 0.4 to 4.0 wt% SiO_2, while formation water was artificially a mixture of seawater with fractions from 0.1 to 1 thinned in distilled water. The flood experiments were performed in 3 different rock types; 500 mD Berea sandstone, 2 Darcy Bentheim sandstone and 9 Darcy quartz sand. They were all saturated first with the artificial formation water, and then displaced by diluted sodium silicate. During the experiments differential pressure was measured, this is the pressure difference between injection pressure and average core pressure, together with the produced ion concentrations that were measured to.

Figure 5, demonstrates the mobility reduction when 2% sodium silicate displaces formation water with 0.5 seawater fraction in Bentheim cores. They both show a stable mobility reduction of 1 before the silicate is injected with 14 and 30 pore volumes individually. Then a visible pressure spike was observed at breakthrough time of the silicate. From there RF slowly declined as more silicate was injected. In both cases, after injecting 10 pore volumes of silicate, a post-flush of 5000 ppm KCl was injected. As a response to the post-flush, some of the permeability was redeemed because of the dissolution of precipitated solids. Similar differential pressures were observed for all flood experiments.

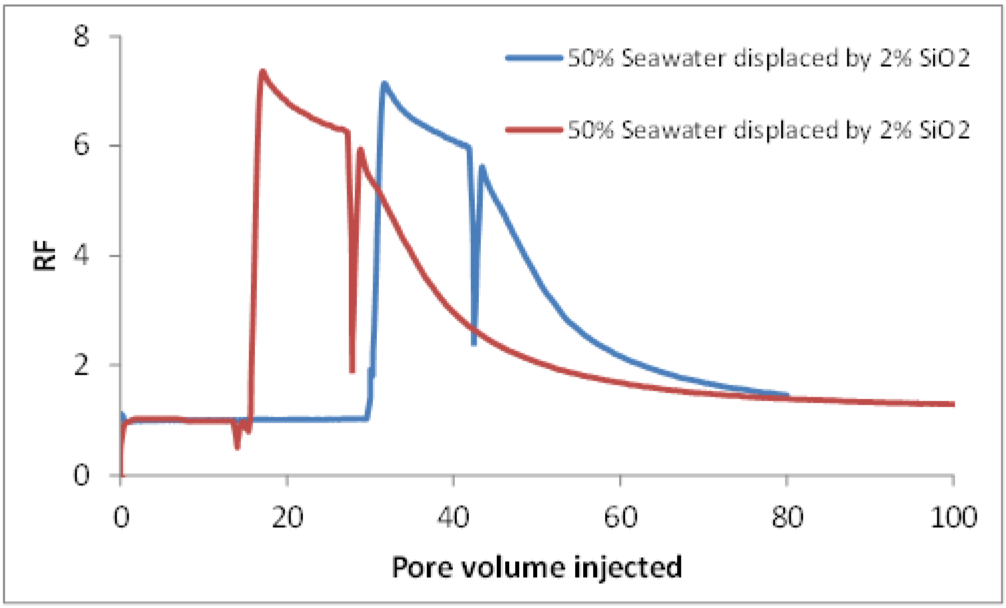

Figure 5; Pressure response when sodium silicate displaced formation water with seawater fraction of 0.5. In the two parallels, sodium silicate was injected at 14 PV (red) and 30 PV (blue).

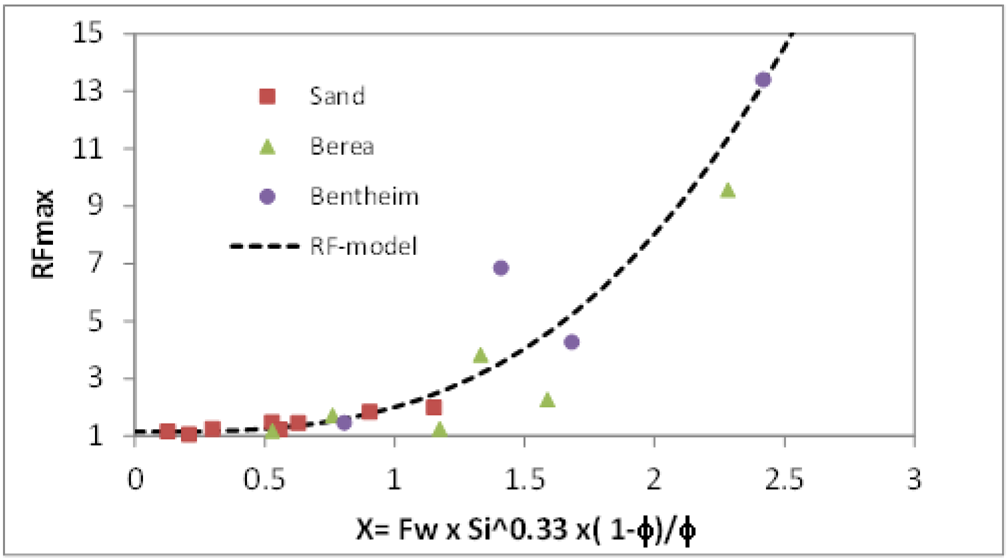

Figure 6; Mobility reduction during displacement of formation water with sodium silicate.

In Figure 6, maximum mobility reduction is plotted versus a scaled parameter X, which represents a function showing when changing concentrations will affect the system. The parameter function; $X = F_w \cdot Si^{1/3} \cdot (1-\varphi)/\varphi$, consists of F_w as the seawater fraction (metals present) in the formation water, *Si* is the normalized silicate concentration and φ the cores porosity respectively. From the plots there is an increasing mobility reduction tendency; this mainly depended on the water salinity, the metal concentrations of calcium and magnesium, but also the sodium silicate concentrations that are illustrated as precipitations of Ca-Mg-silicate complexes. These experiments gave unexpected results. The mobility reduction did not seem to depend on the permeability, but rather on formation porosity. This may be explained with that the permeability reduction is related to the surface area rather than the pore size. Figure 6, also show that the experimental results seem to fit well with the dotted line (RF-model) given by; $RF = 1.15 + X^3$.

It should be noted, that even though the mobility reduction increases with formation water salinity, the maximum mobility reduction (displacing seawater with 4 wt% SiO_2 through a Bentheim rock with porosity of 30%) will be approximately 14 (as can be seen in Figure 6). According to the model, RF is reduced to 7.5 if the silicate concentration dimidiated, but reduced to 2.7 by dimidiating the brine salinity.

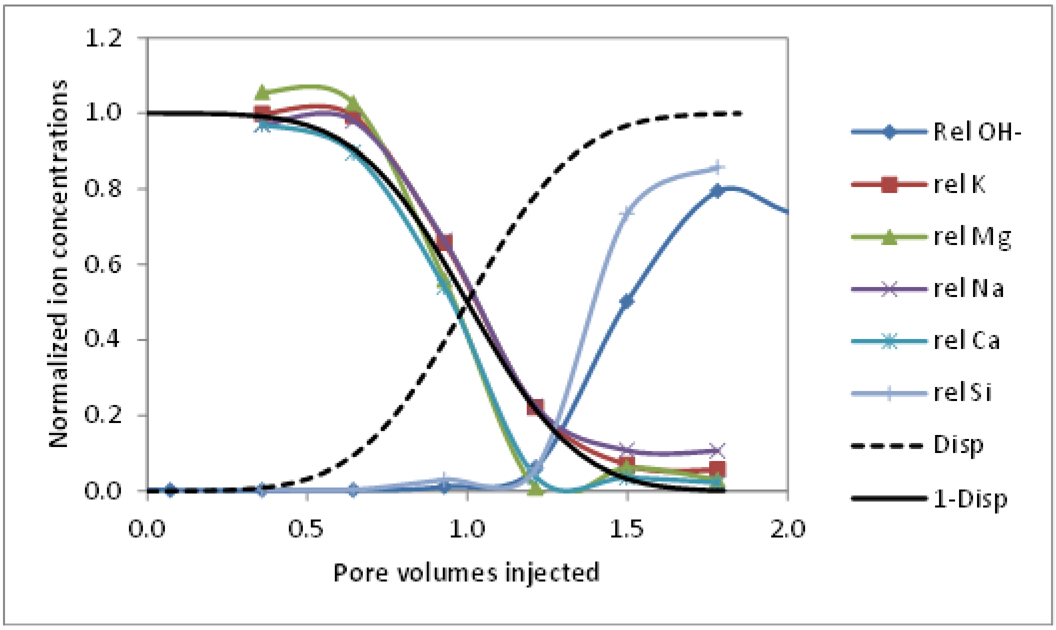

Figure 7; Effluent ion concentrations and dispersion profiles. Injection of 0.4 wt% SiO2 solution through a 500 md Berea core saturated with seawater fraction of 0.75.

Figure 7, illustrates the normalized effluent ion concentrations for the flood experiments in which 0.4% SiO_2 displaced formation water containing a seawater fraction of 0.75. It was assumed that potassium ions (atom K) did not interact with any chemicals, but instead used as a tracer for the system. Tracer is a chemical placed in or around the borehole to measure fluid movement in injection wells. The two main types of tracers used during production logging are the bead tracer (isotope tracer) and the radioactive tracer. All the dispersion curves (in Figure 7) were derived on the basis of the normalized potassium concentration.

Different sodium silicate concentrations were conducted and compared, the effects proves to be different breakthrough times of the silicate. The breakthrough time is at that exact moment when the injected fluid, for instance CO_2 or seawater, reaches the producer. Prior to breakthrough is when the best recovery of oil occurs, because after breakthrough the injected fluids have already made a highway for itself to the producer. This means that the previously untouched oil still remains more or less untouched (D.W. Green & G.P. Willhite 1998). For 0.4% sodium silicate as illustrated in Figure 7, which is a quite low concentration, will experience breakthrough time after 1.5 pore volumes injected. However, with higher silicate concentrations, the breakthrough time was closer to the tracer breakthrough time at 1 pore volume. It is reasonable to conclude that precipitations occurred inside the cores, because measurements of the produced fluids revealed that calcium and magnesium concentrations declined, also white precipitate was detected which contained magnesium, calcium and silicate came out of the core. After using a similar approach as for the mobility reduction, illustrated in Figure 6, it was confirmed that the silicate gel preservation is dependent on the formation water salinity and the sodium silicate concentration. It should be noted that the OH^- concentration (resulting from pH) follows the silicate concentration.

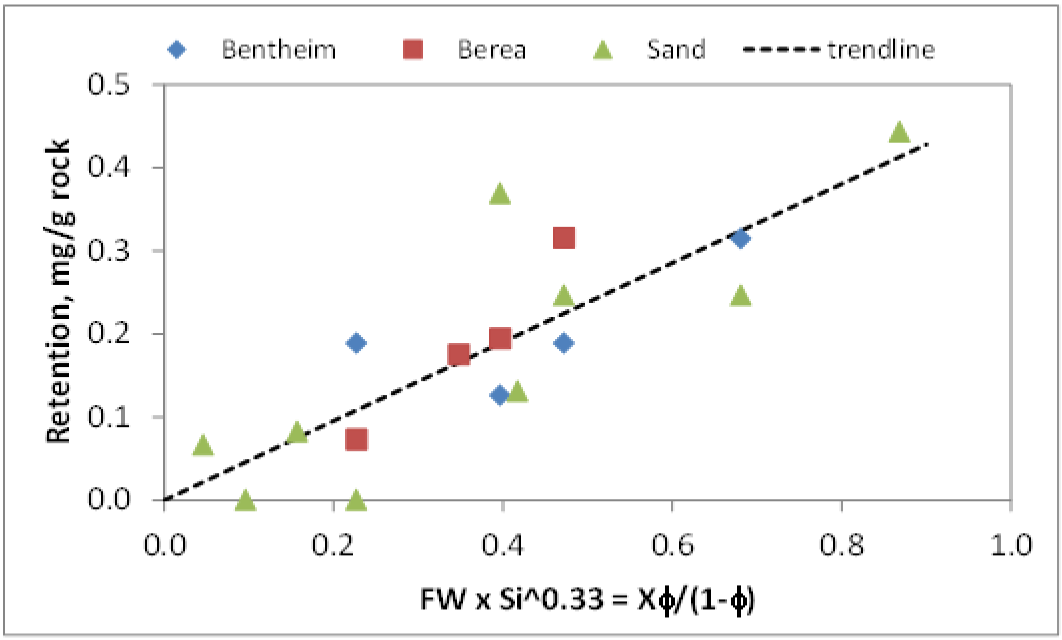

Figure 8; Retention of sodium silicate versus silicate concentration and brine salinity.

Figure 8, illustrates that when sodium silicate solution with low salinity is used, less gelation of the silicate occurs. This indicates that the absorption of silicate is low and that the sodium silicate retention is controlled by the silicate precipitation. Just to clarify, retention of silicate is the ability the silicate solution has to accumulate and generate gel. Because of the low salinity in the seawater, the retention will be less than 0.5 mg/g rock, as seen in Figure 8. This means that for silicate concentrations higher than 1 wt% will have breakthrough times less than 1.25 pore volumes. Also, instead of only using artificial formation water to pre-saturate the rocks, real oil was used from the Snorre field at residual oil saturation. These core flooding experiments behaved in the same way as the previous artificial water saturation cores, and no chemical reactions between the oil and alkaline silicate were detected. Even though there were no reactions between them, and the oil present already were preset at residual saturation, some of the oil was produced. This might be due to the fact that when introducing oil, the interfacial tension (IFT) becomes lower for the system. Interfacial or surface tension exists when at least two phases are present. These phases can for instance be gas/oil, oil/water, or gas/water. Interfacial tension is the force that holds the surface of a particular phase together (Ramey, H.J. Jr. 1973).

Also worth mentioning, similar experiments were conducted by injecting alkaline NaOH (sodium hydroxide) instead of SiO_2 (sodium silicates), also the identical pH was used as the silicate experiments. The different results between these two alkalines are when breakthrough time occurs. With OH^- the breakthrough time was significantly slower, this is because sodium silicate is a buffer while sodium hydroxide is not. A buffer is a solution that can resist pH change with the addition of an acidic or basic (alkaline) component. It is able to neutralize small amounts of added acid or base, thus maintaining the pH of the solution relatively stable. Buffer solutions have a working pH range and capacity which dictate how much acid/base can be neutralized before pH changes, and the amount by which it will change (Brown, et al. 2008). Because of the consumption of OH^-, no precipitation and mobility reduction was observed.

1.2.4 Cation Exchange Experiments

Cations as mentioned earlier, is positive charged ions like Mg^{2+}, Ba^{2+}, K^+ and Ca^{2+} that normally exists in seawater and formation water. The term cation exchange means that a species substitutes another at the surface, and these ions comes in contact with negative charged ions (anions), like CO_3^{-2} (carbonate) or Cl^- (chlorine), and a chemical reaction occurs. The challenge we may face with these kinds of chemical reactions, is the creation of solids also known as precipitations. Such chemical reaction could for instance be; Reaction between calcium cations and carbonate anions that form insoluble calcium carbonate:

Ca^{+2} (aqua) + CO_3^{-2} (aqua) --> $CaCO_3$ (solid)

The reason why precipitation is unfavorable, is as discussed earlier because of pre – plugging, it will decrease the injection rate and plug unwanted zones. Decreasing injection rate may speed up the gelation process, which means that the silicate will not be able to reach the designated area.

So, in order to avoid as much ion exchanges possible when injecting silicate, measures need to be taken. Because mixing the diluted sodium silicate solution directly with the formation water will result in ion exchanges which will lead to precipitations. This is why a pre – flush solution is necessary to displace formation water but also to control ion exchanges from rock minerals. These cations from the formation water and/or rock minerals should be exchanged by the pre – flush, which with the correct solution is able to prevent precipitation. Knowing the size and the ion concentration of the pre – flush is important in order to have this control of ion exchanges. For instance, experiments done with fresh water as pre – flush solution (Stavland et al. 2011b), is able to effectively displace the formation water, but not contribute to cation exchange. This means that when the sodium silicate is injected, with high calcium and magnesium concentrations already present, rapid plugging will most likely occur. For the pre – flush solution to be able to exchange ions, it is essential to add chemicals to the solution. Two different diluted chemical compositions were tested; NaCl (sodium chloride) and KCl (potassium chloride). Both chemicals proved that it will contribute to exchange cation ions from the rock surface, but with sodium chloride it is a chance that clay will swell. Clay swelling is a type of damage in which formation permeability is reduced because of the alteration of clay equilibrium; this is not desirable, since it can reduce permeability in undesirable zones. Clay swelling can be caused by ion exchange or changes in salinity. However, only clays that are directly in contact with the fluid moving in the rock will react; these include authigenic clays, some detrital clays on the pore boundaries and unprotected clay cement. The nature of the reaction depends on the structure of the clays and their chemical state at the moment of contact. The most common swelling clays are smectite and smectite mixtures that create an almost impermeable barrier for fluid flow when they are located in the larger pores of a reservoir rock (Schlumberger oil glossary 2015). However, KCl brine does not contribute to clay swelling, so it was decided to use this as pre – flush brine. Potassium is however less effective since it first needs to exchange the sodium from the rock surface and this will delay the cation exchange.

The controlling parameter in cation exchange is the "cation exchange capacity", CEC (K. Skrettingland 2014). The most common CEC formula is given by the stored charge divided by the mass of rock it is stored on; $CEC = (\sum_i n_i Z_i)/\ Rock\ Mass$.
Where n_i is a species moles, and Z_i represents that atoms charge. CEC is given in meq/kg (milliequivalents/kilograms).

CEC varies a lot by the type of rock material, especially on the type of clay mineral present; CEC is in the range of 5 to 28 meq/kg (Sheng 2011). Several methods are available to measure CEC, direct measurements on rock samples, or estimation from the mineral composition of the rock sample. Another method is to assume that CEC is dependent on rock surface area (Sheng, 2011). At high permeability zones, CEC has a tendency to be unreliable. But it was found that it was possible to estimate CEC from Snorre reservoir core data, Figure 9, shows the CEC for a set of Snorre reservoir cores plottet vs. the surface area, S, given by Carman – Kozeny equation as; $S = 1/4\,(\sqrt{2/\tau}) \cdot (\varphi/(1-\varphi) \cdot (\sqrt{\varphi/k})$. Here τ is the tortuosity, φ is the porosity and *k* is the permeability.

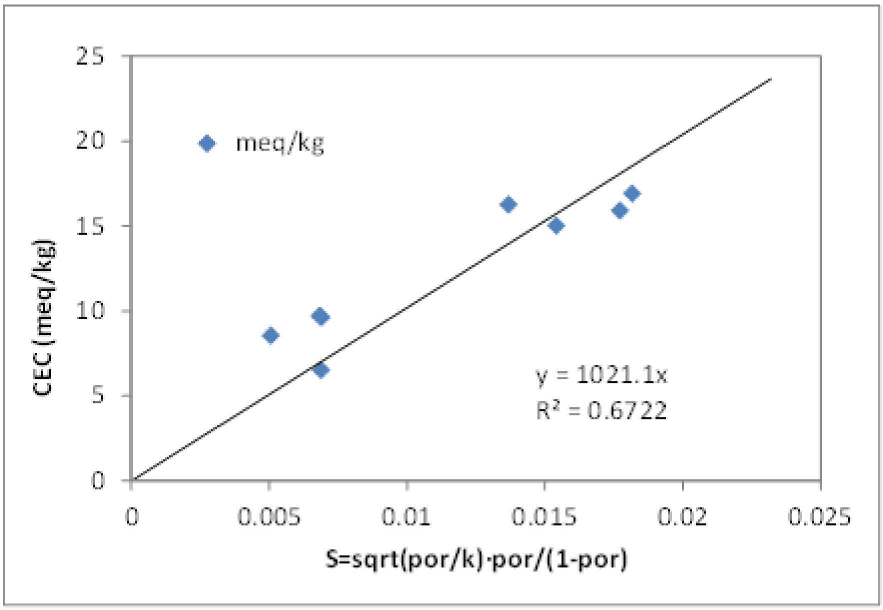

Figure 9; Cationic exchange capacity (CEC) for a set of Snorre reservoir core plugs.

As can be seen from Figure 9, the measured CEC supports the theory on a linear dependency between CEC and the surface area. It is possible to use this approach (since it is linear) to extrapolate in order to find values for CEC where there is higher permeabilities. To extrapolate in order to calculate new values, a known and correct reference point is needed. In Figure 10, CEC is estimated at different permeabilities. And as seen, high permeability corresponds to lower CEC. The lowest CEC value for instance is in the range of 1.8 meq/kg rock.

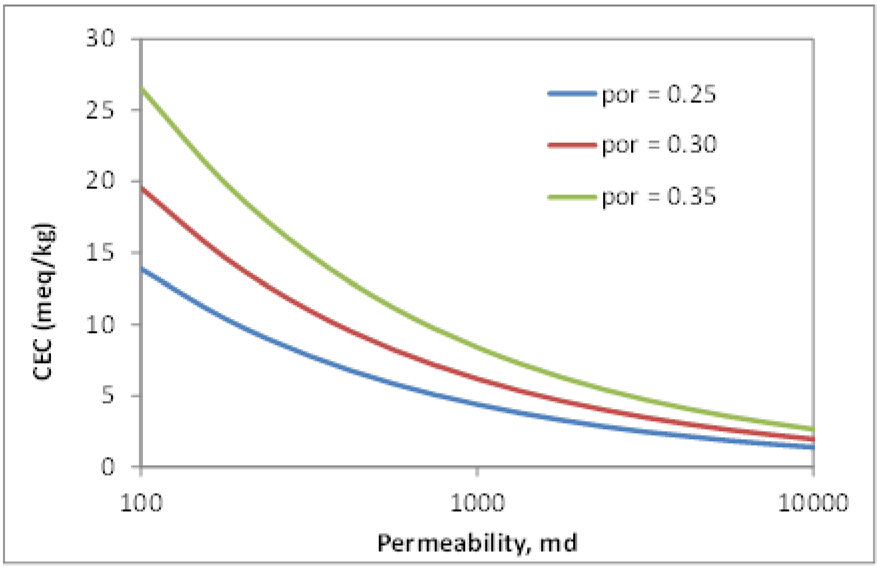

Figure 10; Estimated CEC vs. reservoir permeability obtained from results in Figure 9.

In order to predict the ion chromatography and salinity fronts involving ion exchanges, retardation factor is introduced. Normal formula for retardation factor; $R = 1 + \Delta q/\Delta c$. Where Δq is change in CEC, and Δc is change in concentration. The retardation factor equation can also be presented as; $R = 1 + CEC \cdot d\beta_i/dc_i$ (C.A.J. Appelo et al. 2005), which was used in these experiments. Here CEC is constant, only the equivalent fraction $d\beta$ of the exchangeable ions varies. Also, R can be thought of as the relative time to breakthrough (retardation time) in pore volumes of the injected solution at concentration of dc. Equivalent fractions assumed if seawater has been injected for a long period of time: $\beta_{Na}{}^{+} = 0.6$, $\beta_{Mg}{}^{2+} = 0.3$ and $\beta_{Ca}{}^{2+} = 0.1$, which will always be: $\beta_{Na}{}^{+} + \beta_{Mg}{}^{2+} + \beta_{Ca}{}^{2+} = 1.0$ (C.A.J. Appelo et al. 2005). The detailed calculation of these fractions may be seen elsewhere, but it involves first solving $\beta_{Na}{}^{+}$ from a second degree equation (with only one correct value), then the remaining two fractions can easily be calculated (C.A.J. Appelo et al. 2005).

Figure 11, shows the retardation time to exchange the sodium ions vs. the injected KCl concentration. As can be seen in the plot, at low concentrations of KCl (about 0.1) and at high CEC (30meq/kg) yields unlikely long retardation times and correspondingly large volume of required pre – flush. On the contrary, if CEC is low, the KCl concentration is less critical.

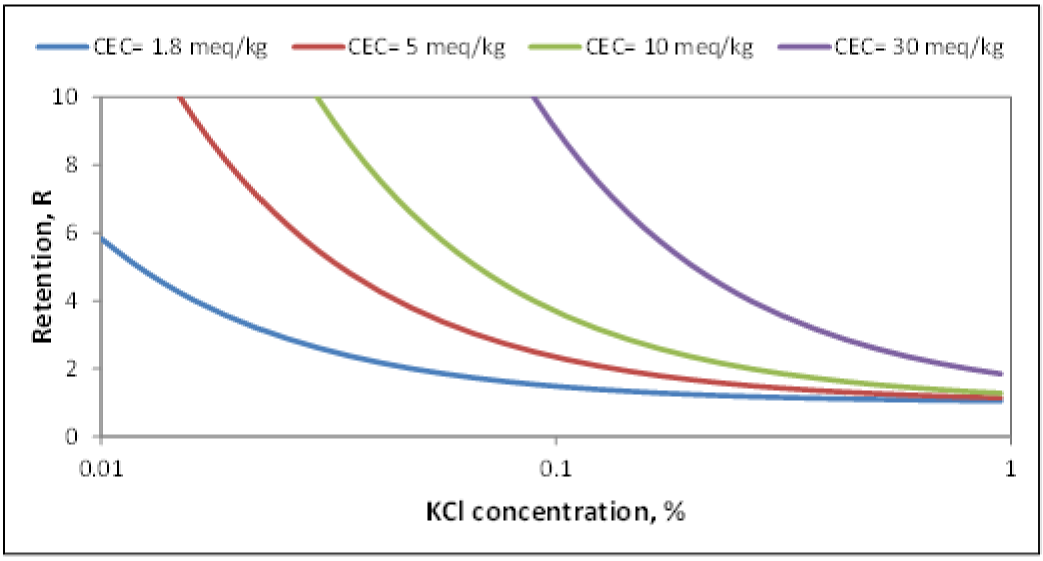

Figure 11; Ion exchange induced retention of sodium vs. KCl concentration for different sets of CEC.

The core flooding experiments discussed above support the approach of including Ca-Mg-silicate precipitation. According to the flood experiments this would then contribute to a moderate reduction in the in-depth mobility along the silicate front. When the cores were pre – flushed with KCl prior to the silicate injection, no calcium peak was observed. It is therefore recommended to properly design the pre – flush to avoid high calcium concentration banks in the silicate front.

1.2.5 Gelation Kinetics Experiments

With gelation kinetics experiments, the goal is to get a better understanding of how rapidly the gelation process is. From clear solution (turbidity ≈ 1 NTU) to the point where filters and the porous media are plugged; this appears when turbidity exceeds 170 NTU. Turbidity method is used to quantify the gelation time in these experiments (Stavland et al. 2011b). It should, however, be noted that the solution is still a liquid at 170 NTU, but with aggregate sizes comparable with the pore size. Gelation time was measured at different temperatures, ranging from 20 to 90°C.

This is of importance because we want to have a decent comprehension of where the silicate will plug. If the silicate pre/post –plugs the porous media, some actions are required, like for instance changing different concentrations in the sodium silicate solution or in the pre/post – flushes and adjusting the injection rate. These different factors that affect the gelation time will be subdivided into three sections.

1.2.5.1 The influence different mixing ratios has on the gelation time

As mentioned in the introduction, temperature is a main factor for the initialization of the gelation development. But with low concentrations of activators present, with activators being salt and/or acid, the gelation process could be vastly delayed. From bulk gelation experiments it was proven that the gelation time at high temperatures (≈80°C), could be delayed from just a few seconds to more than 1 month, simply by varying the activator concentrations. Therefore, the effect of preflush brine and sodium silicate dilution on the gelation time was investigated.

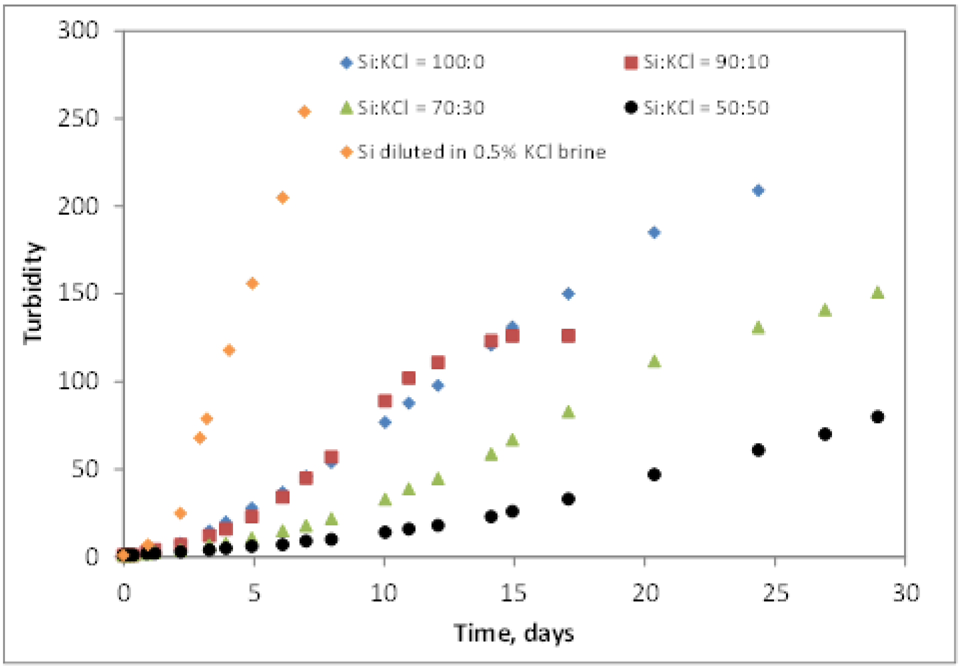

Figure 12; Evolution in turbidity at 60°C for different mixing ratios of sodium silicate and KCl. 4 wt% silicate and 3wt% 2 M HCl in 100 ppm NaCl mixed with 5000 ppm KCl.

Figure 12, displays the gelation time at 60°C as evolution in turbidity vs. time for 4 wt% silicate and 3wt% 2.0 M HCl diluted in RO (reverse osmosis) brine and mixed with 0.5 wt% KCl brine at mixing ratios of 10:0, 9:1, 7:3, 5:5 and 0:10. Blue symbols (10:0 ratio) show the evolution in turbidity with zero pre –flush (KCl), and orange symbols with opposite conditions (0:10 ratio), meaning that the 4 wt% silicate solution is directly diluted in 0.5 wt% KCl. Important to notice is that the silicate concentration is fixed in all these tests (4 wt%), meaning that the gelation time is not depended upon this, but on the makeup brine salinity. In Figure 12, take another look at the blue symbols, the only salinity present is 100 ppm NaCl (since there is no KCl), the gelation time here is longer compared to the orange symbols with diluted silicate in 5000 ppm KCl. However, if the dilution of the silicate solution is taken into account, the gelation time is delayed by dilution of the silicate; take for instance green and black symbols that both have less steep slopes corresponding to increased gelation time.

It should be noted that if the pre –flush salinity is higher than 5000 ppm, the gelation time may decrease by dilution, and if the pre –flush salinity is less than 5000 ppm, the effect of dilution is even longer gelation times. The results in Figure 12, are in agreement with a low risk of rapid gelation because of dilution of silicate and the soft water pre –flush.

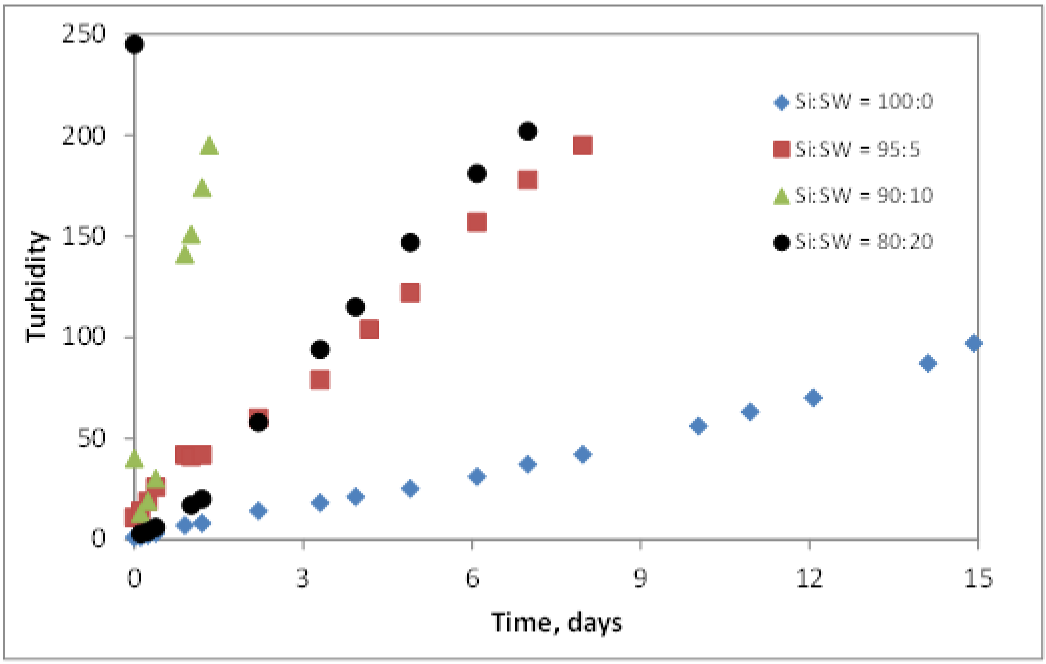

Figure 13; Evolution in turbidity at 60°C for different mixing ratios of sodium silicate and seawater. 4 wt% silicate and 3wt% 2 M HCl in 100 ppm NaCl mixed with seawater.

Figure 13, A sodium silicate solution containing 4 wt% SiO_2 and 3% 2.0 M HCl diluted in RO brine is diluted with seawater at fractions of 10:0, 9.5:0.5, 9:1 and 8:2. If results from Figure 12 & 13 are compared, it can be seen that the gelation development is more rapid in Figure 13 (when silicate is diluted in seawater, see ratio 9:1 in both figures for comparison). Also in Figure 13, seawater fractions of 10% and 20% (green and black symbols) has noticeable instantaneous precipitation at 60°C. The reason why it is assumed to be precipitation, is because gel development this early would be highly unlikely to occur. Green symbols, at time = 0, Turbidity ≈ 40 NTU (precipitation). Also with black symbols, at time = 0, Turbidity ≈ 248 NTU (precipitation). These precipitations are assumed to be a combination of Ca-Mg-silicates, which lowers both the hardness of the brine and the silicate concentration. When combining green and black symbols in Figure 13, at t = 0, the turbidity value for 20% seawater (8:2 ratio) is much higher than for 10% seawater fractions, meaning that more of the silicate will precipitate with 20% seawater fractions. This explains why 20% seawater fraction has a longer gelation time (less steep slope) than 10% fraction, since less silicate concentration remains in the solution after the time the precipitation occurs. The results in Figure 13, clearly demonstrate that rapid gelation and plugging will occur when the silicate solution is mixed with the formation water.

However, it should be mentioned that experiments at lower temperature, no precipitation were observed at these seawater fractions. This phenomenon is not fully understood, and should be further investigated.

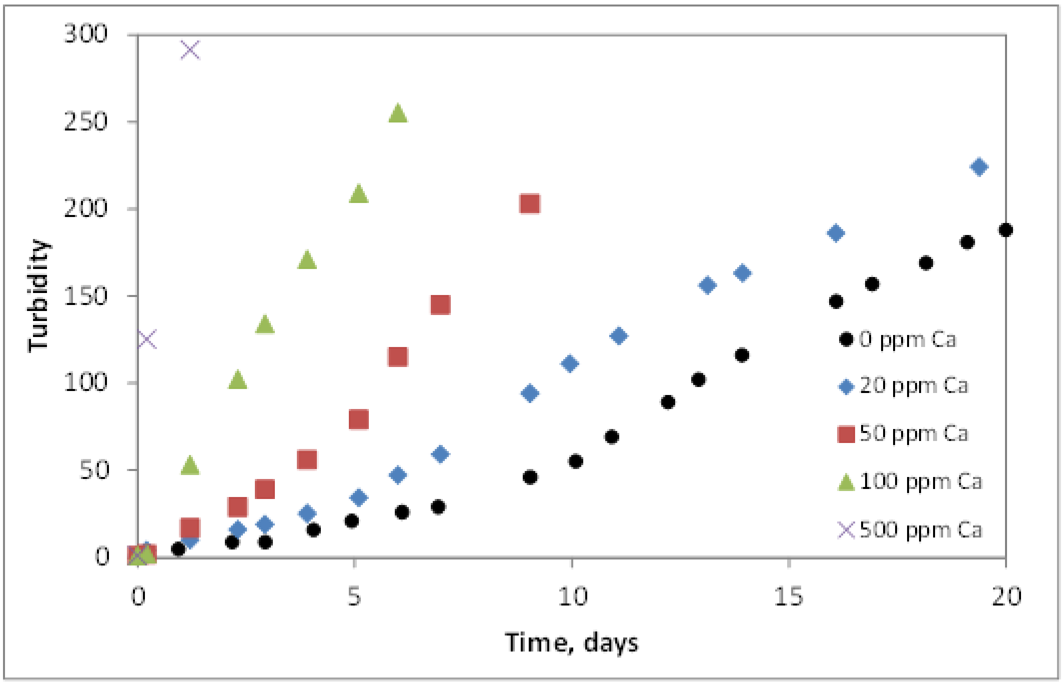

Figure 14; Evolution in turbidity for different calcium concentrations. 4 wt% silicate and 3wt% 2 M HCl in 100 ppm NaCl is added fixed amount of Ca^{2+} ions.

Similar conclusions can be drawn from Figure 14, which shows the effect of different parts per million Ca^{2+} in solutions on the gelation time. For instance, it can be seen that with high concentrations of Ca^{2+}, like 500 and 100 ppm Ca^{2+}, rapid gelation occurs. As with low concentrations, like 0 and 20 ppm Ca^{2+}, a less steep slope is observed, corresponding to longer gelation times (Stavland et al. 2011a). The calcium dependent gelation time tendency was fitted with the equation; $\exp([Ca]^{-1/2})$ (Stavland et al. 2011a).

These core flood experiments is expected to differ from a real reservoir situation since the dissolution of Ca^{2+} into the silicate solution may be in the range of 20 – 50 ppm. Therefore the gelation kinetics in the reservoir may be faster by a factor 2 to 3 than the ones measured in RO brine. This also implies that dissolved calcium can be an internal activator and that the amount of the external activator can be reduced.

1.2.5.2 The influence temperature has on gelation time

Also worth mentioning, experiments conducted with diluted sodium silicate in normal tap water at 40 – 70°C, containing 20 ppm Ca^{2+} and added HCl (acid) under stirring, with intent to measure bulk gelation times. The intension of these tests is to see how the temperature effects the gelation times. As stated earlier, gelation is measured visually when turbidity exceeds 170 NTU (Stavland et al. 2011a). The bulk gelation time was used to tune the gelation model proposed by Stavland et al. (2011a). This model assumes that the dependency of silicate-, activator- and make up water salt concentration can be regarded as individual parameters. As mentioned in the introduction, for most chemical gel reactions, the kinetics is controlled by temperature and the effects are controlled by the Arrhenius equation. Arrhenius equation; $t_g = A \times e^{\alpha[Si]} \times e^{\beta[HCl]} \times e^{\gamma\sqrt{[Ca]}} \times e^{Ea/RT}$. Here t_g is the gelation time (in days), [Si] is the silicate concentration (in wt%), [HCl] is the molar acid concentration, [Ca] is the makeup water calcium concentration (in ppm), E_a is the activation energy, R is the gas constant equal to 8.31 $JK^{-1}mol^{-1}$ and T is the absolute temperature. The constants $A = 2.6\text{x}10^{-5}$, $E_a = 50.6$ kJ/mol, $\alpha = -0.6$, $\beta = -0.7$ and $\gamma = -0.11$ were determined from experiments conducted by Stavland et al. 2011. When turbidity is found, average particle size, d, can be calculated based on the following relationship; $= B * (t - t_0)^{a}$, where t is the turbidity, t_0, B and a are tuning parameters. The gelation time versus HCl concentration is plotted in Figure 15, and the gelation kinetics is basically the same as reported by Stavland et al (2011a). It should also be mentioned that without thoroughly stirring of the solution, local gelation was observed around the acid droplets.

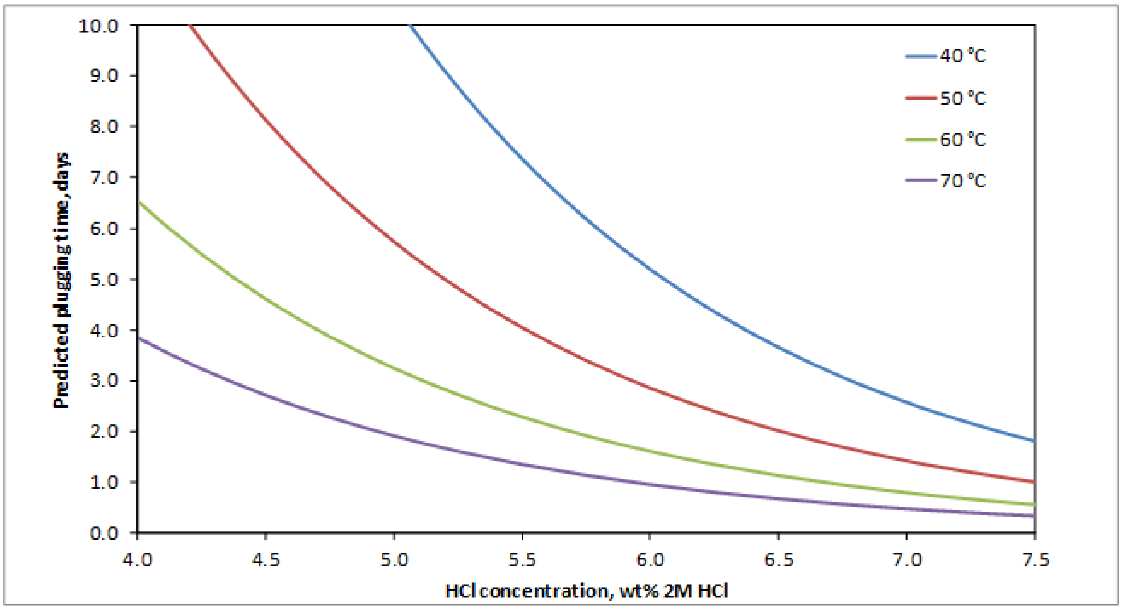

Figure 15; Gelation time vs. acid concentration for 4 wt% silicate in tap water.

In Figure 15, higher temperatures correspond to more rapid gelation, especially combined with high acidic concentrations, and vice versa. Like for instance at HCl = 7,5 wt% and temperature = 70°C predicted plugging time will occur after approximately half a day, while low HCl = 4 wt% and temperature = 70°C roughly after 4 days.

The temperature initiation can be explained as an activation energy that makes collisions between molecules effective. The majority of reactions rates are increased as the temperature increases. The molecules obtain higher energy and speed with higher temperature, causing more molecules to collide and react. And with increasing activator concentrations, will result in more collisions of molecules, thereby, a faster reaction is obtained (D. Hatzignatiou et al. 2014).

1.2.5.3 The influence the injection rate has on gelation time

Experiments were also conducted to focus on how the injection rates affects the gelation process (Stavland, A. 2011). Coreflood experiments with 2 Darcy Bentheim sandstone cores ($L = 25cm\ and\ d = 3.8cm$) show good injectivity for new untested samples. The area is A ≈ 1,15*10^{-3} m^3 and porosity 0.22. These cores were all initially saturated with 0.5 wt% KCl (Pre–flush), then 6 pore volumes of 4 wt% diluted sodium silicate injected through the samples each day with the same rate (ml/min), followed by a low injection rate of 0.5 wt% KCl (Post–flush). The sodium silicate was diluted in tap water, with 2 Molar HCl 6.5 wt%, and the bulk studies were at 40°C (meaning everything is initially 40°C, both the solutions and the cores).

Two different flood experiments were conducted under these conditions mentioned for 2 Darcy Bentheim, but with the exception of different injection rates of the diluted sodium silicate solution. Flood experiment 1 has injection rate 5.0 ml/min, corresponding to a velocity of; v = u/ø = 3.3*10^{-4} m/s, where u = q/A; *u* is Darcy velocity, *q* injection rate, *A* cross section area and *ø* porosity. While flood experiment 2 has injection rate 1.0 ml/min, which corresponds to a velocity of; v = 0.66*10^{-4} m/s. In both experiments it was assumed a linear relation between particle size and turbidity.

Flood experiment 1 (q = 5 ml/min), has initially silicate mobility reduction, RF = 1.35, which is close to the relative silicate viscosity. After 6 pore volumes of sodium silicate were injected at 5 ml/min, a low rate of KCl diluted in saltwater is injected, then permeability reduction, RRF, was 1.0. Same procedure was carried out every day until sustainable plugging take place inside the core. This occurs as previously described when the silicate gel plugs a 3 µm filter (≈ 170 NTU). The evolution of the silicate turbidity was monitored by measuring the turbidity of both the injected and produced silicate on a daily basis; this can be seen in Table 1, with the rest of both measured and calculated data.

Time (Day)	Measured	Measured	Measured	Calculated	Measured	Calculated
	Turbidity injected (NTU)	Turbidity effluent (NTU)	Mobility reduction, RF	Particle size (µm)	Measured permeability reduction, RRF	Predicted permeability reduction, RRF
0	3,06	3,06	1,35	0,05	1	1,01
1	12,2	14,2	1,35	0,23	1,12	1,11
2	36	37,7	1,77	0,64	1,48	1,35
3	72	76,6	2	1,3	1,71	1,87
4	123	121	3,37	2,14	2,79	2,97
5	169	172	Plugging	3	Plugging	5,06
6	208	–	–	3,66	–	–

Table 1; Experiment 1 data, with injection rate 5 mL/min ($v = 3.3 * 10^{-4}$ m/s)

In Table 1, day 0, represents initial conditions. The equation for finding the particle size is the same as presented under "The influence temperature has on gelation time" section. To clarify, this particle represents a silicate particle that grows in size and becomes gel. Predicted permeability reduction is calculated from equation; $RRF = (1 - \frac{d}{R})^{-4}$, where *R* is pore radius and *d* is the particle size, meaning that RRF increases as the particle size, *d*, increases. The pore radius was calculated to be approximately; $R = \sqrt{(8k/\varphi)} = 9\mu m$, where k is absolute permeability and φ is the porosity.

Also in Table 1, there are mentioned two different turbidity measurements. The injected turbidity is the pre mixed sodium silicate solution, while the effluent turbidity is measured from the produced solution. It is expected that the effluent turbidity is greater due to the development of gel over time. Plugging occurs at day 5, which is expected since the turbidity is above 170 NTU and the calculated particle size is 3 µm. Also when the permeability reduction (RRF) exceeds a value of at least 100, plugging can occur. Even though it says “plugged” right after a low number, RRF must be over 100 to be plugged.

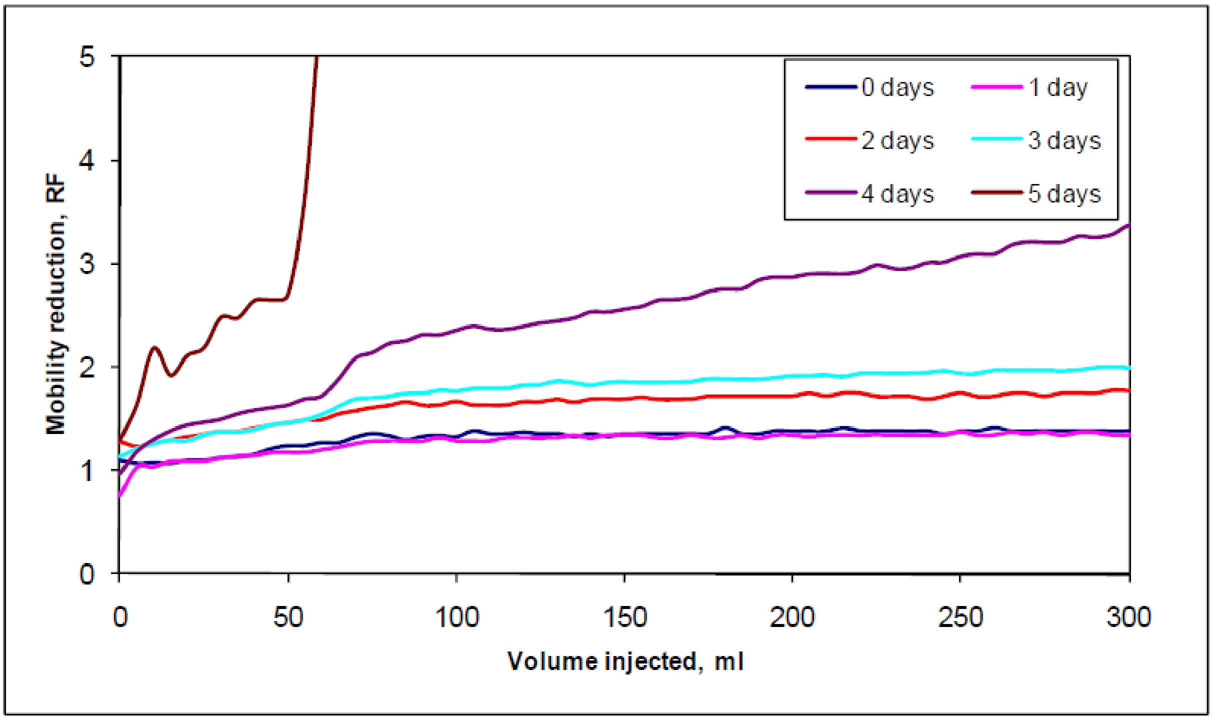

Figure 16; Mobility reduction, RF, for each of the silicate slugs at q = 5 ml/min.

As Figure 16 illustrates, the mobility reduction increases more or less gradually until complete plugging occur at day 5.

Flood experiment 2, was carried out the same way as experiment 1, with the exception of five times lower volume rate injected sodium silicate; q = 1 ml/min. The intention was to see if the injection rates have any impact on gelation time.

Time (Day)	Measured	Measured	Measured	Calculated	Measured	Calculated
	Turbidity injected (NTU)	Turbidity effluent (NTU)	Mobility reduction, RF	Particle size (µm)	Measured permeability reduction, RRF	Predicted permeability reduction, RRF
0	2,29	3,05	1,6	0,04	1,01	1,02
1	11,9	18	1,61	0,2	1,02	1,09
2	35,9	40,1	2,1	0,62	1,09	1,33
3	72,1	79,1	4,2	1,26	1,16	1,83
4	114	278	630	2	1,3	2,72
5	160	–	Plugging	2,81	Plugging	4,48

Table 2; Experiment 2, with injection rate 1 mL/min ($v = 0,66 * 10^{-4} m/s$)

From Table 2, the injected turbidity compared with the data in Table 1 deviates slightly, but not enough to have any significant influence on the gelation time. However, it is interesting to see the difference in the evolution in mobility reduction (RF), because RF seems to increase faster at a lower injection rate, together with the effluent turbidity. The evolution of the permeability reduction (RRF), is expected to increase in the same manner as RF and the effluent turbidity, as in experiment 1 for instance. But in experiment 2, RRF is much lower than expected compared to RF and the effluent turbidity measurements. After 4 days with RF factor of 630, RRF factor is only 1.3. The reason that the RRF measurements is lower than expected, is because the post – flush with KCl brine regains the permeability, the gel was not strong enough so it got produced. Normally a mobility reduction this high means that it is plugged, but perhaps by sheer coincidence the gel was not fully developed. This explains why the effluent turbidity factor can be above 170 NTU and still be produced. But after 5 days it was not possible to regain the permeability, and complete plugging was observed. Also just to clarify, the data given in both Table 1 and Table 2, are results at the end of the day, and not during the experiment as both Figure 16 and Figure 17 illustrates.

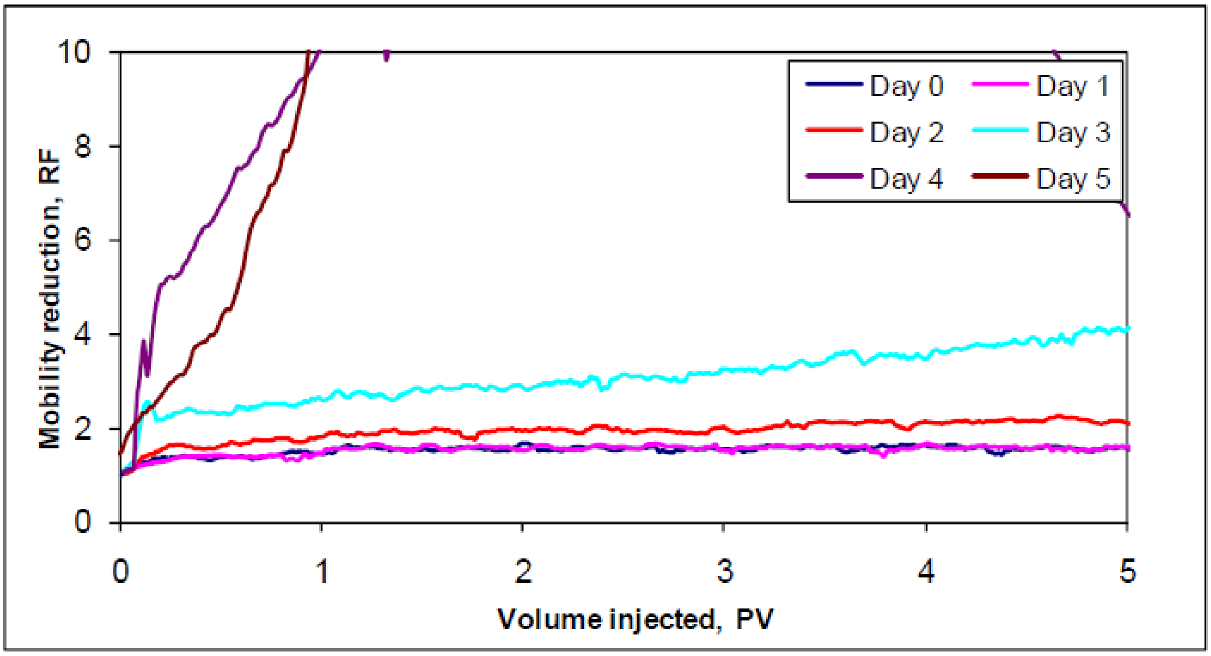

Figure 17; Mobility reduction, RF, for each of the silicate slugs at q = 1 ml/min.

Figure 17, shows the evolution of mobility reduction during flood experiment 2.

Both flooding experiments show the same evolutionary development of RF, predictable increase of RF until a peak is evident/experienced. It is also interesting to notice that in flood experiment 2, the predicted permeability reduction differs more and more each day from the measured values (see Table 2), which means that low injection rates may give more uncertain gel times. It can also be seen in Table 2, that calculated particle size at day 5, is less than 3 μm, which should in theory mean that the core is not yet plugged, even though the core is in reality completely plugged. But in Table 1 (experiment 1), the predicted (calculated) versus measured data seems to be more consistent, which means more predictable plugging times.

These two flood experiments were also conducted with the same conditions in quartz sand columns (length 30 cm and diameter 2.8 cm), with 2 Darcy permeability and 0.22 porosity.

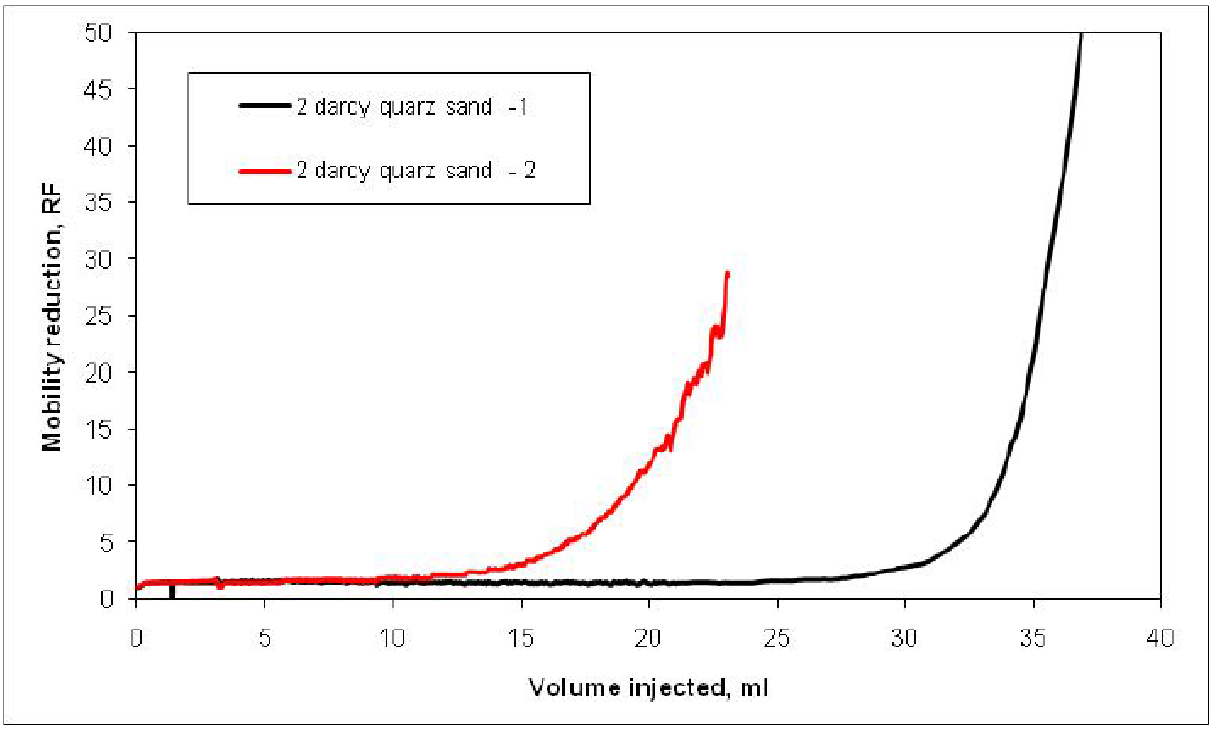

Figure 18; Mobility reduction, RF, for the silicate train injected through 2 Darcy sand columns at 40°C.

In Figure 18, the black graph illustrates injection rate; q = 5 ml/min (Experiment 1). While the red graph is; q = 1 ml/min (Experiment 2). As previous results gained from the Bentheim cores and what Figure 18 shows, with lower injection rate of sodium silicate means earlier development of the mobility reduction, which the red graph (q = 1 ml/min) shows.

Experiments with 9 Darcy quartz sand (instead of 2 Darcy) and 500 mD Berea sandstone, gives the same result, lower injection rates results in earlier gel times. But, the plugging of aged silicate solution at low injection rate was found also to depend on the permeability. For instance, injection rate that plugged a 2 Darcy Bentheim core after 20 hours, also plugged a 500 mD Berea core after about 12 hours.

In core scale experiments it is fairly straightforward to know when the core is completely plugged, since it is easy to monitor the data and the process goes a lot faster compared to actual field operations. So, a method to have a better conjecture is measuring pressure responses. While the core matures (days with injection of silicate solutions), the pressure increases since more pressure must be applied in order to maintain the desirable injection rate. When the core is more or less plugged, the low permeability can be compared with trying to force large amounts of water through a drinking straw, at the same velocity of injected volume as with a big pipe. This is why the pressure increases, and with too high pressure there is a risk of fracture of the formation also, undesirable fracture can ruin the reservoir.

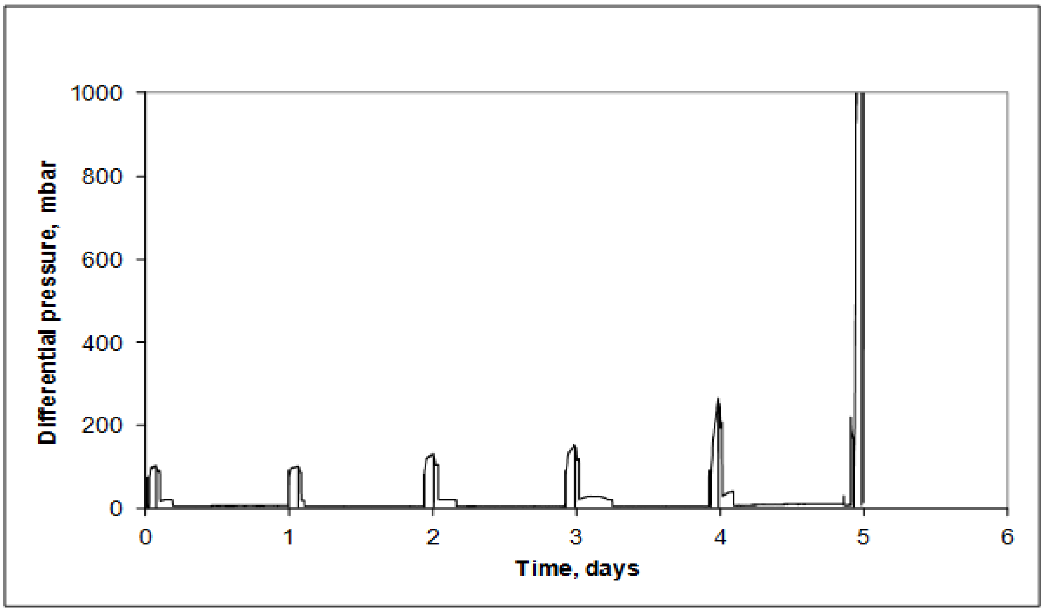

Figure 19; Pressure response when solution of 4 wt% silicate and 6 wt% HCl was injected through a 2D Bentheim sandstone.

Figure 19, illustrates how the pressure response slowly increases each day, but at day 5 complete plugging occurs, evidently due to the high pressure spike. Figure 19, is related to flood experiment 1 (q = 5 mL/min), with bulk temperature of 40°C.

A significant confirmation obtained from the laboratory work, was that it proved that the gelation time of sodium silicate solutions can be considerably delayed by lowering the salinity and acidic concentrations, but it is also important to ensure that the injection rate is high enough. This implies that one of the critical factors for in-depth diversion is fulfilled. Other factors that contributes to the bulk gelation kinetics is the concentration of the silicate solution, where 4 wt% sodium silicate shows good gel strength potentials. Pre and post – flushes with 0.5 wt% KCl was proven to work, does also have an important role to play, such as avoiding precipitation and displacing the silicate solution further into the formation.

In summary, the laboratory experiments demonstrate the possibility of good filter properties of the pre –filtered sodium silicate. As long as the cation exchange in the high permeability sand is moderate, the onset of gelation is triggered by temperature. Therefore, a simple and robust approach to simulate the gelation may be to assume gelation and permeability reduction in grid blocks where both silicate concentration and temperature exceed some critical values.

1.3 Single Well Injection Pilot

This section is based on the work conducted in paper; SPE 154004. This paper contains the results from the single well injection pilot.

Single well injection pilot is only focusing on one injection well. The area of interest is illustrated in Figure 21, from layer 16 to 25.

At this stage, the experimental work has already been carried out and analyzed. With this information, computer simulations are used in order to have a better comprehension of how silicate will behave in a field operation. Since small scale experiments are too limited in itself to directly go from small to large scale. A few cores cannot represent an entire area, and reservoir conditions are extremely different from laboratory conditions. From what is known from the literature, only the simulation program eclipse was used in these simulations. Eclipse is recognized as a reliable reference simulator (commercial simulator). It offers a robust set of numerical solutions for fast and accurate prediction of dynamic behavior for all types of reservoirs and development schemes.

This pilot well was the first ever attempt with in – depth sodium silicate offshore. This field operation is only meant as a test, to get an indication as to whether or not this method holds good EOR potentials. Just to clarify, the intension is not to produce anything or enhance oil production another well somewhere. Hence, it is to see if the sodium silicate could be displaced about 40 meters from the injection well and there become gel that completely plugs the zones. The reason for making a test operation before an actual real reservoir situation is to be sure that it works, because less effort is put into it, both in terms of money and manpower. The amount of sodium silicate used in the large scale operation is about 320 times more than this test operation, and that is only the silicate. Instead of taking the risk and go straight from small scale experiments to the large scale operation, this would be a safer and predictable solution to choose.

1.3.1 General Information About The Operational Field

The reason that this thesis will discuss the Snorre field is because this is the first and only offshore field that has been tested so far with sodium silicate as deep in-depth plugging. The snorre field has an OOIP of 519 MSm^3 and is now a mature under – saturated oil field with roughly 3/4 of the reserves already produced, expected recovery is about 48%, but optimistically one wishes to get out 55% with EOR methods. The total thickness of the reservoir is about 1000 m with net/gross ratio of approximately 0.45, with porosity from 14 to 32 %, and permeability variations from 100mD to 4 Darcy. Total clay content is about 5% to 35%, and reservoir temperature is 90°C with initial pressure 383bar. The formation consists of several rotated fault blocks comprising the Lunde and Statfjord Grp. of Late Triassic and Early Jurassic ages, and it is characterized by complex packages of mainly inhomogeneous stratified fluvial sandstones dipping 6 to 8 degrees. Snorre field is also very heterogeneous; the reservoir is characterized by limited vertical and horizontal communication, particularly in zones with low net/gross ratio. Production started in 1992 with Snorre A platform as producer, in the southern part of the field with sea water injection as the main drive mechanism. Then Snorre B platform started producing in 2001, in the northern part of the field with water alternating gas injection (WAG) as main driver mechanism. Due to the heterogeneous nature of the reservoir, one saw the need for improving the sweep efficiency. This is where the in-depth water diversion method comes into play (Blaker, T. et al. (2002) and Skrettingland (2011)).

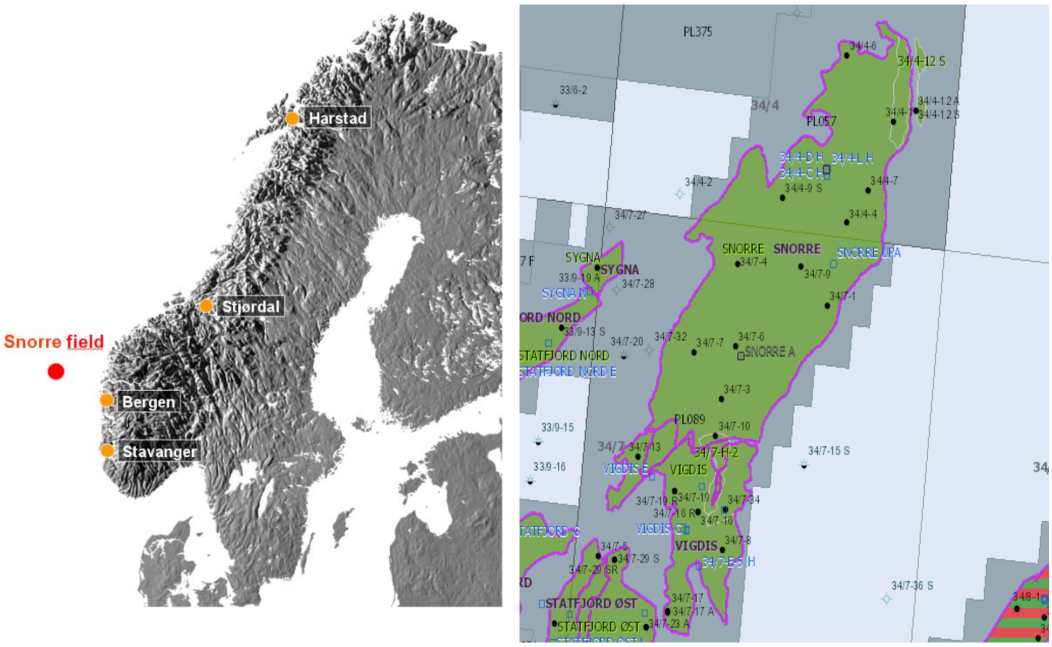

Figure 20; The Snorre oil field, located 150 km from the Norwegian coastline in the North Sea

1.3.2 Pilot Well; P-07

Well P-07 in the Snorre field was drilled in 1994, and originally an oil producer for Upper Statfjord formation. Core samples were only collected from the upper part of the sand, since the formation was too unconsolidated (not compact or dense in structure or arrangement). The core sample was taken at the depths of 4027.00 – 4027.50 meters, and was analyzed by thin sections and XRD, see Table 3. With thin section analysis a thin sliver of rock is cut from the sample with a diamond saw and ground optically flat. It is then mounted on a glass slide and then ground even using progressively finer abrasive grit until the sample is only 30 μm thick, this sample is then observed under a microscope so that rock forming minerals can be identified (Nicolas P. Badertscher* and Martin Burkhard, 2000). X-ray diffraction (XRD) is the primary, non-destructive tool for identifying and quantifying the mineralogy of crystalline compounds in rocks, soils and particulates. Every mineral or compound has a characteristic X-ray diffraction pattern whose 'fingerprint' can be matched against a database of over 250 000 recorded phases, XRD is an essential technique for identifying and characterizing the nature of clay minerals, providing information which cannot be determined by any other method (He. B. B. 2006). Well P-07 has a water cut of 97%, with the water originated from a thin sand of about 1 meter vertical thickness. Because of the high water cut one began to use it as an injector for IOR purposes, and in 2008 the well was used to measure the effects of low salinity water injected by in-situ measurements of the remaining oil saturation before and after injection (Skrettingland et al., 2011). Following the IOR-pilot with low-salinity water injection, the well was shut in because of its high water cut.

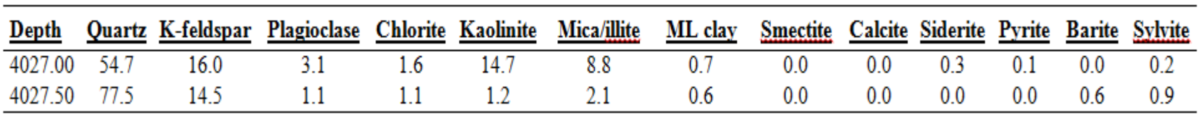

Depth	Quartz	K-feldspar	Plagioclase	Chlorite	Kaolinite	Mica/illite	ML clay	Smectite	Calcite	Siderite	Pyrite	Barite	Sylvite
4027.00	54.7	16.0	3.1	1.6	14.7	8.8	0.7	0.0	0.0	0.3	0.1	0.0	0.2
4027.50	77.5	14.5	1.1	1.1	1.2	2.1	0.6	0.0	0.0	0.0	0.0	0.6	0.9

Table 3; Rock mineral composition of the core material (XRD wt %).

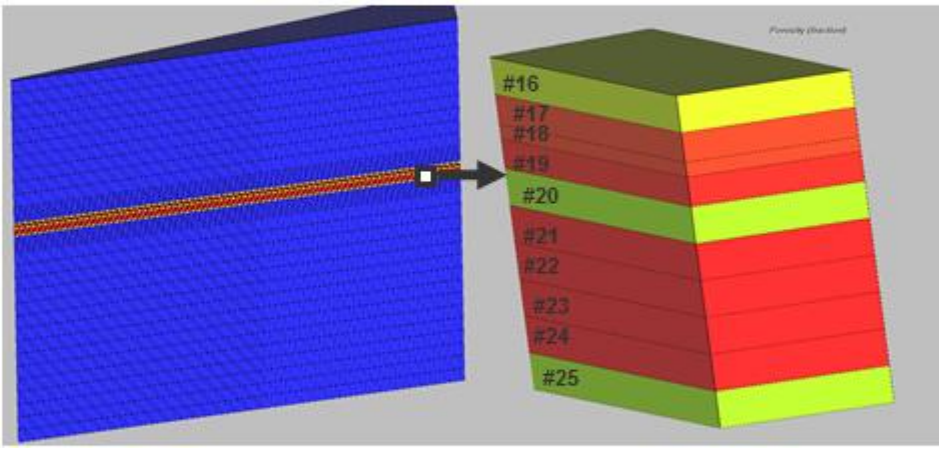

Figure 21; P-07 Radial sector model used for simulations

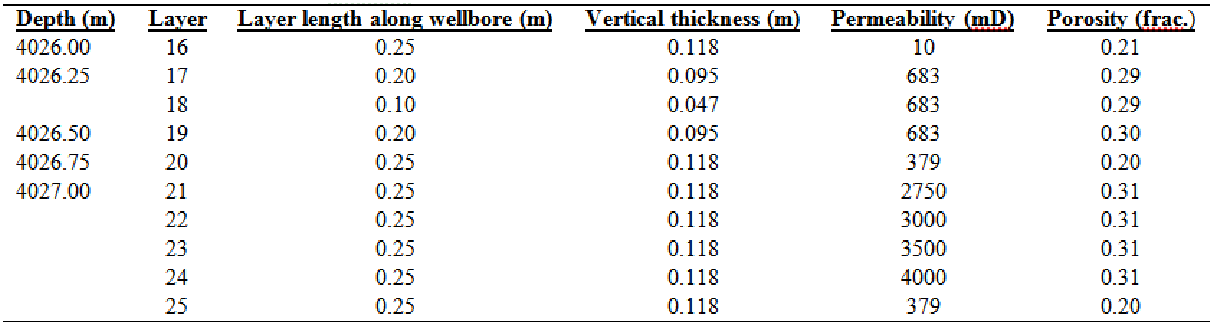

Depth (m)	Layer	Layer length along wellbore (m)	Vertical thickness (m)	Permeability (mD)	Porosity (frac.)
4026.00	16	0.25	0.118	10	0.21
4026.25	17	0.20	0.095	683	0.29
	18	0.10	0.047	683	0.29
4026.50	19	0.20	0.095	683	0.30
4026.75	20	0.25	0.118	379	0.20
4027.00	21	0.25	0.118	2750	0.31
	22	0.25	0.118	3000	0.31
	23	0.25	0.118	3500	0.31
	24	0.25	0.118	4000	0.31
	25	0.25	0.118	379	0.20

Table 4; Layers used in P-07 Reservoir simulation model

In order to get trustworthy simulation results, there must be included data from several layers (Table 4), since vertical connections must be taken into consideration.

1.3.3 The Simulation Model For The Pilot Test

As already mentioned, this pilot well, P-07, was first used as a production well, and then for EOR purposes it was changed to be an injector for testing. This pilot well was selected to be the field test injector for in – depth sodium silicate. Main reason for choosing this specific well is because it is in the same area as the future "real" field operation (in Snorre field), meaning that it contains more or less the same properties/characteristics as the large scale interwell field pilot operation.

As shown in the experimental results, the temperature is the main initiator for the gelation process. In core scale experiments, temperature was not an issue, since it was easy to regulate. The same thing cannot be said about field operations, especially because it is nearly impossible to have a complete understanding of the temperature profile from the injector to the producer. The reservoir temperature is 90°C in Snorre, this is quite high and would result in early gelation, as illustrated in Figure 15. In order to accommodate this challenge, large volumes of seawater is injected directly from the sea, to cool down the reservoir; normally seawater is about 17°C (depending on depth and season) in the North Sea. It should be mentioned that it is only possible to temporarily cool down the reservoir, it will eventually always return to its original temperature. The exact temperature after the cool down is not mentioned in the papers, but after talking to K. Skrettingland, the temperature was about 30 - 40°C near the well. It is expected that the temperature profile from the injector and further into the formation has an increasing tendency, either a linear or an exponential increasing temperature function. This means that the deeper the silicate is displaced into the formation (horizontally), the higher the temperature will be. Eventually during this displacement the silicate solution will be initiated by high enough temperatures, and the gelation process starts, with that permeability reduction.

As just explained, the Snorre field is about 90°C, so in order for the silicate to reach 40 m into the formation, it has to be cooled down prior to silicate injection. Simulations with eclipse helps to give an estimation of how much volume of injected fluids is needed. Not only the sea water that cools down the reservoir, but also the rest of the injected fluids.

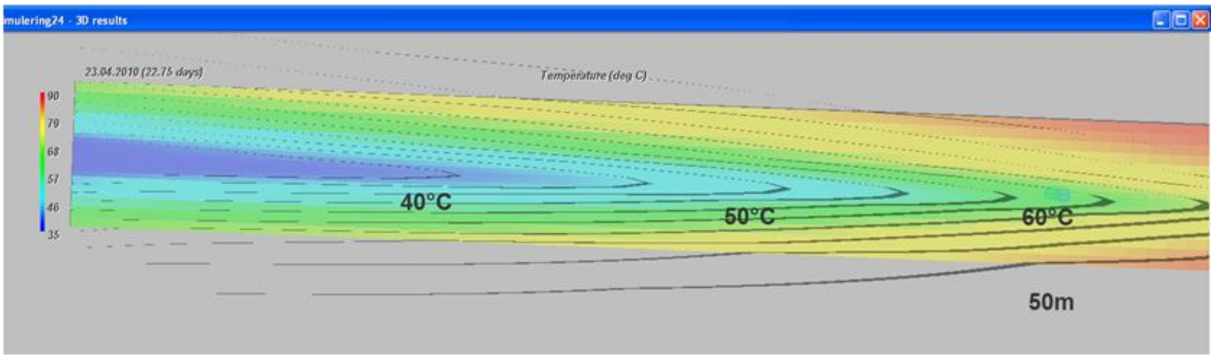

Figure 22; Snapshot of the simulated reservoir cooling

Figure 22, shows the simulated temperature profile in the lower part of layer 22, after injection of seawater to about 50 meters from the injection well. Near the well it is somewhere around 35°C, as the dark blue colour indicates. If the temperature before 40 meters reaches roughly 55°C, simulations show to early gel development of the silicate, in order to reach the desirable area.

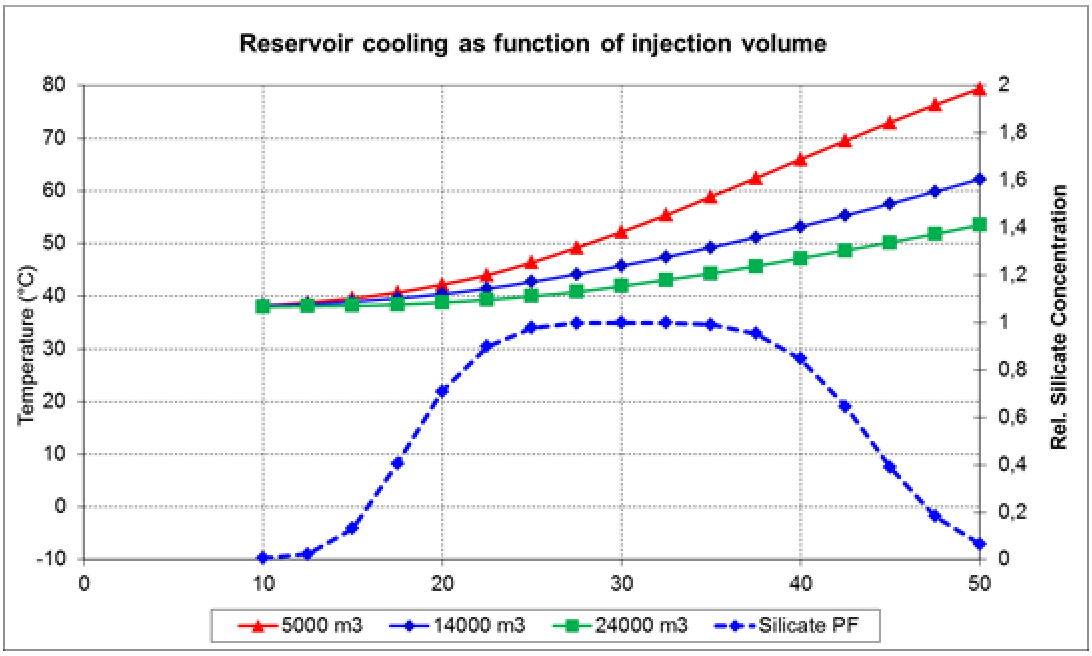

Figure 23; Simulated reservoir cooling vs. volume seawater injected. Sodium silicate injection volume is 800 m^3 and displacement volume 200 m^3.

In Figure 23, simulations of different volumes of sea water are shown, together with a fixed volume of sodium silicate. The x – axis illustrates meters from the injection well, the reason for both the cooling seawater and silicate fluids begins at 10 meters, is because of the post – and pre flushes of KCl that displaces them. The KCl flushes are not illustrated here, because the volume injected is too small to make an influence on the temperature profile.

It should be mentioned that Figure 23, only represents the lower part of the sand in layer 22. This is because layer 22 represents the high permeable zones, as shown in Table 4, layers from 21 to 24 is the highest ones.

Simulation results gave indications that injecting 14000 m^3 cold seawater gave a sufficient robustness in temperature of the target area. As could be seen in Figure 23, the injection of 24000m^3 which is almost twice the amount as 14000m^3 did not give any substantial impact on the temperature. This means it is a waste of time injecting a lot more, and still come to the same conclusion. The temperature predictions did also match historical temperature data from adjacent wells.

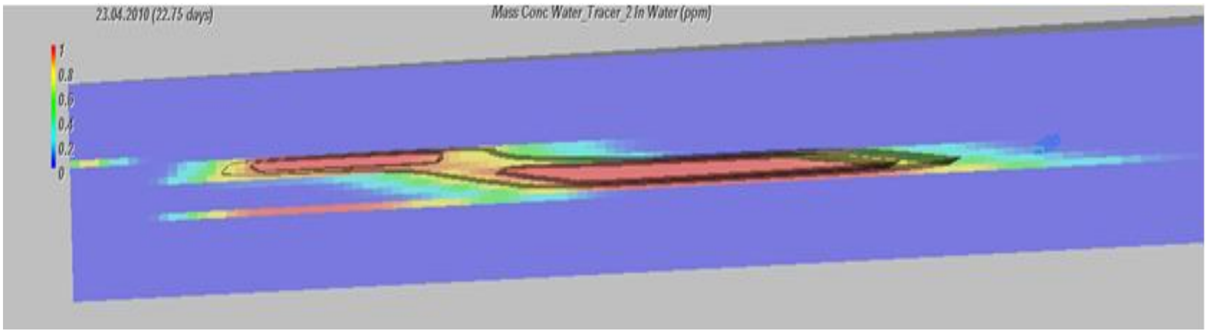

Figure 24; Snapshot of the simulated silicate plugging

Figure 24, shows the estimated sodium silicate placement in lower part of layer 22, especially the red area, which represents plugged zones. Figure 24, should be seen together with Figure 22, to better understand the silicate placement. The silicate bank is found to be about 20 – 50 meters from the injection well, as can be seen in Figure 24. This snapshot is taken after all the injection steps were conducted (see the injection steps taken below), together with the actual volumes and concentration used to give the best simulation result. The part in between the two red areas is believed to be a zone with lower permeability; it could for instance be a salt barrier. This could explain why silicate plugging is not seen here. It will be given an explanation based on the actual operational data collected later in this thesis.

As previously stated, this pilot well is a test well. The purpose was to upscale the laboratory experiments reported by Stavland et al. (2011a and b) together with the simulation work to prove the ability to create a permeability restriction in the reservoir at a chosen distance of approximately 40 meters from the wellbore, with a radial slug length of the sodium silicate solution of roughly 20 meters (See Figure 22-24).

The results were; The injection pilot were mainly chosen to have the following 5 injection phases:

1. Injection of 14 000 m^3 sea water to cool down the reservoir temperature around the P07 wellbore.
2. Injection of 400 m^3 0.5 % KCl brine to separate sodium silicate from the injected sea water.
3. Injection of 760 m^3 4.0 % sodium silicate solution.
4. Injection of 200 m^3 0.5 % KCl brine to displace sodium silicate solution into the reservoir followed by 70 m^3 LVP (Low Vapor Pressure oil) for hydrate prevention in the wellbore.
5. Injection of 10 m^3 every second day to monitor injectivity and record transient falloff data.

The injection process is assumed to be a piston like displacement. Details surrounding the injection process are elaborated later on.

1.3.4 Designing Criteria For The Pilot Test

For the actual injection operations on the pilot, a supply vessel was chosen among the ones that are regularly used to transport drilling fluids and bulk material to the Snorre field. The vessel was temporarily modified for this operation, with pumps and fluid mixing equipment installed only for this purpose. The total tank capacity for both sodium silicate and KCl fluid was 1400 m^3, these fluids have the mixed considerations of 400 m^3 pre – flush, 760 m^3 sodium silicate solution and 200 m^3 post – flush. What the vessel carries of silicate and KCl at the time, is the only volume available. No more came later. The reason for using a vessel to do this test operation and not the active platform, is to avoid interfering with the activity that is already in progress on the Snorre A platform.

Based on maximum allowable downhole injection pressure and well injectivity, the planned water injection rate of 1000-1200 m^3/d was chosen. At increased injection resistance the rate was limited to max allowed estimated downhole injection pressure of 350 bar. Stavland et al. (2011a) reported limited static gel strength in core floods using 3 wt% silicate and an improved static gel strength at 4 to 5 wt% silicate concentration; therefore, a 4 wt% sodium silicate solution was chosen for the injection pilot in P07.

If the pumping process would cease during the silicate injection, the temperature will start to increase; slowly in the formation just above the perforation interval, but rapidly in the wellbore. This was observed in similar wells and conditions as this well, the temperature there at top perforation was observed to increase from about 40 to 60 °C when the injection process stopped for 6 hours. This makes a huge difference in the gelation time, as temperature is the main initiator for the gelation process in field operations. Both foreseen and unforeseen occurrences could for instance be bad weather or wear and tear on the equipment that results in operation stops. The primary requirement for the sodium silicate gelation kinetics is that even at 6 hours of pumping stop for instance, premature gelation should not occur. Second requirement is limiting the gelation time to reduce the time needed for response measurement because of the risk to displace the silicate too far from the injection pilot, but also to finalize the monitoring of the permeability reduction prior to a coming four weeks maintenance stop at the Snorre A platform. To fulfill these requirements, an acid concentration of 6 wt% 2 M HCl was chosen; gelation time at 40 °C was 5 days which would allow pumping of the 760 m^3 volume, even at flow rates substantially lower than the planned 1000 m^3/d, and would also allow for a pumping stop of more than 6 hours. See Figure 15, for illustration of the gelation time at these conditions.

The dilution of the sodium silicate and KCl was conducted before loading it onto the supply vessel. As for the acid (HCl), it was kept separate from everything else in its own compartment onboard the vessel. Then offshore the acid is continuously mixed into the silicate solution under the injection process, so that the wt% of acid (acidic concentration) can be changed as desired. The vessel was connected to the x – mas tree of well P07 by a 2’’ hose, where all the injected fluid goes through. As previously discussed one of the few things that can be controlled to obtain the planned gelling time, is the mixed acid concentration. For instance at pumping stop, the temperature will start to increase, but then it is possible to accommodate this problem by lowering the acidic concentration, so that the gelation time is less affected. This is why the accuracy of the acidic mixing is important, because with increasing acidic uncertainty, comes the risk of increasingly premature gelling. To ensure sufficient accuracy, the flow rates and pH were measured. Before the offshore operation the mixing process was tested and optimized in a full scale yard test, the accuracy in the fractional acid rate was found to be within 1% which from gel the kinetic model indicated accuracy in the gelation time of less than 10%. Operationally, injection of 4.0 wt% silicate with an HCl concentration of 6.0% 2M HCl, at an injection rate of 1200 m^3/d (833 l/min) implies onshore diluted silicate solution to 4.18 wt% with injection rate of 798 l/min and 10 % HCl at injection rate of 35.3 l/min. The pH of the injected silicate solution will be 11.04 and the density at 20°C was measured to 1.040 g/cc, which agreed well with the calculations.

In the light of the results from the experimental work, in order to avoid rapid plugging, more than acidic accuracy needs to be done. That is where pre – and post flush comes in, especially pre – flush is important since it separates the silicate solution from both the injected seawater and formation water, but also controlling the cation exchange. Here 0.5 wt% KCl was applied, the reason for using KCl instead of NaCl is because clay swelling is then avoided. The core flood experiments demonstrated that precipitation of silicate would not cause permeability reduction as long as the relative sea water concentration was below 10%. Relative seawater concentration is a commonly used term for cations, such as Mg^{2+} and Ca^{2+}. The length of the mixing zone is assumed to control the location of plugging. Some estimates of the mixing zone between the KCl pre – flush and the seawater can be made assuming ideal conditions. In linear core floods, the length of the mixing zone, Δx, can be calculated as $\Delta x = x_{10}-x_{90} = 3.625\sqrt{K_l t}$ (Green and Willhite, 1998). Here x_{10} and x_{90} are the distances (in feet) at which the relative concentrations are 10 and 90%, respectively, K_l is the longitudinal dispersion coefficient and t is the time (in hours). Using this approach with $K_l = 3x10^{-4}$ ft^2/hr, Δx will be less than 1 m, indicating that the pre – flush volume is not critical. However, as pointed out by Green and Willhite (1998) widths calculated by dispersion theory must be considered as minimum widths.

For the P07 well, field data from the low salinity water injection tracer tests (Skrettingland et al. 2011), can be used to quantify the length of the mixing zone. The production rate was about 20 m^3/hr. These data are plotted in Figure 25, and compared with dispersion curves using different Peclet numbers, N_{Pe}. As can be seen, N_{Pe} = 20 matched the P07 tracer test well. However, calculations of N_{Pe} indicate that $N_{Pe} = v * l/K_l$ is significantly larger and above 1000. This implies that the mixing zone, with N_{Pe} = 20 will be in the range of 0.7 to 1.5 pore volumes. For a pre-flush volume of 400 m^3 this means that in-depth mixing of alkaline silicate and brine with salinity larger than 10% sea water may be possible. Peclet numbers is dimensionless and used to determine the relative importance of advection and diffusion on low permeability environments (M. Huysmans et al. 2004) such as this, due to the gel plugging.

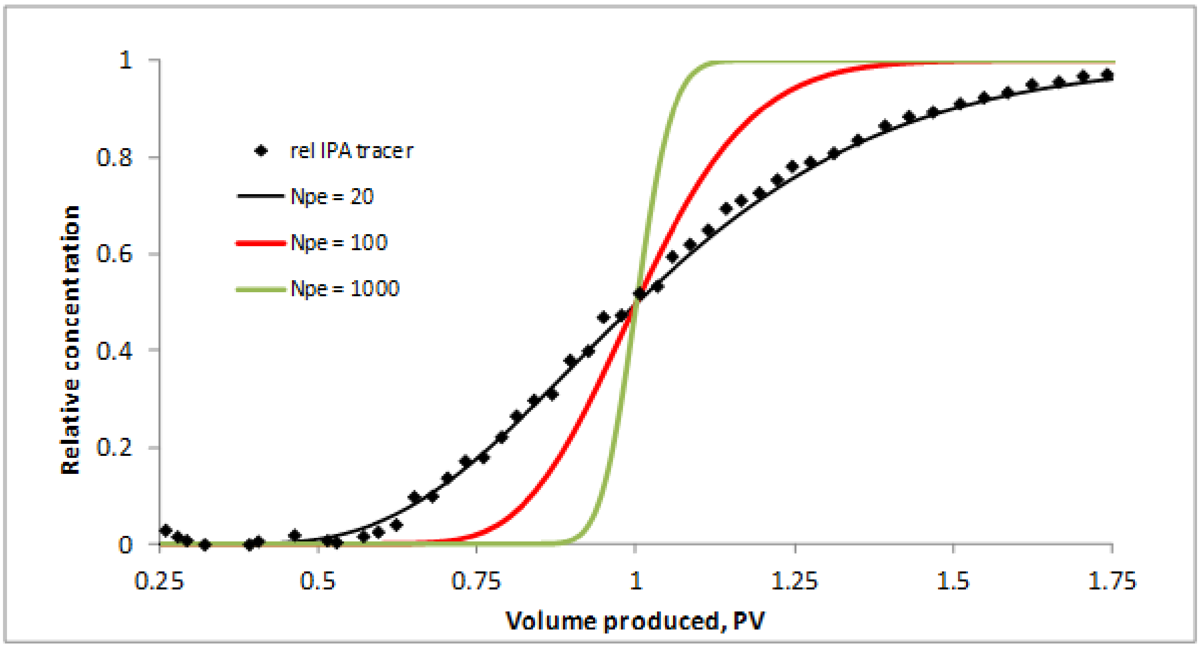

Figure 25; IPA tracer from P07 low salinity SWTT test 2, matched with Peclet numbers of 20, 100 and 1000, IPA data from Skrettingland et al. (2011).

In Figure 25; IPA is another word for the alcohol isopropanol, which was used as a tracer in this test (Lovelock 2006 et al.). A tracer is a chemical or other substance placed in or around the borehole to measure fluid movement in injection wells, for instance a bead tracer or a radioactive tracer (Brigham, W. E. 1987). SWTT is short for: single well tracer test, and is an in – situ method for measuring fluid saturations in reservoirs. The method works by injecting a reacting partitioning tracer (ester) that produces a non-partitioning tracer (alcohol) in-situ. During back – production, the ester alternates between the moving water phase and the immobile oil phase and is slowed down, compared to the alcohol. This alternation (denoted partition coefficient) is fixed for a given oil/water system and is measured in the lab beforehand (Romero, C. 2011 et al.). See Figure 26, for illustration of SWTT.

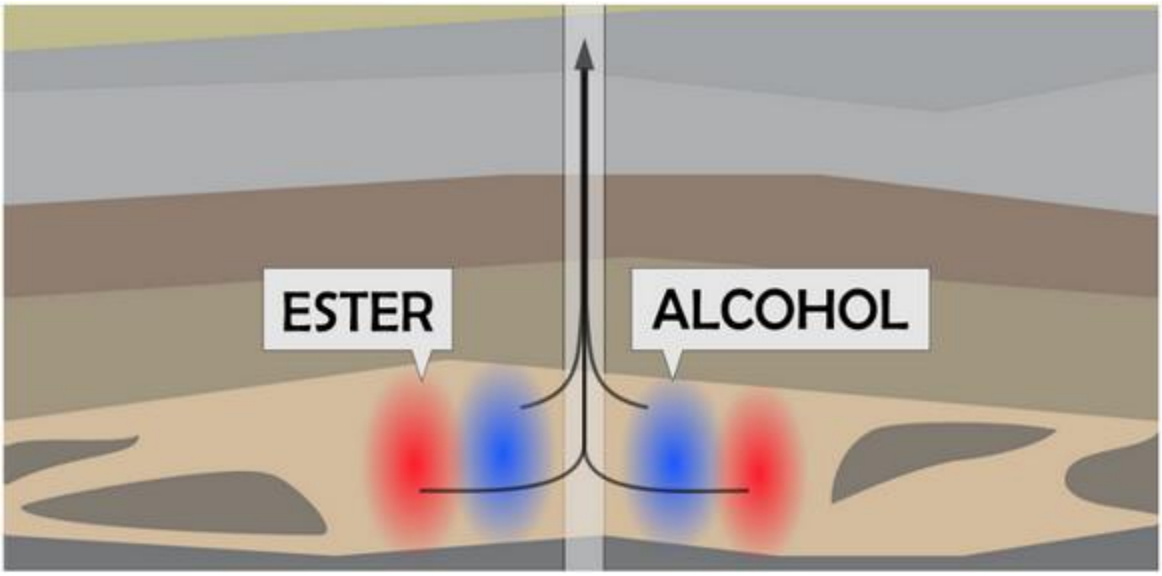

Figure 26; Illustration of the single-well chemical tracer test (SWTT) principle

In Figure 26, during a SWTT, ester is injected into the formation. Parts of the ester react with water (hydrolyze) to form alcohol. During back – production the partitioning ester lags behind the alcohol and the time-difference is directly related to oil saturation in the formation. In other words, oil saturation in the test-zone is found from the time – delay between production of the ester and the alcohol in the producer (Romero, C. 2011).

When injection of the silicate starts, the 400 m^3 KCl pre – flush has then reached a front position of about 31 meters in the high permeable layers. And when 200 m^3 silicate has been injected, the pre – flush is located from 38 to 22 meters, this constitutes a slug thickness of 16 meters. The thickness becomes smaller as more silicate is injected. This is indicated by the blue curve in Figure 27. Both the silicate front and the seawater tail are dispersed. The following three cases are plotted in Figure 27;

1. Mixing zone lengths represented by 0.25 to 1.75 pore volumes (Worst case, the red curve),
2. Base case lengths represented by 0.5 to 1.5 pore volumes (The green curve)
3. Best case lengths represented by 0.75 to 1.25 pore volumes (The violet curve).

The worst case scenario indicates mixing of silicate and seawater after the injection of 200 m^3 of silicate, while the best case indicates that no mixing will take place during the injection of the 760 m^3 of silicate. Base case is somewhere in between the two other cases.

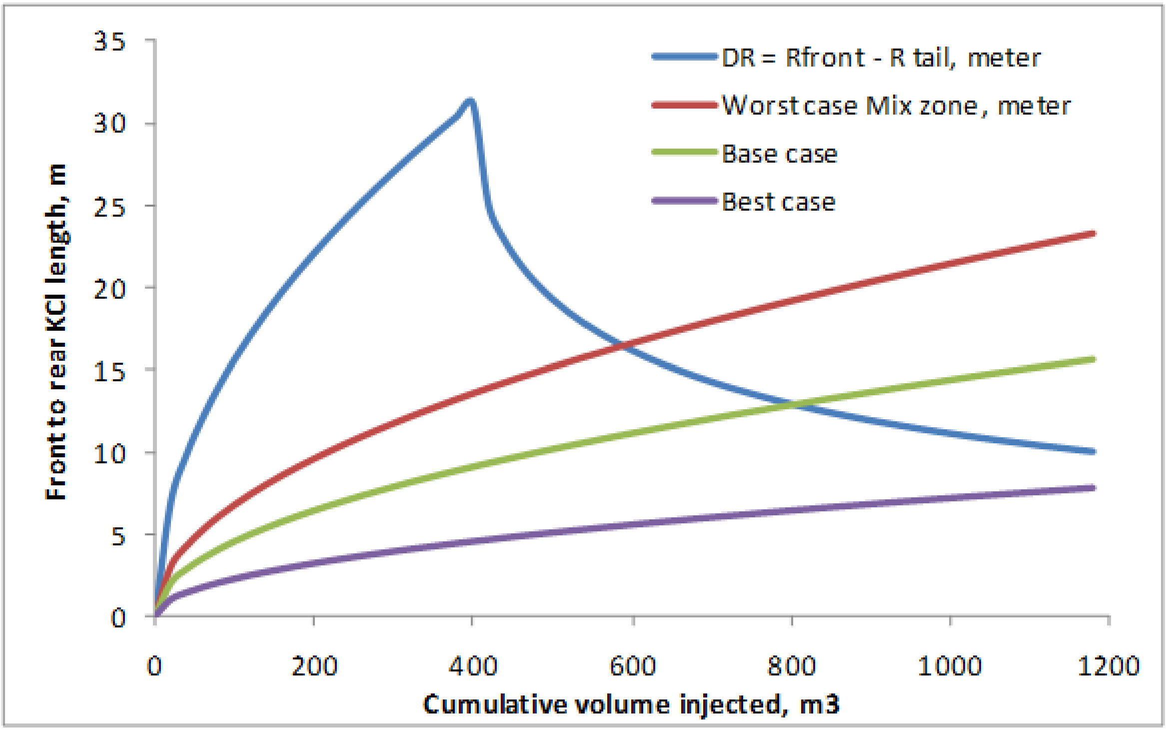

Figure 27; Estimating the evolution of pre-flush size and the possibility of silicate/seawater mixing.

Due to the heterogeneous permeability nature in this reservoir (shown in Table 4), higher viscosity and deeper invasion in the high permeability bottom layers will occur. This may impact on the mixing of silicate and seawater, because the pre – flush volume entering the low permeability zones is only 14% of the total volume, and the front position is correspondingly lower. Assuming that the fluid fraction entering the high permeability layers 21 to 24 is 0.86, it is then easy to estimate at which injection volumes the silicate front in the high permeability zones overlaps with the seawater tail in the low permeability zones by simple radial front position calculations.

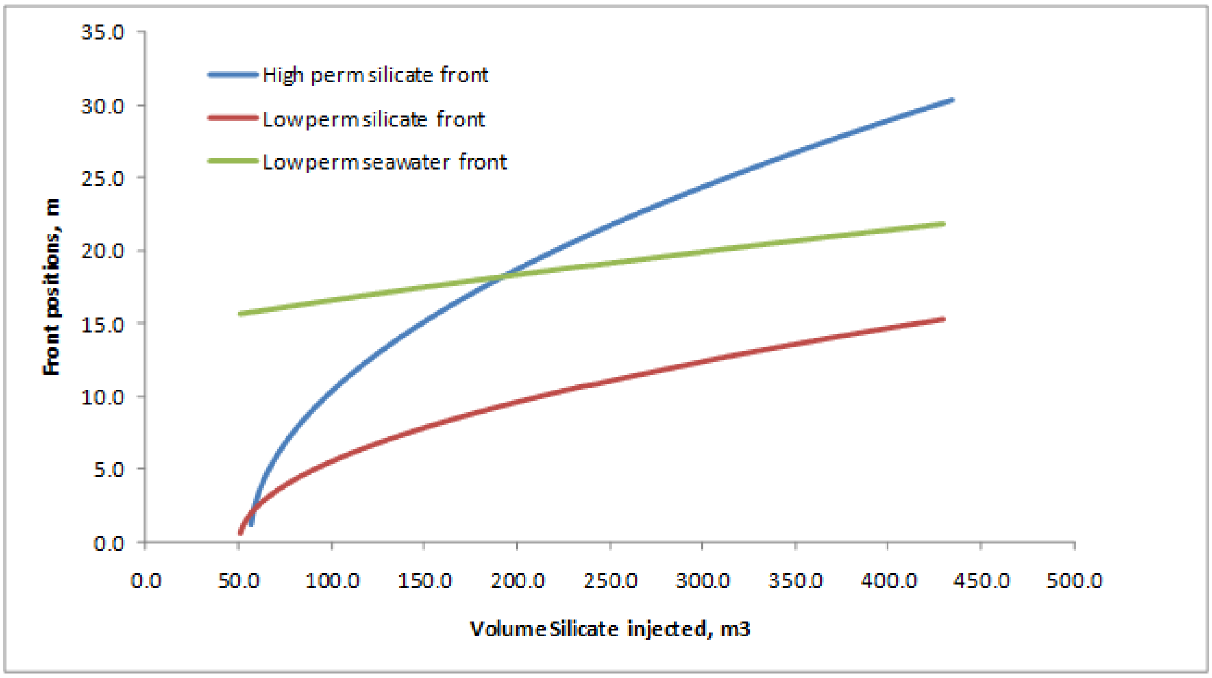

Figure 28; Seawater/silicate mixing fronts at the interface between high and low permeability layers.

Figure 28, shows the silicate front position in the high permeability layer and the sea water front in the low permeability layers, both versus the injected volume of silicate. Where the high permeability silicate (Blue curve) crosses with low permeability seawater (Green curve) at about 200 m^3 injected silicate and front position about 17 meters, is similar to the worst case scenario shown in Figure 27. In an ideal reservoir, including vertical communication and neglecting crossflow because of nearly no viscosity contrast, the silicate front will after injection of 200 m^3 catch up the low permeability sea water front. As more silicate is injected, formation of a thin layer barrier in the high to low permeability contact is possible. The barrier is formed because of the combination of Mg-precipitation and the higher salt concentration which causes a rapid gelation. Such a barrier will most likely introduce a decline in the injectivity but not a complete blocking. Using Figure 24, as an example, a salt induced barrier will most likely reduce the risk of crossflow between the gel located in the low and high permeability layers.

This indicates that both of the above explanations seem possible. Larger pre-flush volumes would most likely improve the silicate injectivity. Also note that the pre-flush slug size may be used as a design parameter for in-depth placement. Detailed simulations will however improve the quality in the above mentioned estimates.

The in-depth location of the gel can be estimated by falloff tests or productivity calculations. However, in heterogeneous reservoirs there is a risk of separating the gel located in the high and low permeability layers. Optimizing the injection volume may however eliminate such a risk. Simple estimates using Darcy law calculations demonstrate that with separations of the silicate gel plugs, the maximum reduction in injectivity is given by the high to low K_H ratio, regardless of the permeability reduction across the gel plugs. This is expressed by the following equation:

$$I_r = \frac{1 + 1/F}{I_{ri} + 1/F} \tag{1}$$

Here, I_r is the relative injectivity, I_{ri} is the relative injectivity for single layer and F is the high to low K_H ratio, $F = {K_H h_H}/{K_L h_L}$. For the current model, see Table 4; $F = \frac{\sum_{21}^{24} K_i h_i}{\sum_{16}^{20} K_i h_i + K_{25} h_{25}} = 6.2$. If $RRF > F$, post water will crossflow and I_{ri} is found by setting $RRF = F$ in Equation 2. This implies that with crossflow, the minimum relative injectivity will be 0.90. On the contrary, if the silicate gel plugs overlap, or the crossflow can be eliminated, the relative injectivity will decrease as the gel strength increases. In radial geometry we have the following:

$$I_r = \frac{\ln\left({r_e}/{r_w}\right)}{\ln\left({r_e}/{r_w}\right) + (RRF - 1)\ln\left({r_f}/{r_t}\right)} \tag{2}$$

Here, RRF is the permeability reduction across the gel plug, located between the tail, r_t and front r_f. Also, I_r can also be called relative injectivity index and I injectivity index.

1.3.5 The Pilot Test Operation

Now when the designing criteria are set, the actual offshore operation can be conducted. Two different methods were chosen to give response measurements on the permeability reduction as a consequence of the silicate injection;

- Calculated the injectivity index from measured pressure and rate
- Transient falloff test analysis

In an injectivity test, the well is shut – in until the pressure is stabilized and then injection is initiated at a constant rate while recording the bottomhole pressure. If the injected fluid has exactly the same properties (density, viscosity, compressibility, and wetting characteristics) as the reservoir fluids, an injectivity test would be identical to a pressure drawdown test except that the constant rate, q, would be negative (Sabet, M.A. 1991).

A pressure falloff test is usually preceded by a long injectivity test. Injection is then stopped while recording pressure. Therefore, a pressure falloff test is similar to a pressure buildup test, but only if the properties of the injected and reservoir fluids are the same (Kazemi, H. 1974). It should also be mentioned that with falloff tests it can be confirmed that the fluids injected after the in – depth gelation is actually diverting into new areas, and not that the fluids just moves slower through the reservoir.

During shut – in periods there is a risk of having hydrate formations occurring; to prevent this produced oil from second stage separator at 11 Bar (LVP) was injected for the injectivity and falloff measurements. Hydrate is a compound formed by the chemical combination of water and some other substance. In a reservoir situation it often reacts with gas, and creates an icy – like solid that form when free water and natural gas combine at high pressure and low temperature. Details concerning gas – hydrate chemistry, physics and oilfield engineering are found in Makogon, Y (1997) and Sloan, E (1990). Also clarifying what LVP (low vapor pressure) oil is, its purpose is to achieve higher vacuum (lower pressure) than is possible by use of positive displacement pumps alone. The pump relating to the use of LVP is called oil diffusion pump (R. Witty 1947).

The different injection steps do not all use the same pumps. The operational steps are listed in detail in Table 5. The injected seawater that cools down the reservoir used a water injection pump that is located at the platform. Also LVP for hydrate avoidance and response measurement was pumped from LVP – pumps at the platform. But KCl, sodium silicate and HCl were all injected from each of their pumps that were located on the vessel. It should also be mentioned that well P – 07 wellbore volume is 50 m^3.

The operational window of the LVP-pumps was limited by a minimum required pump rate of 140 m^3/d. Good response data were acquired until the injectivity became too low, approximately 20 days after the sodium silicate placement. After 23 days, 03.08.2011, when the injectivity was too low for continuous injection, 50 m^3 LVP was injected by applying continuously an incremental pressure of 70-90 Bar across the permeability restriction during 12 hours. The injectivity index from the 12 hour pumping was 1.0 m^3/day/bar.

The pumping sequence is listed in Table 5, and the corresponding pumping pressure when injecting the preflush – silicate – postflush fluid train is shown in Figure 29.

Date	Operation	Fluid	Rate (m3/d)	Total volume (m³)	Purpose
24.06-08.07.2011	Injection	Seawater	1000-1200	13800	Reservoir cooling
08.07.2011	Injection	LVP		10	Hydrate prevention
08.07-09.07.2011	Well shut in				Hook up pipeline from vessel to the well P-07
09.07-10.07.2011	Injection/falloff	0.5 % KCl brine	800-1200	400	Pre-slug as spacer between sea water and sodium silicate, reference falloff analysis.
10.07-11.07.2011	Injection	4 % silicate	800-1200	760	In-depth permeability reduction
11.07.2011	Injection	0.5 % KCl brine	700	200	Post-slug as spacer between silicate and LVP. Displace silicate away from the well.
11.07.2011	Shut in well				Disconnect pipeline from vessel
11.07.2011	Injection	LVP	550-350	70	Hydrate prevention, displacement of sodium silicate and preparations for response measurements.
11.07-15.07.2011	Shut in well				Wait for gelation
15.07-31.07.2011	Repeating injection (10 m³) and falloff	LVP	210-140	80	Response measurement; injectivity and transient pressure falloff analysis. Hydrate prevention.
31.07-03.08.2011	Shut in well				
03.08.2011	Injection	LVP	0-170	50	Response measurement; too low injectivity for continuous injection. Discontinuous pumping for 12 hours
03.08-14.09.2011	Repeating injection (5 m³) and falloff	LVP		20	Response measurement; too low injectivity.

Table 5; Detailed operational summary on test well P – 07.

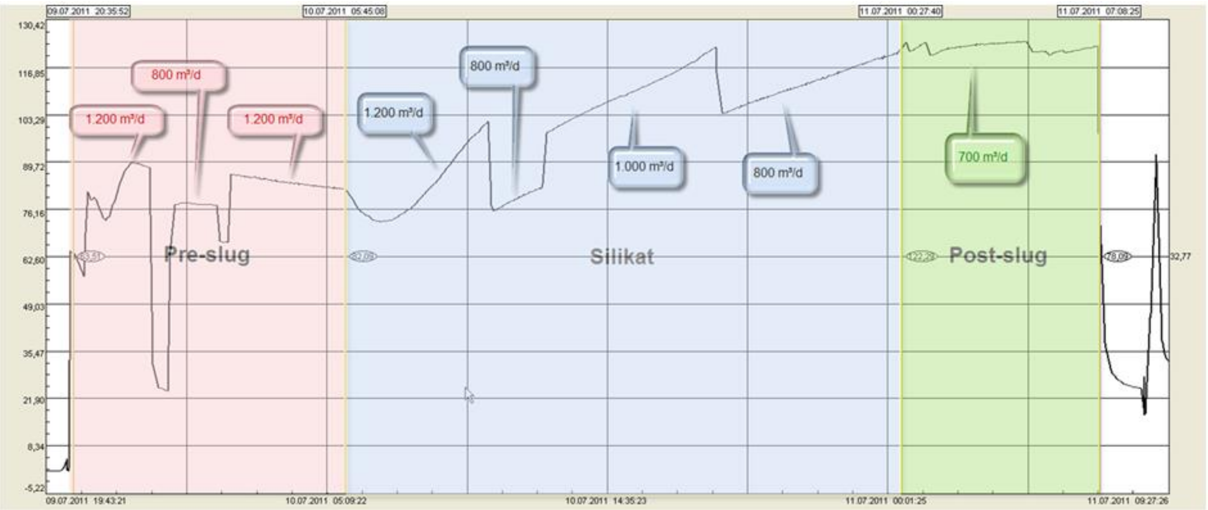

Figure 29; Surface pumping pressure (Bar) during the injection of KCl pre – flush, sodium silicate, and KCl post – flush.

1.3.6 The Pilot Test Operation Results

Both pH and the turbidity of the injected silicate were regularly measured during the process. The pH was stable at; $pH = 10.84 \pm 0.02$, this was slightly lower than the laboratory experiments, where it was; pH = 11.04. At silicate injection start, the turbidity was measured to be about 3 NTU. This is more or less the same as the core flood experiments in Bentheim cores started off with; see turbidity values in Table 1 and 2.

During the injection of the pre – flush, silicate and post – flush the wellhead pressure and injection rates varied. The pressure was normalized using the injectivity index approach; $II = {}^{q}/_{\Delta P}$ where ΔP is the drawdown pressure and q is the volume rate. The following effective hydrostatic pressure corrections were made: ΔP_{SW} = PWH + 15.6 Bar, $\Delta P_{KCl} = \Delta P_{SW}$ + 5.0 Bar, $\Delta P_{Si} = \Delta P_{SW}$ – 10 Bar and $\Delta P_{LVP} = \Delta P_{SW}$ + 54 Bar. The objective of pressure normalizing is to present a robust diagnostic method for drawdowns that did not suffer from noise and data scatter, as is typical of the standard well test derivative. The solution involves using a pressure integral curve as the base curve for noisy drawdown analysis (Samandarli, O. 2012).

Initially the premade silicate viscosity was 1.3 mPas, which is slightly higher than water. During the silicate injection the productivity index (PI) is lowered (It should be mentioned that injectivity index is the same as productivity index!) The concept of PI expresses the following: Once the well production is, in some sense, stabilized, then the ratio between the production rate and the pressure drawdown (difference between the reservoir average pressure and the well average pressure) is practically independent from the production history or even from the operating conditions. The higher the value of the PI the better the performance of the well in the reservoir is (Aulisa, E. 2009). The PI is stated here as the volume delivered per Bar of drawdown at the sandface (m^3/day/Bar).

As earlier stated the silicate viscosity will increase during the gelation process. This forces the silicate PI to decrease. But when the silicate PI declines to levels lower than expected, it was expected to give the same result as in core flood experiments, stable injectivity in fresh silicate solution. But this clearly did not occur in this test operation. It can then be concluded that the reduction in the injectivity is caused by reduction in the permeability. There are two possibilities for this premature permeability reduction:

1. The mixture of silicate and seawater because of dispersion and too low KCl pre – flush volume.
2. Mixing of silicate in high permeability layer with seawater on low permeability layers.

The injectivity reduction seemed to start when the silicate front reached about 10 meters; this is earlier than expected compared with the simulation results, which was approximately 15 meters, see Figure 24. Although there was greater permeability reduction than anticipated, this will not pose a significant difference in the objective, which was to plug approximately 40 meters from the injection well.

During the falloff tests, the PI can be estimated from the effective injection rate and corresponding pressures prior to the falloff. The last injection test, see Table 5, with 5 m^3 gave response measurements; too low injectivity. Since it did not produce at stable injection rates and the estimated injectivity indexes are not accurate. Even so, a large reduction in the injectivity rate 6 days after injection of the silicate, see Figure 30, for the evolution of RRF. This is fairly in agreement with the core flood experiments conducted, which gave a gelation time of 5 days, see Table 1 and 2.

The injectivity reduction during the LVP falloff tests is thought to have a combination of (These two gelation explanations are also discussed under filterability experiments);

1. Filtration of silicate gel near the silicate front, at 45 meters. Since the gel particles have grown during these 45 meters, and will eventually grow as large as the permeability area. This silicate gel will accumulate with time, resulting in intensified permeability reduction.
2. The other combination is most likely in high permeability layers approximately 25 to 45 meters from the injection well. The gel particles here do not plug because it is not large enough to get stuck. But will grow in – situ, under shut – in periods and as the layers age with rising temperature.

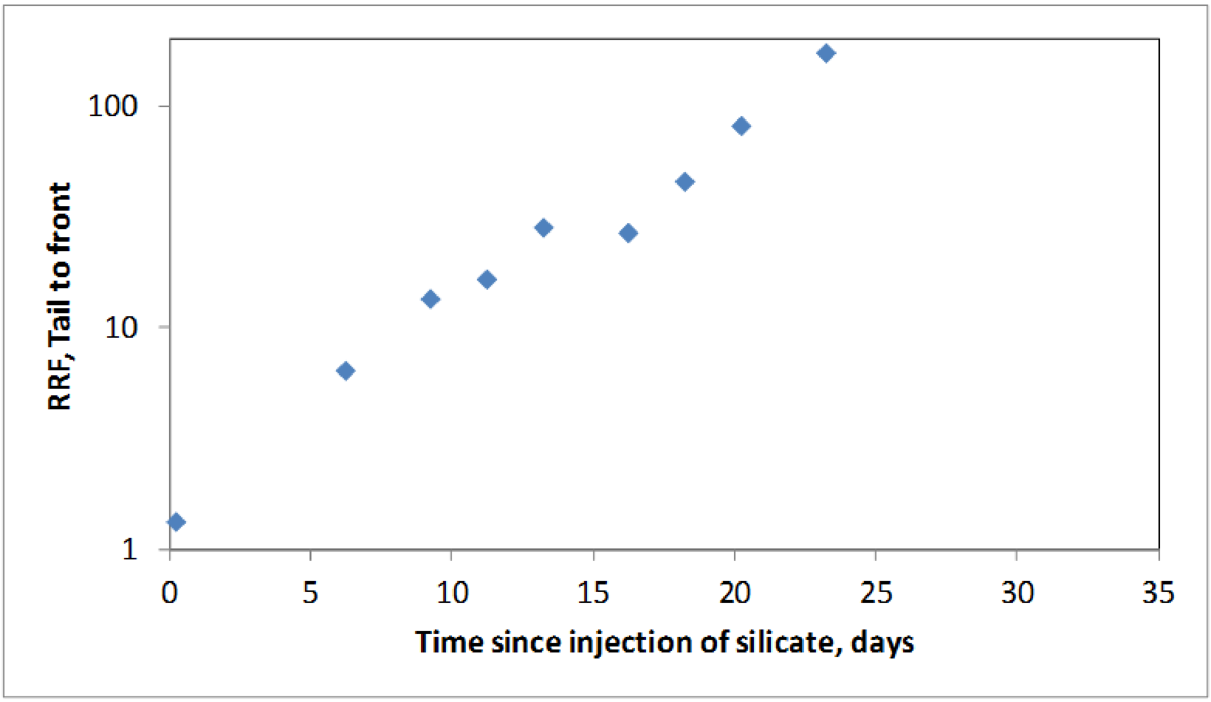

Figure 30; Permeability reduction across the silicate slug assuming uniform gelation in the injected silicate slug.

Figure 30, is only based on the theory that the injectivity reduction is caused by in – situ gelation that grows over time, the gelation which occurs at 25 – 45 meters. It should also be mentioned that the permeability reduction (RRF), was derived using equation 2, under "Designing Criteria For The Pilot Test". In Figure 30, RRF increases more or less linearly with aging time.

The opposite approach is assuming RRF caused by in – depth filtration, which is presumed to occur 45 meters from the injection well, as Figure 31 indicates. Here RRF is plotted versus the estimated thickness of the silicate plug. It is not only the accumulation of the silicate particles that reduces the permeability, but the increasing compression of the particles, see Figure 32 for accumulation illustration.

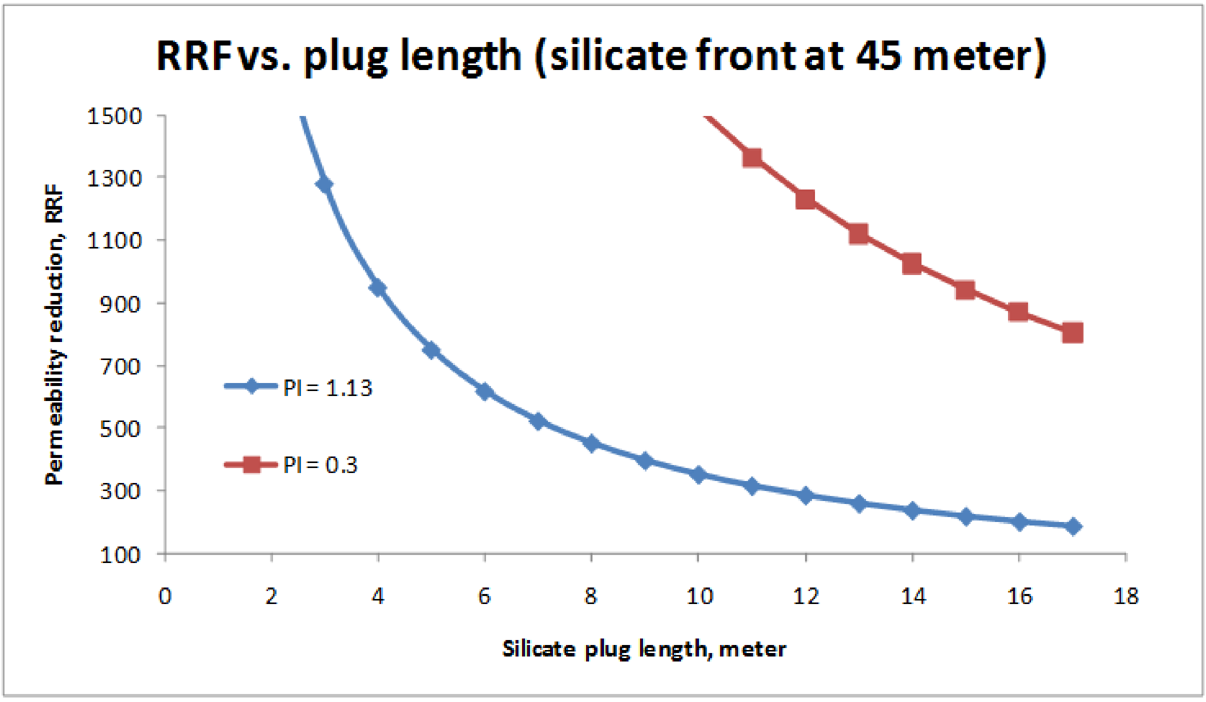

Figure 31; Permeability reduction versus thickness of the plug.

Figure 31, shows two cases, one pre – estimated result the other actual results measured. Both for the same date, 03.08.11;

1. Actual results with productivity index of 1.13 m^3/day/bar (blue curve)
2. Estimated results with an productivity index of 0.3 m^3/day/bar (red curve)

Even though they show different PI, in both cases the RRF > 100 and RRF increases as the size of the assumed restriction area decreases (meaning compression of the filter cake). It was predicted; $PI = 0.3$, which means it was predicted a more effective RRF at this time than what the reality gave. But some margin errors must be taken into account, at least the most important criteria is held here; To avoid too early gelation.

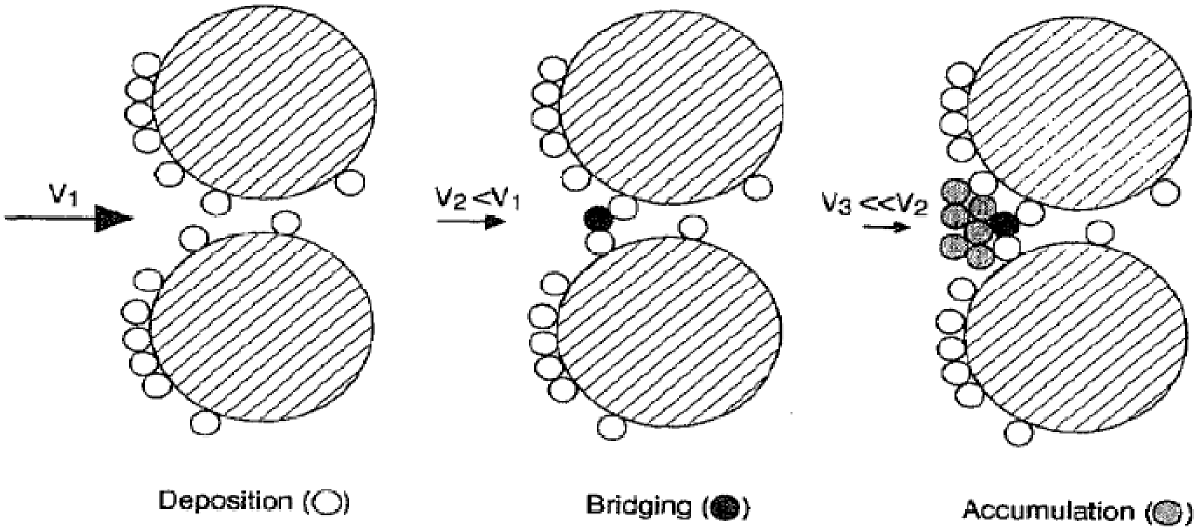

Figure 32; Retention at the grain/pore level

Nabzar et al. (1996), which introduced a model for formation damage, which includes bridging of particles. The effect of fluid velocity on bridging is illustrated in Figure 32; at high velocities, no bridging occurs. This is probably because of the high viscous forces. At lower velocities bridging is initiated, which may lead to accumulation of particles. It seems obvious that the criterion of bridging is that the distance between the deposited particles must be of the same order of magnitude as the particle diameter. This implies that bridging is favored by small pore throats. It is likely that bridging of the charged silicate particles will initiate silicate growth resulting in larger silicate aggregates. Regarding the velocity, since the filtration occurs further out in the formation (about 40 meters), velocities is obviously significantly reduced here, and it will be even further reduced if it continues deeper in the formation. But the point being, as Nabzar et al. (1996) pointed out, velocities must be low enough for the silicate to start accumulating.

This is also why it is very important to have high enough injection rate (velocity), when it comes to avoiding near well gelation, since avoiding premature gelation is first priority, see "The influence temperature has on gelation time" under experiments conducted for more on the importance of injection rate.

The simulation result shown in Figure 24, has this gap in between the red areas. It was speculated on if the silicate slug possibly revealed a high and low permeability transition between layers, which lead to crossflow of the post slug. With the probability for bypassing of the gel slug in the lower high permeability part of the sand, both simulations and analytical calculations show limited injectivity reduction and that the injectivity was independent of RRF. But without bypassing, the relative injectivity would decrease by increasing RRF.

The reduction on injectivity resulting from the injection tests reveals that there was no bypass flow and that both the high and low permeability part of the sand was actually plugged. This could be understood as either a silicate induced barrier separation of the high and low permeability layers or by invasion of silicate from the high permeability into the low permeability layers. Either way, the conclusion is that it is plugged.

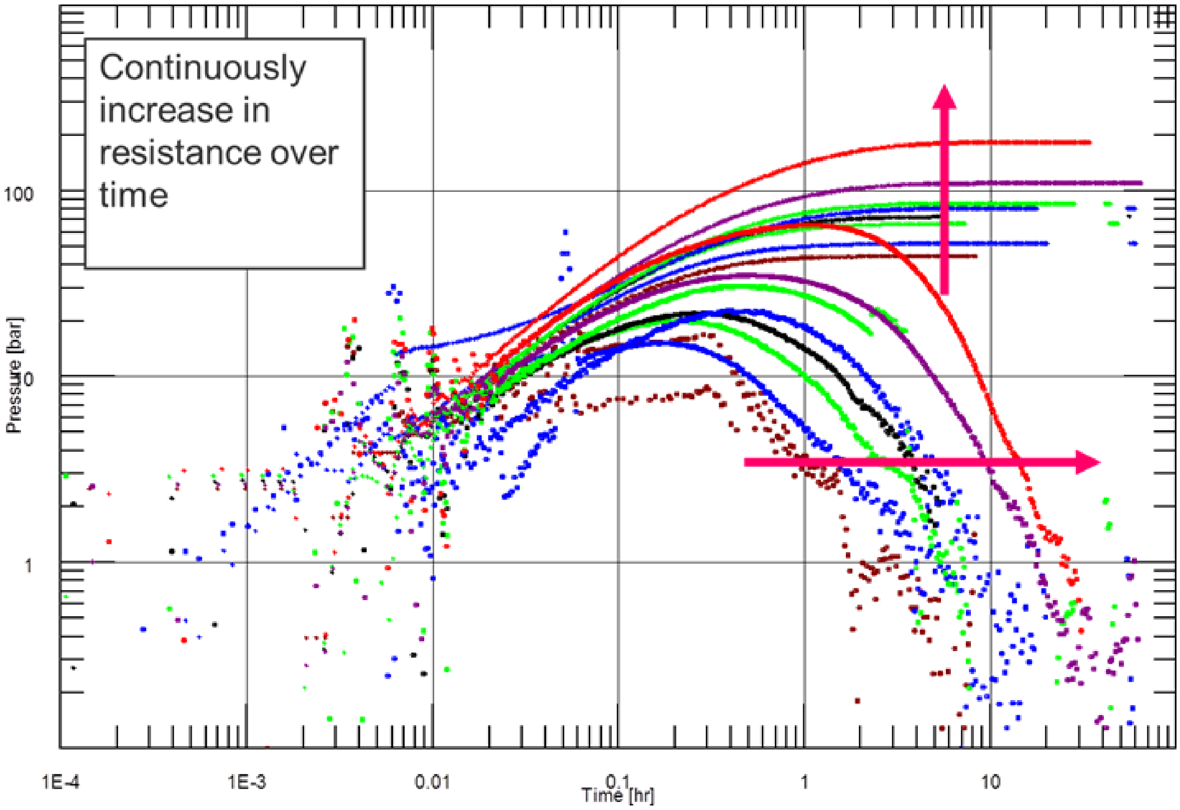

Figure 33; Transient falloff test data from day 4 to day 20 after sodium silicate injection.

Figure 33, illustrates how the pressure increases for each transient falloff test from day 4 to day 20, the increased pressure corresponds to increased resistance, in other words increasing permeability reduction factor. As can be seen, the curves with the same color are the same falloff test. Except some of the tests at random have the same color, two green and two blue tests. All together its 8 transient falloff tests conducted, where the red curve represents the last test at day 20, and brown the first at day 4. Figure 33, was interpreted using radial flow from the pre – silicate falloff data as basis, pre – silicate is shown in Figure 34.

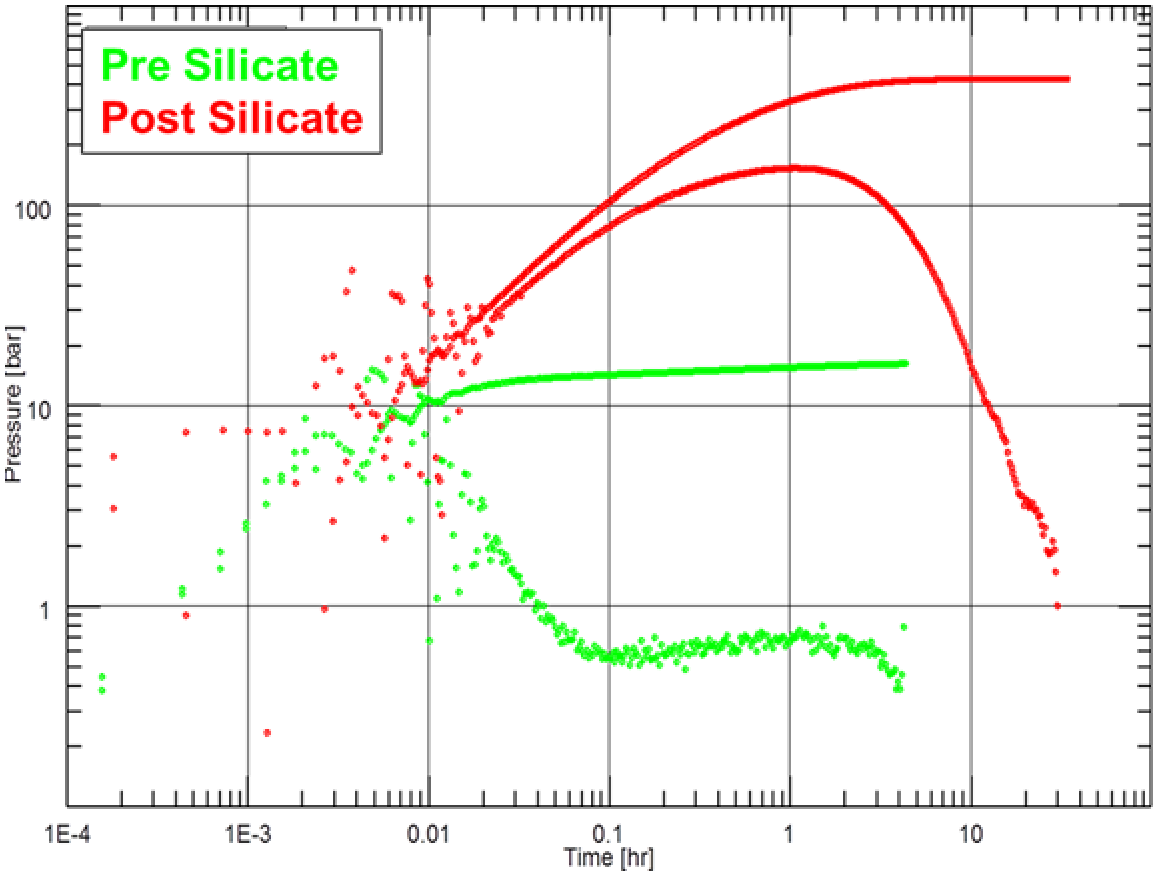

Figure 34; Transient falloff data before sodium silicate injection and 20 days after injection.

Several transient falloff tests were performed before the KCl pre – flush and sodium silicate injection, during the reservoir cooling seawater process tests were conducted. This is what the pre – silicate (Green curve) represents in Figure 34. The interpretation gave permeability of 3600 mD for a radius of investigation of nearly 1.5 km. When the silicate was displaced to a radius of roughly 40 – 45 meters injection tests with 1 – 1.5 hour injection followed by transient falloff tests were performed frequently. The reason that the data information stops on day number 20, is because after that time it was not possible to conduct additional tests, due to low injection rates (velocities).

Interpretation of transient falloff data 20 days after silicate injection showed an average mobility reduction factor of 170 in a radial interval from 7 m to 70 m from the wellbore compared to the near wellbore data and far from wellbore. The injectivity index after 20 days was 3 m^3/day/bar with the injectivity decreasing further to a value lower than 1 m^3/day/bar after the final falloff test.

1.3.7 The Pilot Test Operational Conclusions

The main objectives of the pilot test was sustainable in – depth plugging about 40 meters from the injection well, avoid too much precipitation, premature gelation and post mature gelation. This was achieved and confirmed by fluid injectivity measurements and transient falloff tests. The actual operational results seemed to be consistent with the experimental results.

The planned gelation time was set to be 5 days, after the reservoir was cooled down to a temperature of 40°C. This would secure injection of the planned volume before onset of gelation and included safety margins for potential pump stops. When it comes to gelation time, the challenge was to ensure plugging about 40 meters from the well. Salt was too complex to use as a controllable factor, and trying to control the placement with injection rate (velocity) is just not achievable. The temperature profile inside the formation involves too many unknown factors to be used for this purpose. The best way is using acid (HCl), since this can be mixed on the go and the amount of HCl can easily be controlled by the acid injection rate. With high concentrations of HCl in the silicate solution, would result in fast gelation for instance, and the opposite tendency for lower concentrations.

The injectivity of the sodium silicate before the gelation was good. This and the permeability reduction were pretty much in agreement with core flood experiments. However, in the mixing zone between silicate and seawater a permeability reduction in the range of 10, caused by precipitation of $Mg(OH)_2$ was detected. It should probably have been a larger KCl pre – flush volume used, since this would have reduced the risk of mixing silicate and seawater (or formation water), and less precipitation would have been created close to the injection well.

Again the planned gelation time was after 5 days, but distinct permeability reductions were seen after 6 days in the field. One day does not make a difference, so this is thought to be a good match. But the predicted permeability reduction missed some, but this does not affect the results. Because as long as the permeability reduction is above a factor of 100 it is acceptable, plugging will then occur anyways. Injectivity measurements were performed during a period of 75 days.

The conclusion of this offshore test pilot in well P – 07 at the Snorre field Norway is considered to be a success. It is also recommended to perform fluid mixing and injection from a vessel linked up to the platform to minimize the operational interference with the ongoing work on the platform. This demonstrated that sodium silicate can be used for deep in – depth gelation.

It can be noted that sodium silicate is primarily intended to be used for sandstone reservoirs like the Snorre field, since carbonate reservoirs normally does not have high permeability problems, it is more likely to have the opposite, too low permeability. But silicate gel could be used for plugging fractures for instance.

1.4 Large Scale Interwell Field Pilot

This section is based on the work conducted in paper; SPE-169727. This paper contains the results from the large scale interwell field pilot.

General information concerning the operational field has already been reviewed under the "Single Well Injection Pilot" section. This large field operation will also be conducted on the Snorre field, same as the pilot test. Virtually the same principle as the test pilot will be attempted here, only it is up – scaled. This means that the conditions and experiences gained from the test pilot P – 07 can be implemented here, which was the purpose of the test pilot. It should also be mentioned that several wells are included in this large operation, not only one as the pilot test.

The main objective of this large scale operation is to actually produce more oil than it would have done without the use of this technique, silicate in – depth plugging resulting in diverted injection fluids. Also it must be economically responsible in the long run for it to be thinkable to perform this large scale operation. So before actual field operation work can be conducted, steps like interpretations of simulations results must be completed. These results will describe the sub surface in order to evaluate the economic potential, designing the volumes and the timing for the actual operation.

The economic potential is based on whether all expenses ultimately are lower than the financial gain in the long run. Therefore, it is important to consider all types of costs, not only the major costs. This could for instance be performing the field operations in the summer time, instead of performing it in the wintertime. In the wintertime, the weather will be more extreme, which can lead to more wear and tear on equipment and postponement of the project. Another argument to perform this operation in the summer is that problems like premature development of silicate will be a smaller risk. Due to greater probability of pump stop in the winter. At pump stop, the temperature in the reservoir will start to increase. This is why both the pilot test and the large scale operations were conducted in the summertime.

Before the operational part is demonstrated, it will initially be explained a little more in detail about the area and the wells that are involved. Then the next step is interpretation of the simulations, and from there on to the actual operational implementation.

1.4.1 The Large Scale Pilot Area

The pilot area targets everything that is in some way affected by the silicate in – depth placement. Which means for instance conducting simulations on the entire Snorre field for this operation is completely unnecessary, since only a specific area is affected (often called a segment), see Figure 35. The area is located in the segment containing producer P – 15 and injector E – 4 H. The segment did originally also contain the producer P – 11, but it was only open for about a year (1995-1996). The producer P – 15 and the injector E – 4 H both started up in August 2002. The STOIIP (stock tank oil initially in place) in the drained area of the model (main fault segment) is about 7.6 MSm^3. STOIIP is the volume oil in a reservoir prior to production (Schlumberger glossary 1998). The water breakthrough came after about twelve months of injection. The silicate injection in injector E – 4 H started July 2013, approximately 9.4 MSm^3 of water have been injected so far. This has resulted in a production of 3.1 MSm^3 oil and 5.9 MSm^3 water.

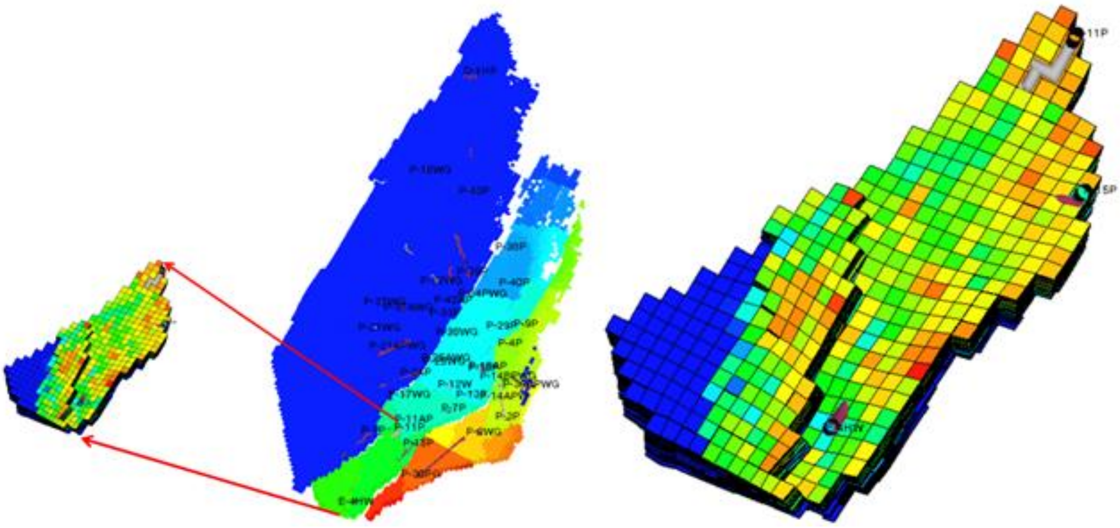

Figure 35; Full-field model and the segment model. Left: segment model location in the full-field model: Right: segment in more details including the water injection well E-4 H and the production well P-15.

Figure 35, shows the simulated segment geomodel in 3D (3 dimensions). The actual 3D model is usually made by a petroleum geologist. This geomodel is then passed on to a reservoir engineer who performs the simulations. In Figure 35 right side, the segment also includes the production well P – 11 that was only open for a short period of time, this well is seen at the top right corner. The other production well P – 15 is located a little south east from production well P – 11. The injection well can be found far south compared to the two production wells.

The stratigraphic column for the pilot area consists of the Statfjord Grp. The upper part of the group has a high net to gross and well connected channel sands. Pebbly sands with very high permeability is found in this part, and is most likely a location for a potential thief zone between E – 4 H and P – 15. The thief zone discussed here is another word for the highway/shortcut the injected water travels through to get to the producer. This is what the silicate should try to plug. The lower part of the Statfjord Grp has a lower net to gross and more isolated sand bodies. Net to gross (NTG) is the fraction of reservoir volume occupied by hydrocarbon bearing rocks (A. Maharaja 2007). The injection well E – 4 H and the production well P – 15 in the Statfjord Grp was correlated by logs, in order to link the matching layers to each other.

1.4.2 The Large Scale Reservoir Simulation Model

As the experiments and the test pilot did confirm, the main initiator for the sodium silicate gelation is the temperature. There are however other factors affecting the gelation rate and the adsorption like for instance pH and the presence of divalent cations, which are not considered necessary to be included in the large scale simulations. Therefore, to predict the IOR effect of the injected sodium silicate, it was chosen to simulate temperature, oil saturation, water saturation, and silicate concentration. The simulation setup, the modelling of the water diversion and the simulation results estimating the IOR potential for this interwell pilot will be outlined.

The same simulation program Eclipse 100 was used in both the large scale interwell pilot and the test pilot. Since in Statoil Eclipse 100 is considered to be the default simulation program, but also because there are several partners included in this process, and a commercial simulator like Eclipse is desirable. Additionally, the resulting simulation model had simulation times that did not make it feasible for usage in more advanced simulators specialized for EOR processes. Therefore, this conventional reservoir simulator was used.

As previously explained under "The Pilot Area", the area of interest is everything the silicate process effects. So, the small segment seen on the right side in Figure 35, is considered to be more or less isolated from the rest, meaning that the flow in/out of the segment can be neglected.

When the silicate completely plugs an area, the following injected fluid will then be diverted in several directions, not only horizontally but also vertically. This means that the simulations need to get a necessary vertical resolution to accommodate this behaviour. This is done by assuring that the vertical grid resolution of the geomodel is sufficient. The aim of gridding blocks in reservoir simulation is to turn the geological model of the field into a discrete system on which the fluid flow equations can be solved. A simple 3D grid is the regular Cartesian grid (Figure 36). Cells in such a grid may be simply identified using their "i,j,k" index values. Each of the grid elements will be assigned a single permeability or porosity value for instance. In this case, it is possible to obtain the transmissibility value, meaning fluid flow from one block to the next (Young, L.C. 1999).

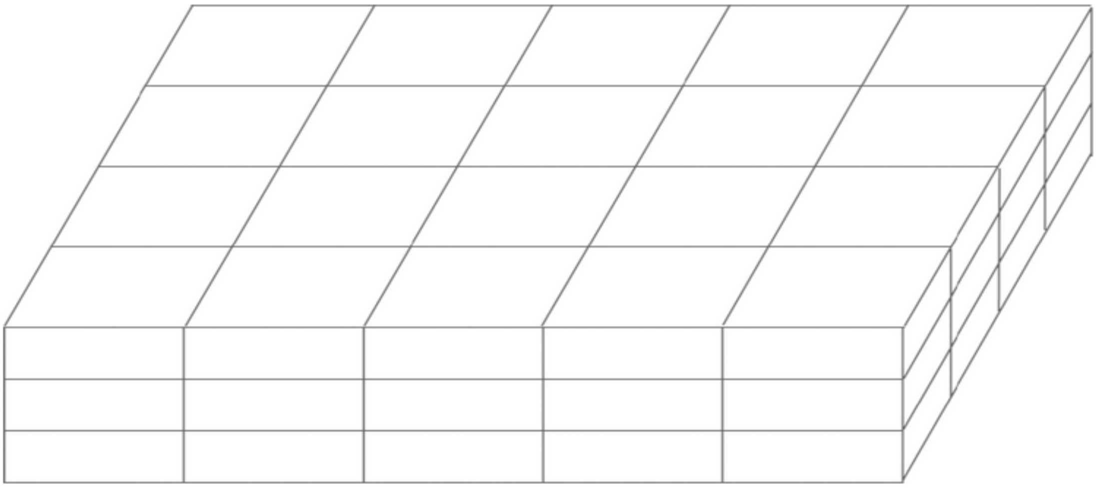

Figure 36; Grid block illustration

The smaller the grid blocks are (in volume or area, depending on if it is 3D or 2D) the higher resolution of the reservoir will be. In theory, one would want the maximum resolution possible, but this requires tremendously high computer power, and the simulation process is very time consuming. There are different methods to keep both a decent stable resolution and avoiding too long simulations, for instance using IMPES (implicit pressure, explicit saturations). To avoid going too much into the details concerning this, the reason the simulation process is faster with this method is because of the explicit part (Doleschall, S. 1985).

Initial simulation tests indicated the need for refining the grid laterally (horizontally) to reduce the numerical dispersion in both the silicate flow simulations and the temperature simulation. The grid was refined laterally by a factor of three in both the x – and the y – direction, leading to even longer simulation times. However, it was also kept a model with the coarse lateral resolution that enabled quick and rough simulation iterations during the work process. With coarse resolution the grid blocks are larger compared to the opposite fine grid resolution model, resulting in lower correctness, but much quicker simulation runs. The issue with coarse grid is that you may miss vital information about the reservoir, like for instance the presence of faults. The rock properties were not re – modelled on the refined grid, but simply mapped from the coarse full – field model.

Concerning the temperature simulations, in order to allow heat exchange throughout the chosen segment (see Figure 35), temperature simulations also includes grid cells that were inactive for flow simulation; like shales, small cells and etc. Basically this means activating all grid cells, and setting permeability to zero for the relevant grid cells. In addition, 10 thicker grid layers were added for the shale above and below the reservoir. This allows the temperature to exchange with the surroundings. These additional grid layers were chosen to have a thickness of 140 meters, both above and below the reservoir.

The final simulation model that were used for history matching had a resolution of about 30 meters in the *x* and *y* direction (horizontal), and with 1 meter in the *z* direction (vertical). The model consists of 140 layers in the reservoir and the 10 extra layers for the shale under and above the reservoir. The total number of active cells for the temperature simulation is approximately 500 000, and for the flow simulations are approximately 300 000.

As discussed above, it was important to establish the resulting temperature gradient from the injection of cold sea water into the higher temperature reservoir since May 2002. The input parameters for the temperature modelling are the rock thermal conductivity and the specific heat capacities of both rock and fluids present.

1.4.3 The Large Scale History Matching

The main objective of history matching is improving and validating a reservoir model until it closely reproduces the historic behavior of a reservoir. The historical data such as production, pressures and etc. are matched as closely as possible with the created simulated model. The accuracy of the history matching depends on the quality of the reservoir model and the quality and quantity of the data available (production, pressure and etc.). Once a model has been history matched, it can be used to simulate future reservoir behavior with a higher degree of confidence, particularly if the adjustments are constrained by known geological properties in the reservoir (Schlumberger glossary 1998). It can also be used to identify unusual operating conditions, like for instance faults and fractures, and how this again affects the fluid flow in the reservoir. Without a reasonable trustworthy history matching, this operation would most likely be unsuccessful.

The simulated model for this large scale interwell field pilot were history matched using bottom – hole pressures, historical oil and water production, tracer data, produced seawater fraction and temperature in the producer.

It was not possible to match the actual pressure from the segment area with the geological realization considered to be most representative for the entire field, so it were then selected for the full field model. However, geological considerations supported the probability for a more sand rich geology for this part of the field. So, it were then decided a more sand rich representation resulting in a better pressure match. Additionally, the relative permeability was updated to a more optimistic case to match the breakthrough time of the formation water.

A tracer was injected in the E – 4 H well February 28th, 2008. After 6 – 8 months the tracer broke through at producer P – 15, Figure 37. The recorded breakthrough was October 15th, 2008 after about 600 000 Sm^3 of water injected.

Both the tracer breakthrough time and the measured seawater production seen in Figure 37, indicated that a thief zone had to be introduced in the model. In addition, Production Logging Tool (PLT) results and geological considerations indicated that the thief zone was located in the zone SN 11.3, which is in the upper part of the Statfjord Grp. Since PLT provides a good average permeability of an entire zone, it is also useful in order to locate barriers and fluid contacts. The depositional environment for the zone is shallow marine with wider and more continuous good-quality sandstone belts than for the zones below. The zone above is also of lower quality for the wells in this area. Two different thief zone geometries were tested, one narrow and one wide. They were described by channels with width of about 250 meters and 750 meters, respectively. Moreover, both thief zones were described by a thickness of about 5 meters. The pore volume for both the narrow and the wide thief – zone was approximately 650 000 Rm^3. The bulk volume of the wide thief zone is higher, but the pore volume had to be reduced to get a history match in this case, thus resulting in a similar pore volume as for the narrow thief zone. The thief zones can be seen as the red areas in Figure 38.

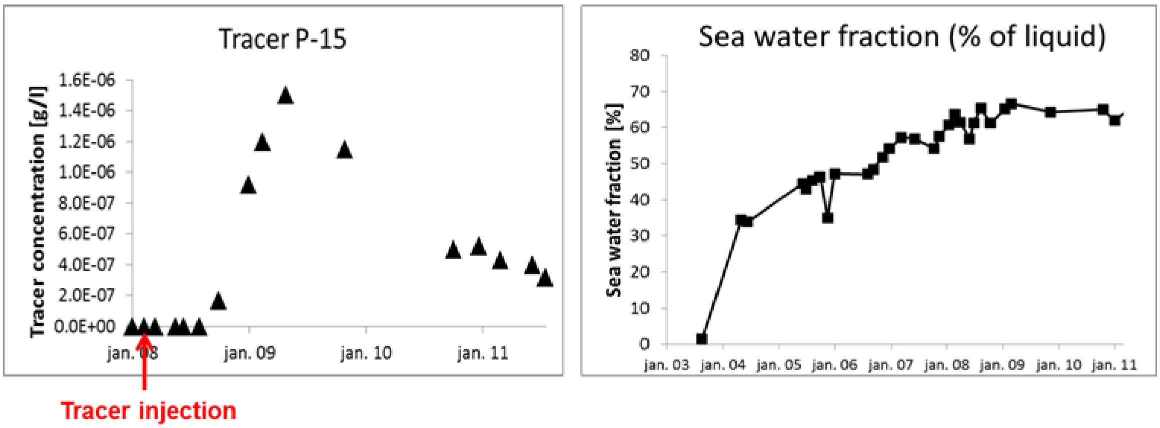

Figure 37; Tracer concentration (left) and measured sea water fraction (right) in the production well P-15.

In Figure 37, the tracer was injected in well E – 4 H, located at a distance of about 2 km from the producer, at the end of February 2008. The graph shows a tracer breakthrough time of about 6 – 8 months, which corresponds to about 600 000 Sm³ of water injected. Both the tracer response and the sea water fraction indicated high – flow channels between the injector and the producer.

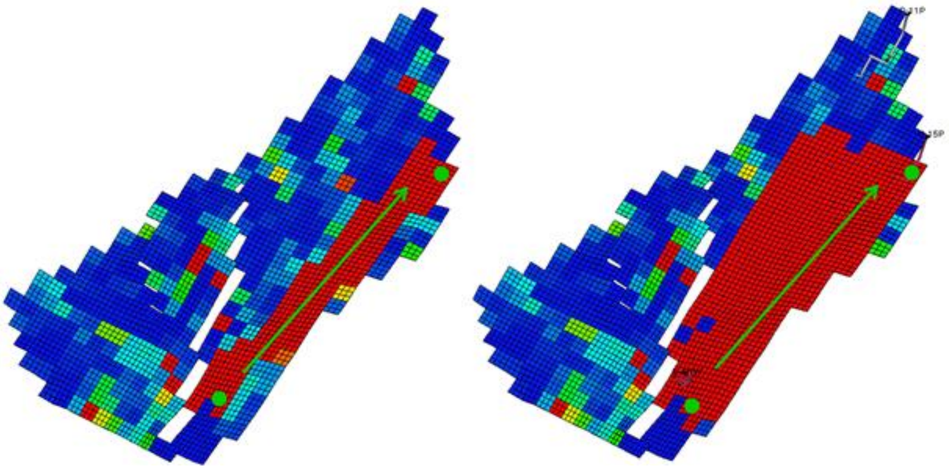

Figure 38; The red continuous areas indicates the narrow (left) and wide (right) thief zones in the simulation model.

In Figure 38, only one layer of the model is displayed in the figure. The green disks indicate the relevant wells, and the green arrow indicates the flow direction.

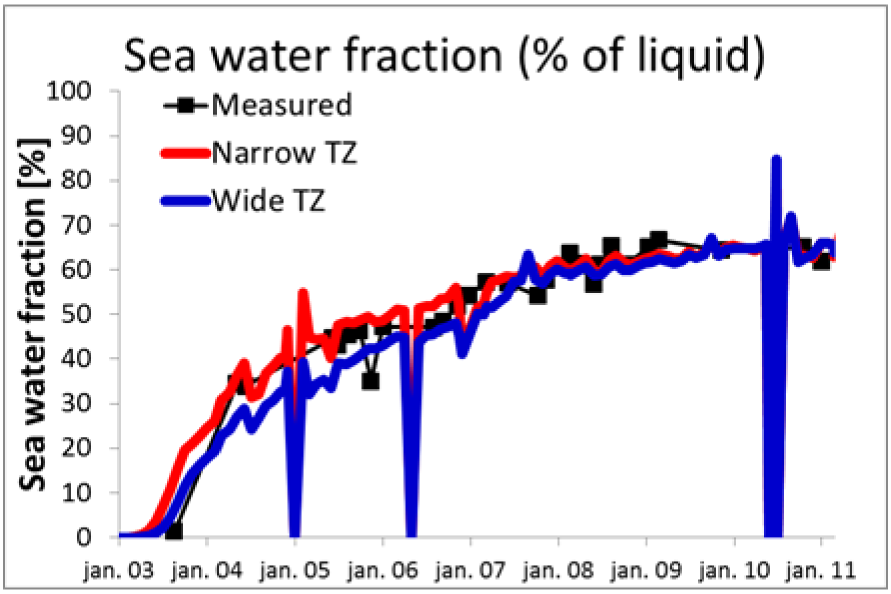

Figure 39; Historical data and history match of narrow and wide thief zone for sea water fraction as percentage of liquid.

A close history match to the cumulative oil production was obtained. The pressure, oil rate and water cut were matched quite well for both thief zone geometries. The water breakthrough is somewhat earlier in both cases, but the later development of the water cut matches well. The simulated sea water cut was tracked by a tracer on the injected water. The match of the sea water cut for both narrow and wide thief zone model can be seen in Figure 39. Both cases match the seawater cut well.

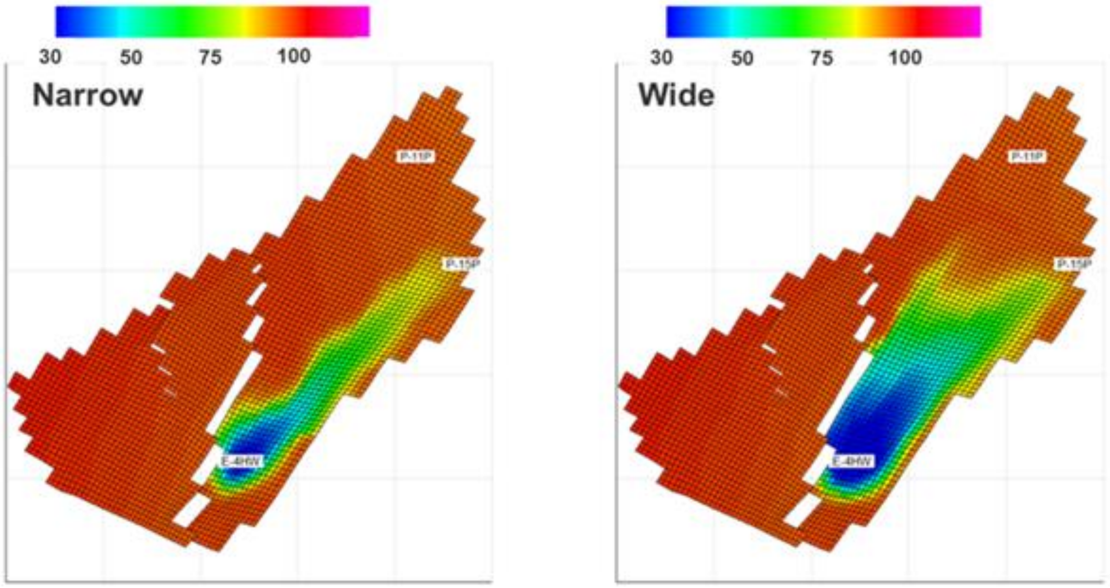

Figure 40; Simulated temperature in July 2013 for the narrow (left) and wide (right) thief zone models. The temperature front has propagated a bit further for the narrow thief zone.

Temperature is measured in the producer P – 15, where the initial temperature is still observed. However, the simulations gave a small temperature decrease in P – 15 at the end of the history; the narrow thief-zone model resulted in lower temperatures. Figure 40, shows the temperature profile for the narrow (left) and the wide (right) thief zone geometries at the time of silicate injection (July 2013).

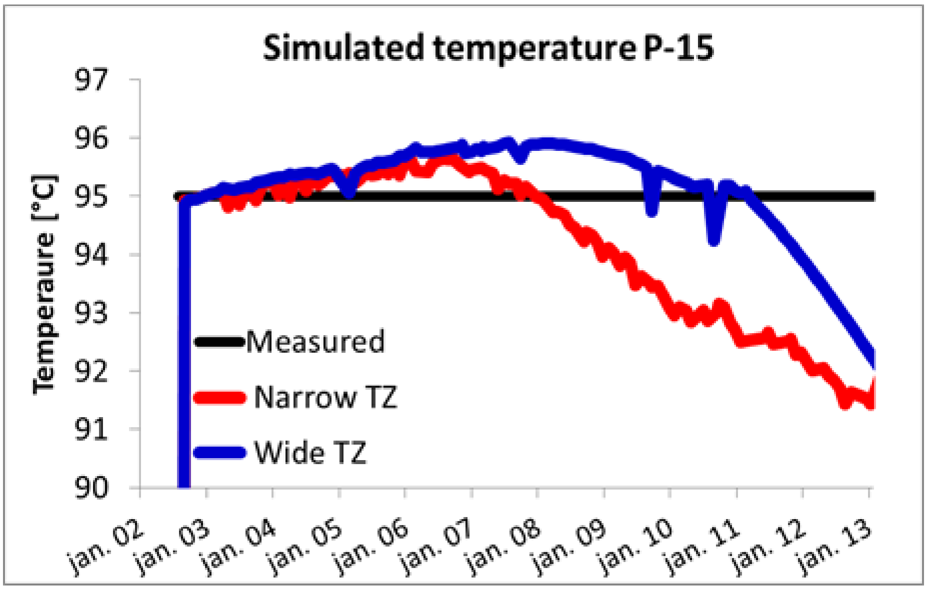

Figure 41; Simulated and measured temperature in P-15 for narrow and wide thief zone models.

Figure 41, shows the simulated temperature in the producer P – 15. No temperature decrease has been observed in the producer. This was difficult to match in the simulation model. There is a slight decrease in the production temperature of about 3°C for both cases. The temperature was matched mainly by tuning the rock thermal conductivity, as changing any other parameters would ruin the pressure and production match. The case with narrow thief zone needed a more extreme value for the rock thermal conductivity than the wide thief zone. Since the geometry of the thief zone is unknown, allows either cases, or something in between to be possible. Reasonably good history matching were obtained for both cases. However, it was more problematic to match the seawater cut using the wide thief zone and more difficult to match the temperature using the narrow thief zone.

1.4.4 The Large Scale Water Diversion Modelling

As previously mentioned in the introduction, it exists other in – depth plugging methods which is based on viscosity increase. Especially the BrightWater method, since the permeability reduction process resembles a lot. The chemistry and process behind BrightWater has been thoroughly researched. It took them about 10 years before it was considered fully developed. However, the method is quite expensive and the ingredients are admittedly hard to come by, so this creates room for better solutions. More on this work can be seen in Garmeh et al. (2011) and Galli et al. (2012). In their work they used advanced reservoir simulators with specialized functionalities. But, the simulation model used for sodium silicate did not use specialized functionalities for temperature triggered water diversion, at the time the simulations were conducted. Since only the commercial program Eclipse were used.

Due to these restrictions, a creative solution for the silicate viscosity increase had to be invented. That is why silicate was chosen to be treated as a water tracer, since there was no need for a water viscosity modification since diluted sodium silicate has water – like viscosity prior to gelation. Due to the seawater cooldown, there is a large temperature gradient between the injector and producer. In order to accommodate this, an adequate good approximation was to model the flow restriction based on a preselected temperature threshold. The flow restriction was modelled by a script filtering on silicate concentration and temperature, for instance if the silicate concentration were above value “x” and the temperature higher than a preselected value “y”, then the block permeability is reduced by a certain factor estimated by the laboratory experiments. The script then automatically continues the simulation with the updated permeability field and steps into the next time interval. At the new time interval, a new filtration occurs and the permeability field is updated again, if all criterias are met. The frequency of filtering and permeability updates were chosen to be checked weekly for the first year after the start of the silicate injection, and then monthly for the next 1.5 years.

Different gelation triggering values were used in the script for temperature and silicate concentration, due to the uncertainties and the potential for optimizing those parameters. However, as a base case, 70°C for the temperature and 1 wt% for silicate concentration were selected. For the permeability reduction factor a value of 10,000 was used for the base case; i.e. this will essentially cause blocking of the grid block and loss of the silicate located inside the grid block.

Both narrow and wide thief zone models were studied. The behaviour was quite similar, as the pore volume of the thief zone was almost the same for both cases. As the production data were more easily matched for the narrow thief zone, this model was chosen as the base case. The results in the following section will therefore focus mainly on the narrow thief zone model.

The base case used had:

- The narrow thief zone,
- Sodium silicate concentration of 4 wt%,
- 2 months injection time (~240 000 Sm^3 of sodium silicate solution),
- Activation temperature of 70°C,
- Activation concentration of 1 wt% (silicate) and
- Permeability reduction factor of 10,000.

To study the uncertainties and robustness of the water diversion modelling, and for potential optimization of the key parameters influencing the process, it was performed sensitivities around the base case.

1.4.5 The Large Scale Simulation Results

The simulated pathway of the sodium silicate slug for the base case is illustrated in Figure 42. The white area in all three pictures illustrates silicate concentrations above initiate value of 1 wt%. The base silicate of 1 wt% is not enough to actually plug, but helps initiate the gelation process in – depth. In Figure 42, all three pictures illustrates three different stages (times) of the silicate with concentrations above 1 wt%. The first (to the left) is at 2 months, the second (middle) is at 5 months and the third shows the placement of the higher concentrated plugged silicate gel. If the third picture is seen together with Figure 40 (Narrow thief zone), then the estimated temperature would be around 70°C.

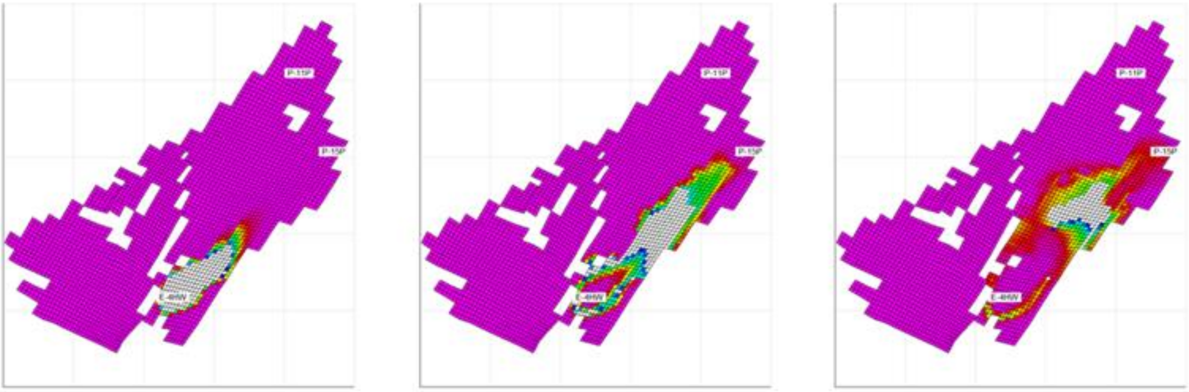

Figure 42; Simulated pathway of the silicate slug

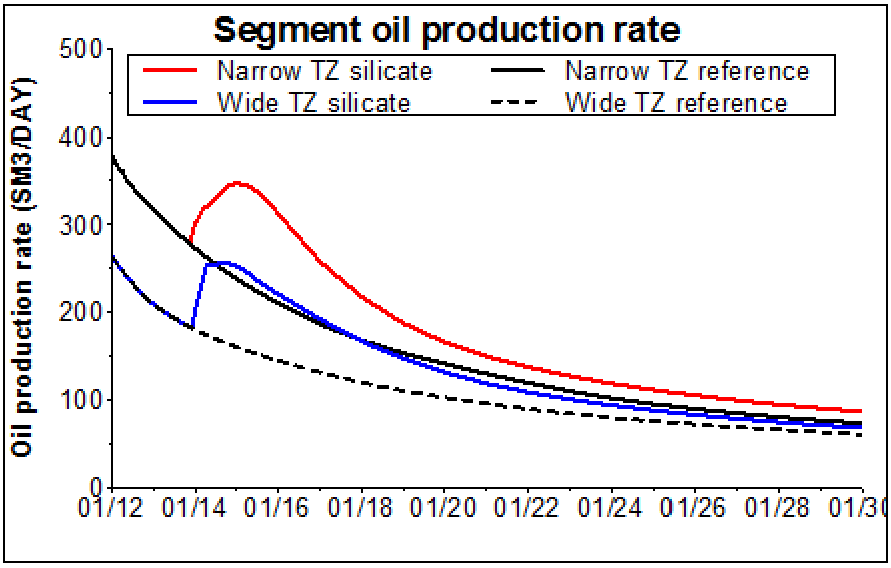

Figure 43; IOR – volumes for the narrow and the wide thief zone. The reference cases start at different oil rates as there are small differences in the history match.

Figure 43, shows the oil production rate versus January every other year both for narrow and wide thief zones. The curves with colour (red and blue) illustrate injections with silicate gel, and curves without colour illustrate injections without silicate gel (reference cases). In both cases, the oil production rate will be higher with silicate gel. The increase is about 70 Sm³/d, when compared to the time before the silicate response and about 120 Sm³/d compared to the simulated production prognosis. The estimated IOR – volume from the silicate pilot is 207 000 Sm³ in 2030. Different maps showed that the silicate gel improved the formation sweep in both horizontal and vertical directions.

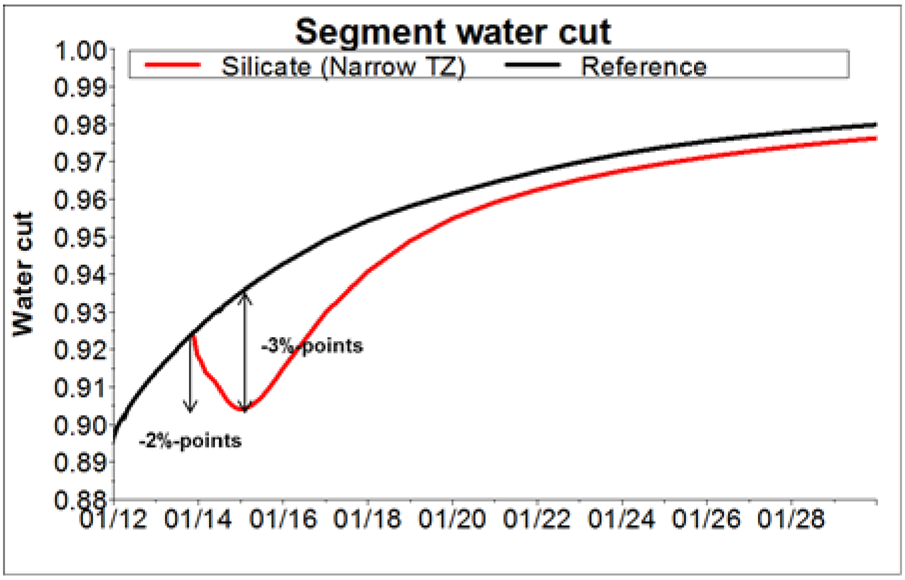

Figure 44; Water cut for reference case and silicate base case.

Figure 44, demonstrates only water cut for the narrow thief zone, with and without silicate gel. The decrease in water cut is about 2% - points, if compared to the time before the silicate gel effect. And 3% - points compared to the simulated production prediction. The drop in sea water fraction of total liquid production was estimated to be about 7% - points.

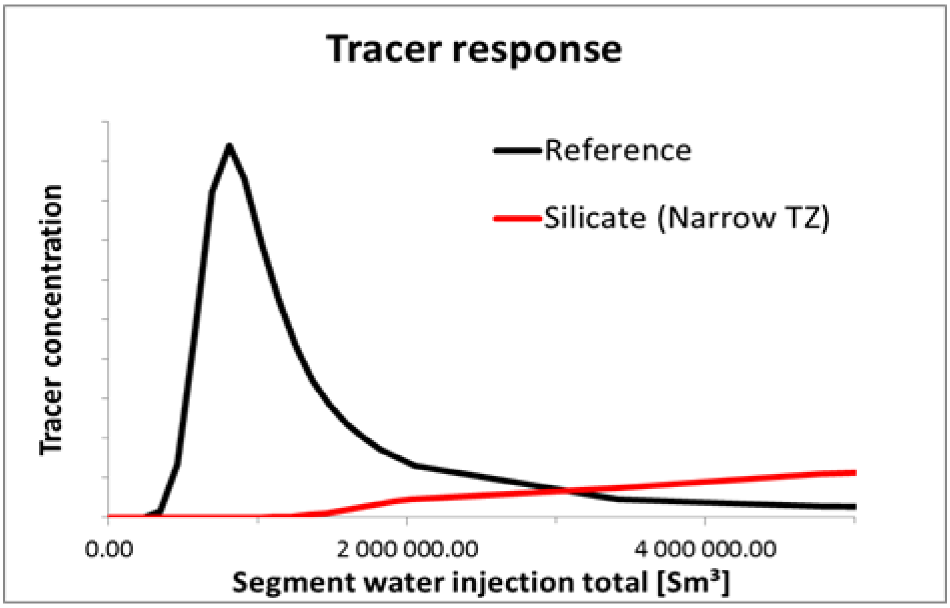

Figure 45; Tracer response for the reference together with the silicate case.

Tracers are injected at different dates, to find out how much impact silicate will provide. Instead of using breakthrough time for the tracers, volume is used. Since injection rate can vary a lot for several reasons, injected volume will then give a more accurate picture. A tracer has been injected April 2002, and another tracer will be injected after the silicate is supposed to have gelled. The difference in amount of injected volume is measured when it arrives at the producer. If a tracer arrives later than expected, then it is probably because it has been diverted into new areas. In the model a tracer was injected one year after the start of silicate injection, for both the reference and the silicate case. The reference case is without silicate. The model shows a large difference between these two tracers. In the silicate case around 1 000 000 Sm^3 additional water was injected at the time of tracer breakthrough, if compared to the reference case, as can be seen in Figure 45. The tracer concentration is also much lower for the silicate case, caused by the diversion of the fluid.

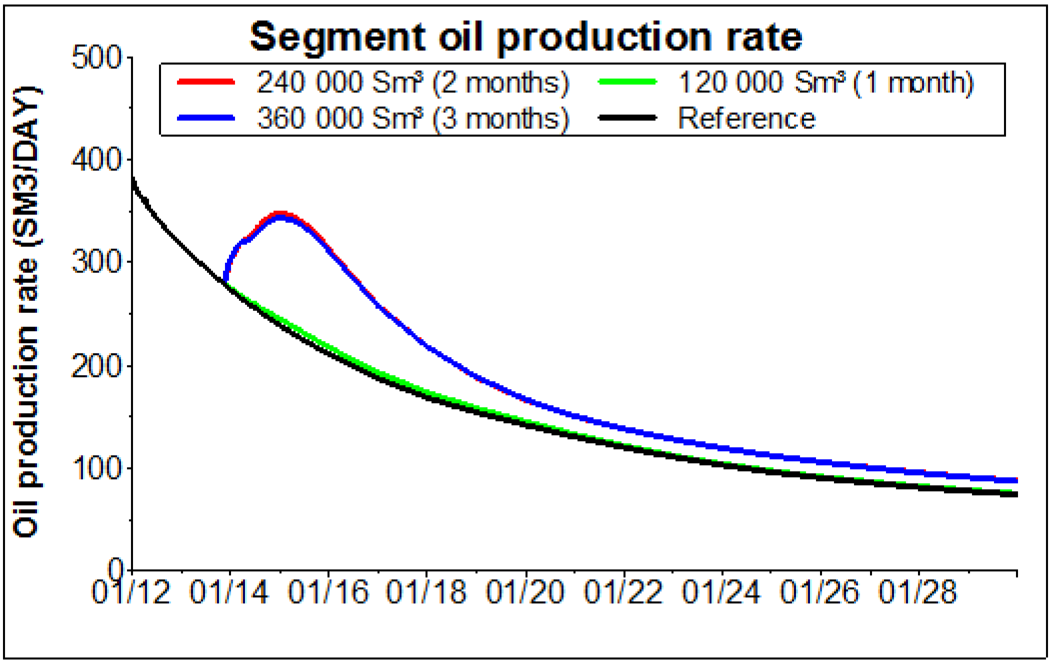

Figure 46; IOR-volume from sensitivity of slug size 1-3 months.

Different kinds of sensitivities were tested in order to examine the silicate slug size, activation concentration, temperature, thief zone geometry, silicate induced permeability reduction, silicate injection concentration and the effect of precipitation of salts behind the front.

The base case silicate solution slug contains 4 wt% silicate injected for a periode of two months resulting in a slug size of about 240 000 Sm^3. Sensitivities with shorter and longer injection periods were tested out. In Figure 46, the IOR-volumes for 120 000 Sm^3, 240 000 Sm^3 and 360 000 Sm^3 of injection can be seen. Injecting only half the silicate volume gives a dramatic reduction in the IOR-volume to 16 000 Sm^3. Increasing the slug size with 50% results in basically the same IOR-volume as the base case. A further investigation of the effect of several slug sizes ranging between 120 000 and 240 000 Sm^3 confirmed that the base case silicate volume gave the largest IOR-volume.

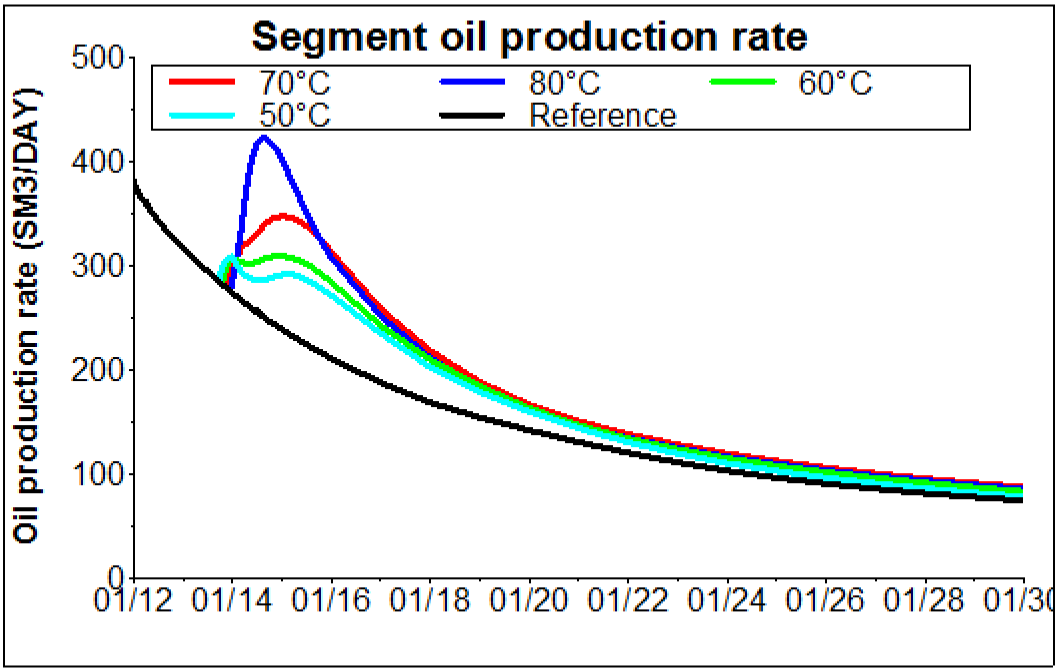

Figure 47; IOR-volume from sensitivity of activation temperature.

The activation temperature can be chosen by designing the silicate slug. In the base case, an activation temperature of 70°C and an activation silicate concentration of 1 wt% were assumed. Tests with activation temperatures of 50°C, 60°C and 80°C were performed. A test with a lower activation concentration of 0.5% was also carried out.

The IOR-volumes from the sensitivity on activation temperature can be seen in Figure 47. An activation temperature of 80°C, giving a restriction closer to the producer, causes a small increase in the IOR-volume to 213 000 Sm³. Activation temperatures of 60°C and 50°C, meaning a restriction closer to the injector, gave a decrease in the IOR – volume to 154 000 Sm³ and 118 000 Sm³, respectively. The simulation results indicate that a slow system, gelling closer to the producer, will give the best IOR – effect.

The narrow thief zone was chosen for the base case, but also the wide thief zone was studied. The IOR-volume is slightly lower for the wide thief zone, as seen in Figure 43. The IOR – volume from the wide thief zone is approximately 12% lower than the base case.

Lab experiments show permeability reductions in the range of 1 000 and 1 000 000. A low case with permeability reduction of 1 000 and a high case of permeability reduction down to zero were tested. The base case IOR – volume is 207 000 Sm³. A permeability reduction close to zero, gives a very small increase of the IOR – volume to 209 000 Sm³. The low case with a permeability reduction of 1 000 has a reduced IOR – volume of 186 000 Sm³.

The base case injection silicate concentration was 4 wt%. Injection of 6 wt% and 8 wt% silicate were also examined. The IOR – volumes are very similar for all these cases. The onset of gelation was in the base case at silicate concentration of 1 wt%. Changing the activation concentration to 0.5 wt% had a very small impact on the results.

The effect of silicate precipitation because of mixing with seawater was investigated. A twenty-fold permeability reduction in the reservoir blocks from which the silicate slug has passed through, was therefore tested. The permeability near the injector has not been changed. Precipitation close to the injector is unlikely because of the pre – flush with desalinated water. The effect on the IOR – volume was very small. Precipitation will also involve loss of the injected chemical. This is not modelled, but the sensitivity with respect to the amount of silicate needed for plugging is tested via other sensitivities mentioned above.

The IOR-volume for the base case was 207 000 Sm³. After examining the sensitivities the base case result was kept as the expected volume. Based on uncertainties and the simulated sensitivities a high and low volume was also estimated.

1.4.6 The Large Scale Simulation Summary

It was possible to show a substantial IOR-effect from silicate gel based water diversion deep in the formation using flow simulations. Post gelation injected water is diverted both horizontally and vertically. The simulations indicate best results for a silicate volume close to 240 000 Sm^3 and a slow system gelling close to the producer. There are substantial uncertainties in the modelling, history match and the actual silicate diversion. However, the sensitivities performed indicated robustness. As long as a sufficient amount of silicate was injected, a significant increase in oil production was obtained, and no flow obstructions were observed in or around the wells.

By knowing the temperature profile, as indicated by Figure 43, the activation energy and bulk gelation times, the actual gelation time for the injected solution can be estimated. At an injection rate of 4 000 Sm^3/d the time from injection to onset of gel will be approximately 4 months for the narrow thief zone and 5 months for the wide thief zone. If the effective injection rate is lower, i.e. 2 800 Sm^3/d, the gelation time is prolonged to 6 and 7 months, respectively. For all these combinations, the actual front temperature is approximately 70°C, which is similar to the simulated base case.

1.4.7 The Large Scale Field Operation

Performing such a large scale operation requires high injection rate, to avoid early mobility reduction. See experiments “The influence the injection rate has on gelation time”. Also very large volumes will be injected, the total liquid volume of 400 000 Sm^3 with an injection rate and pumping pressure all the way up to 4 000 Sm^3/day and 345 Bar, respectively. Sodium silicate is incompatible with divalent cations (such as Mg^{2+} and Ca^{2+}), as proven under “Cation Exchange Experiments”, in both the formation water and the previously injected seawater. To eliminate premature gelation when it comes to salinity in all injected fluids, a lot of the salinity is removed from the seawater on the vessel. For this to work, a fresh water storage on the vessel up to 4 000 Sm^3/day was used.

In order to perform such an extensive pilot injection a new concept of injection large volumes was developed. A shuttle tanker was modified and connected directly to a water injection well at a subsea template, and the injection was performed from temporary installed high pressure pumps on the vessel. Just to clarify, this shuttle tanker is not the same that were used for the test pilot operation, which was a modified supply vessel. Because that specific supply vessel would have been much too small for this operation. The operational concept of performing well injection from a shuttle tanker was proved to be reliable and robust.

This 35 000 ton shuttle tanker was modified and reclassified as a stimulation vessel to perform the comprehensive pumping operation. In order for this modified shuttle tanker to allow a higher number of personnel and the possibility of replacing personnel onboard additional accommodation modules, larger lifeboats and a helicopter deck were installed. A mezzanine deck was built to allow for installation of temporary equipment. For the desalination of the seawater a reverse osmosis plant and power generators for the RO – plant were temporarily installed, acid tanks, mixing units for dilution of concentrated fluids (KCl brine for pre – and post – slug, sodium silicate and HCl acid for pH adjustment of the sodium silicate solution) with desalinated seawater and for adding diluted HCl at a defined mixing ratio while injecting sodium silicate into the well. Temporarily installed high pressure pumps and the mixing equipment were remotely operated from a control cabin on the deck to ensure high HSE standards.

A 3 inch high pressure hose was pre – installed with an IMR vessel and anchored with a riser anchor to the seabed and positioned at the seabed (the water depth were 290 meters) for pick – up from the shuttle tanker. The shuttle tanker was connected to the subsea injection well with a 3 inch hose positioned with a Lazy-S configuration and connected with an emergency release device to the bow loading system of the vessel, see Figure 48. The shuttle tanker was equipped with a dynamic positioning system to keep the vessel within a predefined sector area with the vessel engines without anchoring. The operation limitations for the vessel were 45 knot wind and significant wave height of 4.5 meters to ensure operating within max allowed 7 ton dynamic force on the 3 inch hose. The vessel was disconnected four times due to weather limitations during the 5 months of operation, and the vessel went to shore for up to 6 days to perform repairs and replacement on pumps and the reverse osmosis plant.

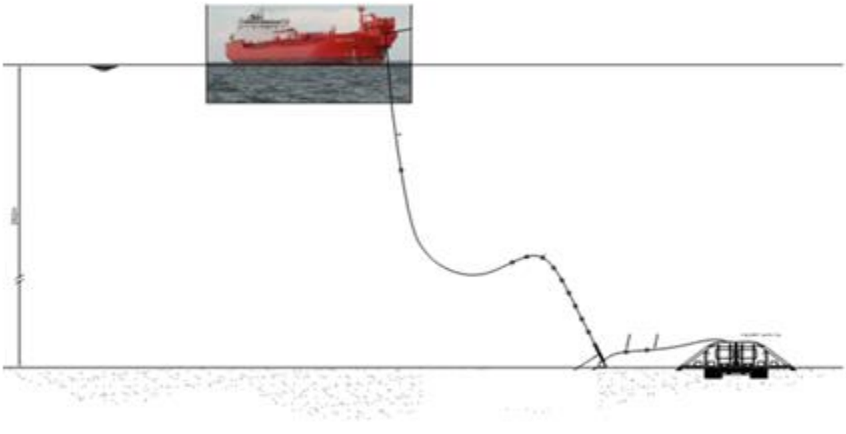

Figure 48; Connection of shuttle tanker to subsea water injection well.

The injection operation was performed during the summer and autumn 2013:

- 113 500 m^3 KCl preslug – 1.5 month duration
- 240 000 m^3 sodium silicate – 3.0 months duration
- 49 000 m^3 KCl postslug – 0.5 months duration

All the injected fluids were filtered through a 10 micron absolute filter after dilution and mixing. This is done in order to remove large particles to maintain the desired injection rate.

The 14 separate tanks of the vessel were equipped with separate pumps in each tank, and the lines and manifold outline was adapted to eliminate the risk of fluid contamination. The tanks were dedicated to each type of fluid; diesel fuel (vessel engine, generators and high pressure diesel pumps), desalinated seawater, concentrated and diluted sodium silicate, concentrated KCl brine and diluted KCl brine. The available tank volume on the shuttle tanker allowed for loading approximately 50% of the concentrated sodium silicate volume. The remaining volume of concentrated sodium silicate was transported to Snorre with a sister vessel with similar dynamic positioning system, and transferred to the shuttle tanker by a vessel – to – vessel transfer while performing the continuous sodium silicate injection from the shuttle tanker.

The main challenges during the pumping operation that caused injection downtime and lower injection rate than 4 000 Sm^3/d (see Figure 49), were low regularity of the reverse osmosis plant due to challenges with pre filtration, pumps and e – savers and low regularity of the high pressure injection pumps due high wear of packing from silicate pumping, and hence need for much maintenance. The achieved average injection rate throughout the whole operation was approximately 2 800 Sm^3/d.

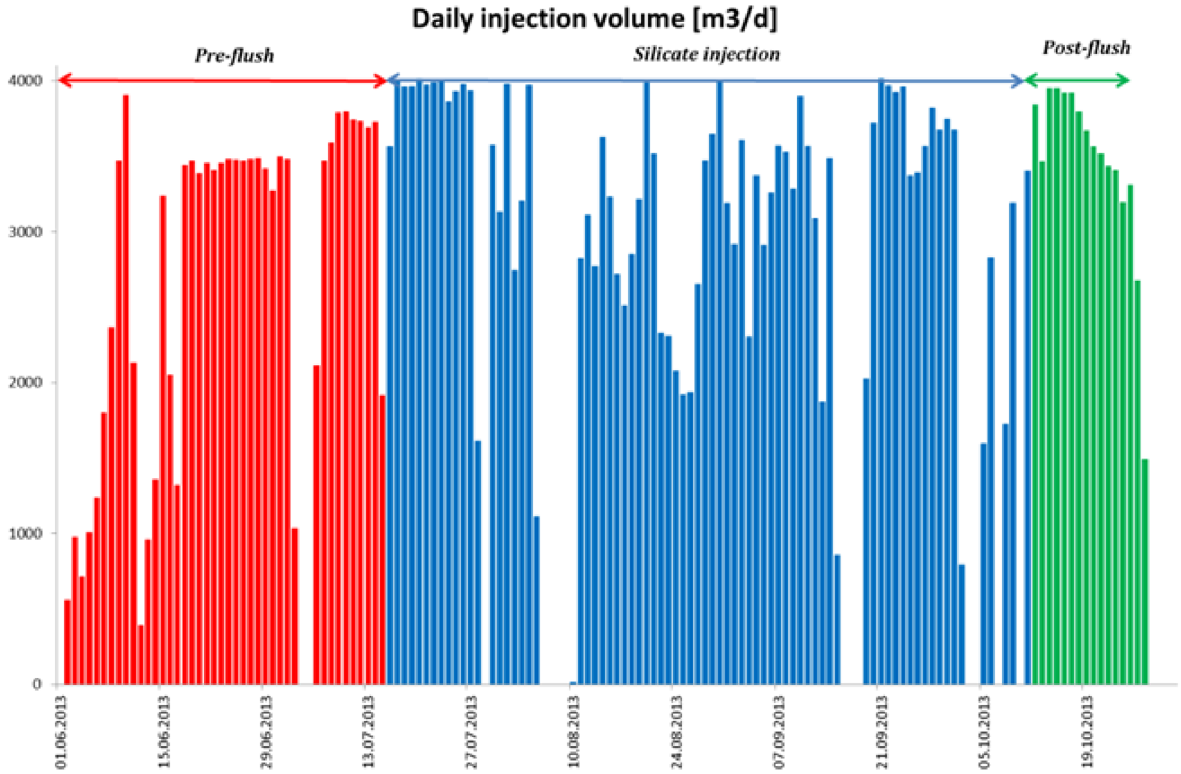

Figure 49; Daily injection rate

The logistic for supplying concentrated sodium silicate included transport with transportation trucks, temporary storage in tank farms, transport on river barges and temporary storage on tank vessel before transfer to the shuttle tankers for the first and second batch respectively. Keeping the sodium silicate clean was crucial, and the quality of the fluid was confirmed by filtration of all concentrated sodium silicate through 5 μm absolute filters on the vessel prior to dilution, and from regular testing of physical properties and gelation time of samples of the sodium silicate as pumped into the well.

1.4.8 The Large Scale Data Acquisition

Data acquisition from the injection well (E – 4 H) like injection rates and pressures is measured. In Figure 50, the wellhead pressure and injection rate during the silicate injection is shown. In order to avoid that the injected fluids migrates out of the desired pathway, especially when it comes to a maximum injection pressure, a limit was set. Another reason is to prevent undesired fracturing of the reservoir. At the end of the injection period, the well had to be choked back as it reached this pressure, and as a result, the rate declined. The injection pressure increased during the whole injection period, and it is believed that this was caused by precipitation of salt in the reservoir.

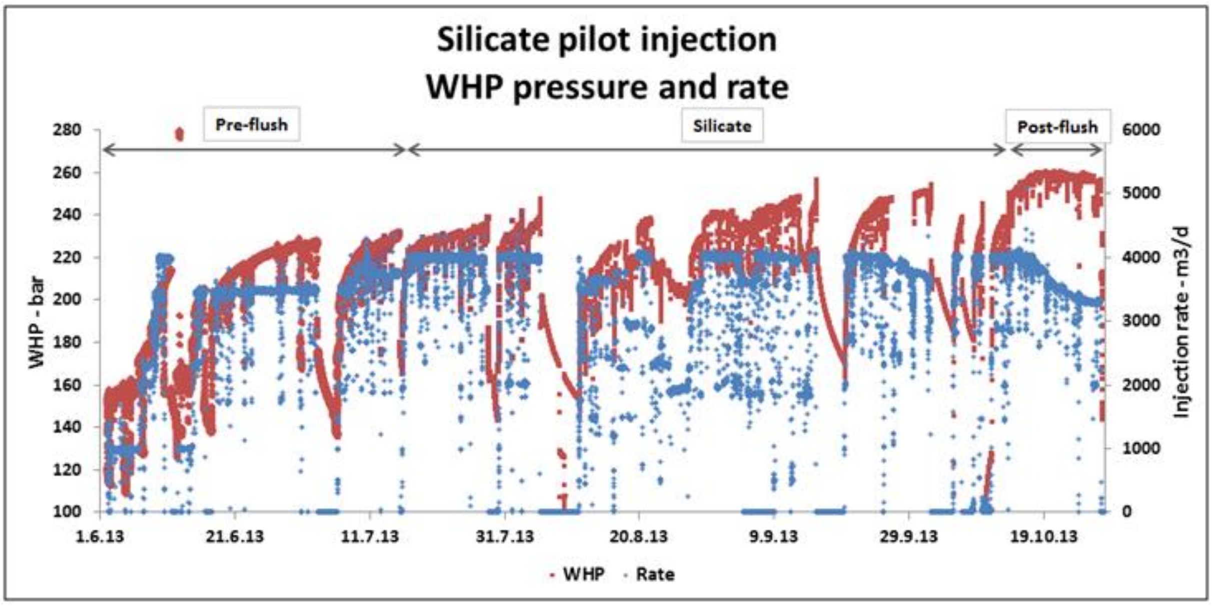

Figure 50; Wellhead pressure (red) and injection rate (blue) during silicate pilot injection.

The production well (P – 15) status has been frequently tested prior to and during the silicate pilot to monitor oil production and water cut, and get a respectable base line to monitor the effect of the silicate injection. The water cut has been very stable in the period prior to the silicate pilot and during the pilot. The simulation model indicated a reduction in water cut of approximately 3%, Figure 44, as a result of the silicate injection as mentioned above. With continued focus on testing, it should be possible to see water cut changes in this range.

The oil production in P – 15 has been on a declining trend during the last year because the voidage in the area has been negative, Figure 51. Based on the results from the simulation model the oil production is expected to increase slightly as a result of the silicate injection, Figure 43, and will be followed up closely. The productivity of P – 15 has been monitored during the injection period by performing multirate tests. But no changes have yet been observed. Multirate tests can be conducted in both oil and gas wells. In these tests, several stabilized flow rates, q_i, are achieved at corresponding stabilized flowing bottomhole pressures, p_{wf}. The simplest analysis considers two different stabilized rates and pressures (Russell, D.G. 1967).

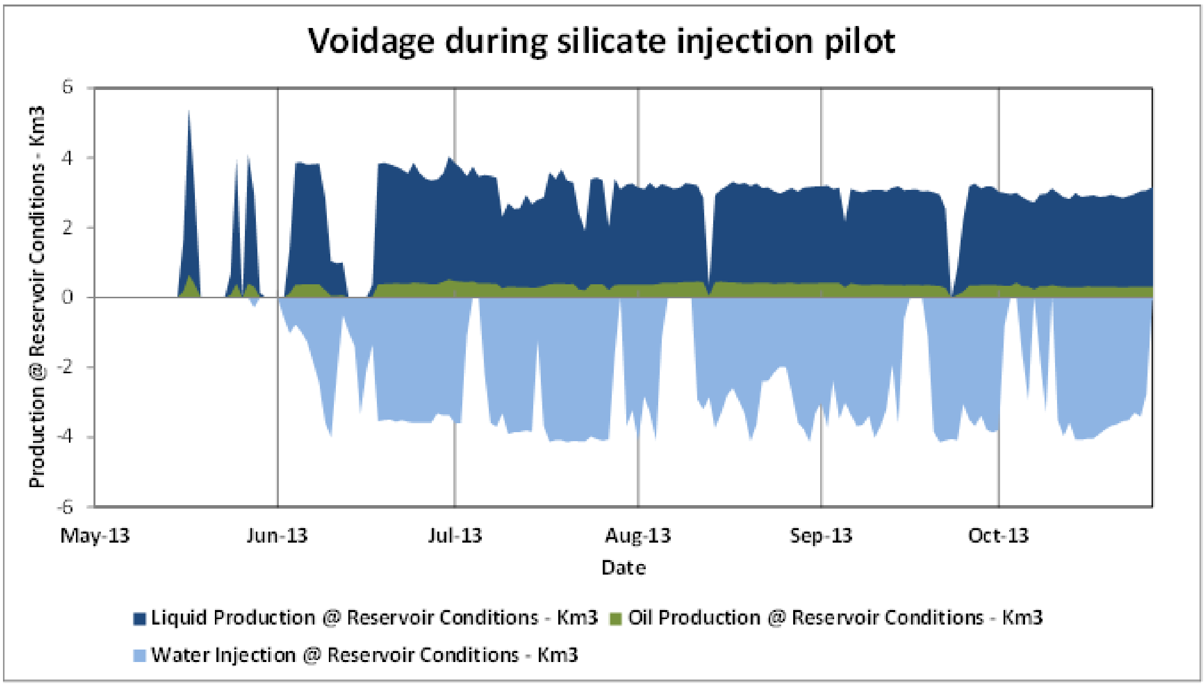

Figure 51; P – 15 and E – 4 H Voidage during silicate injection pilot.

P – 15 has been producing more than E – 4 H has injected during the pilot period, Figure 51. As a result, the voidage in the P – 15, E – 4 H area has been negative, and the reservoir pressure declining. Cumulative voidage in the period was -44 K m^3.

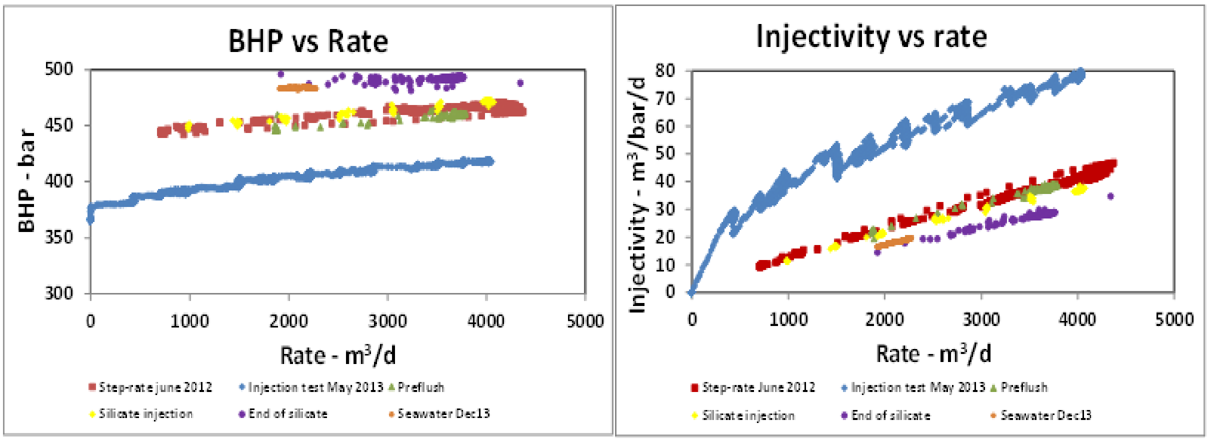

Figure 52; BHP and injectivity vs. rate.

Analysis of E – 4 H injectivity is displayed in Figure 52, it displays the bottom – hole pressure (BHP) and the well injectivity $II = Q/(P_{res} - P_{inj})$ versus water injection rate. These plots can indicate if there are changes in injectivity caused by changes in reservoir parameters where the water is injected, for instance pressure, permeability, injection zones, fracturing and skin.

Early injection data during the pre – flush period were following the same trend as the injection test in May. However, as the reservoir pressure around E – 4 H increased, the trend moved towards the trend observed in June 2012. At the end of the pre – flush period, the injectivity was the same as in June 2012, green points in Figure 52.

Early injectivity data during the silicate injection were also overlaying the trend from June 2012, yellow points (in Figure 52), however, at the end of the injection period, the injection pressure started to increase. As a result, the injectivity decreased, purple points in Figure 53. Since the voidage has been negative in the pilot period, this decrease cannot be caused by higher reservoir pressure. It is, however, believed to be due to precipitation of salt.

Currently, seawater is being injected into E – 4 H, and the injectivity trend is similar to what was observed at the end of the pilot, orange points in Figure 52, the injectivity is stabilized.

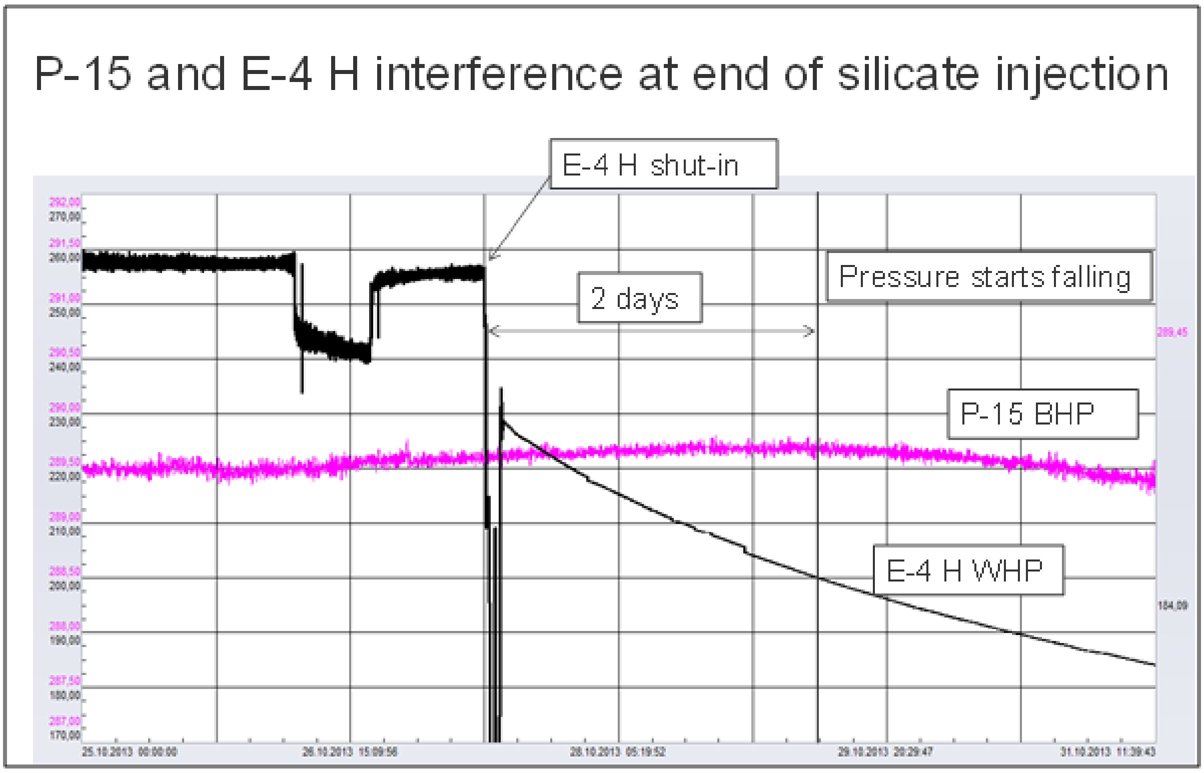

Figure 53; Interference between P – 15 and E – 4 H.

Detection of injected tracers in this segment of the reservoir is assumed to be very important data acquisition with regards to defining the success of the silicate pilot injection. Reservoir simulations show that 1 MSm^3 additional water is injected prior to water breakthrough when silicate is injected in the reservoir. Figure 45, shows the tracer response from the reservoir simulation model.

A tracer injection in E – 4 H was performed in 2008. This tracer was observed in P – 15 after approximately 0.6 MSm^3 had been injected in E – 4 H and 0.6 MSm^3 liquid had been produced in P – 15.

Another tracer was injected in April 2012. This tracer was observed after approximately 0.5 MSm^3 had been injected in E – 4 H and 0.6 MSm^3 liquid had been produced in P – 15. This confirmed the breakthrough time of the tracer injected in 2008.

Several tracers were also injected during the pre – flush and post – flush periods of the silicate pilot, and the plan is to inject a tracer approximately 6 months after the pilot as well, below is the planned tracer program for E – 4 H:

- Tracer injected in start of pre slug – injected to get a pre warning of silicate slug approaching the production well
- Tracer injected at end of pre slug – injected to get a pre warning of silicate slug approaching the production well
- Tracer injected in post-slug – injected to check if response in P – 15 after silicate injection in E – 4 H has changed
- One tracer injection is scheduled about 6 months after the end of the pilot.

Water samples for ion analysis are taken every time P – 15 is tested. Figure 38, right plot, shows the seawater fraction of produced liquid versus time, based on ion analysis. This shows that the percentage sea water production has been quite stable over the last years. It is expected that the level of produced sea water will decrease as a result of a success of the silicate injection pilot. The reservoir simulation model indicates a reduction of produced seawater of 7 – 8 %, Figure 45. If the measured % seawater production is maintained at the current level, the ion analysis can contribute to quantify if the pilot has been successful.

1.4.9 The Large Scale Operational Conclusion

It is important to emphasize that even though the silicate process was completed in the end of year 2013, it is still too early to come up with an absolute conclusion of the field operation. Not enough time has passed and not all tracers have reached the producer yet, in order to conclude whether or not silicate has the anticipated effect on incremental oil production. However, the actual field operation at the Snorre field is considered to be a success, meaning that the silicate was displaced within the expected in – depth position and at this in – depth position plugged the thief zone resulting in diversion of the later injected fluids.

Figure 49 and 50, both show how the injection rate varies. It can also be seen that some of the days illustrates no activity; this can be due to maintenance / replacement of equipment or for instance bad weather. Since these injection operations were conducted in the summertime, the weather had little impact. When there is a pumping stop, the temperature will start to increase rather quickly and the risk of premature gel development is present. But the injection stops did not last long enough to do any significant damage to the process.

The future plan for data acquisitions is to monitor regular acquisitions of P – 15 and E – 4 H, this will continue for the coming years. The plan is to test P – 15 frequently to monitor oil rate, water cut and downhole temperature. Water samples for ion and tracer analysis will be taken every time P – 15 is on the test separator. Tracer will be injected approximately 6 months after the pilot. Transient testing will be performed in both wells as well. This is the latest public information published concerning the large scale operation in the Snorre field.

2 Results

The objective of this thesis was to study different aspects of sodium silicate as an enhanced oil recovery method, following the steps from conducted experiments, simulations then to field operations. By firstly carrying out the test pilot operation in the Snorre field, in order to confirm that it was actually possible to plug about 40 meters from the injector. This was considered to be a success, which made one dare to carry out a much larger field operation (Large Scale Interwell Field Pilot). The main objective of the large scale operation is increasing the oil recovery, using sodium silicate. It is too early to conclude that it was worth the effort, this will be more discussed under discussion and conclusion. But what can be said is that the practical work (the operational part) went quite well, except for some later reported near well precipitations (quote K. Skrettingland). After having gone through these steps, it is definitely confirmed that sodium silicate gel is able to completely plug in – depth thief zones.

Regardless of how much the silicate method will have on the increased sweep efficiency in the long run, following conclusions can be made concerning the operational aspects:

- The concept of using a modified shuttle tanker as a platform for this large scale operation, which again was connected to the subsea injection wells, proved to be a solid solution.
- Seawater was taken directly from the sea, then desalinated in order to become fresh water at a rate up to 4 000 Sm^3/day in the reverse osmosis plant located in the stimulation vessel. Concentrated KCl (for pre and post – flush) and sodium silicate is then diluted in this fresh water, then filtered to remove any impurities and lastly injected into the reservoir. This went as anticipated.
- The pre – flush containing KCl, designed to prevent injectivity reduction during the injection of the silicate and delaying the gelation time was considered to be adequate.
- The injection of the sodium silicate solution went as estimated, same with the in – depth placement and permeability reduction.
- The pre – flush displaced the sodium silicate with the injectivity as anticipated.

Following conclusions/results can be made:

The objective of the injected silicate solution is to avoid premature gelation, but again generate in – depth plugging while the injectivity is at a satisfactory level. The gelation kinetics was controlled by the reservoir temperature gradient, pre – filtration of the sodium silicate and the added activator (HCl).

Even though the magnitude of the large scale operation did generate logistically tough chemical injection challenges, the gel kinetics obtained from small scale experiments were fairly similar.

The experimental work and the test pilot both illustrated that sodium silicate concentration of 4 wt% was sufficient to plug in – depth zones and that the gel strength was able to withstand the conditions present in the reservoir. Even though it is not official that it was also used 4 wt% in the large scale operation, it can more or less be concluded that it did. Why suddenly change something that has been proven to work.

The simulation results predicted in advance that the operation will show an IOR effect of approximately 200 000 Sm^3 with a reduction in water cut of 3%. This prediction has yet to be seen.

A comprehensive data acquisition program including tracer tests, ion analysis of produced water, transient testing, and injectivity and productivity tests are initiated and will be used to report the effects of the sodium silicate field test.

3 Discussion and Conclusion

Even though the operation was considered to be a success, improvements can be made regarding the simulations and operational tasks, elements which have not been taken sufficiently into account in the long run.

The pilot area was sand rich and relatively well flooded outside the thief zone. Thus, the EOR potential for diverging was estimated to be moderate. The most important thing for a technology pilot, is to be able to measure the response and to conclude on whether or not the technology works (quality assurance of the technology). The pilot area was suitable for measuring the response, since it was an isolated segment with a well pair, both water injection and oil producer. At the same time, there was no gas injection and a stable high water cut in the oil producer. The injection well was a subsea well, therefore this operation could be conducted without interrupting the ongoing work on the platform significantly (Snorre A). The producer was a platform well, hence frequently measuring of the response parameters were readily accessible (rate watercut and liquid/tracer analysis).

If this technology had been quality assured in another area/reservoir, one could perhaps argue that starting this operation earlier in the producer lifetime could gain more oil. This is due to the moderate oil reserves volume left in the segment. However, since this is a pilot technology the risk of losing oil reserves is largely present. This is why this segment is suitable for being a pilot area.

Simulation limitations:

For instance the use of a too basic simulation program for the gelation process may turn out inaccurate. As reported by D. Hatzignatiou et al. 2014, they also used a commercially simulator like Eclipse. Limitations like for instance some of the injected water are also integrated into the gel structure, but it appears not to be feasible to integrate the water contribution into the simulator chemical reaction. In addition, the chemistry of silicate is complex, and the process in the simulation model is a simplified one based on a predefined chemical reaction.

The gelation kinetics may not have been fully understood because a commercially simulator model tends to create a significant amount of gel right away, while in reality, the silicate solution would start to gel at the designed gelation time. In reality, the viscosity of the silicate solution increases to a point at which it is too viscous to move. Thus, it plugs the pores. Also, the increase of the molecular weight affects the gelation process because silicate solution gets stuck more easily in the pore throats. This is also a weakness in a basic simulator (D. Hatzignatiou et al. 2014).

Also the effect of ions in the formation may not have been sufficiently taken into account. For instance calcium is not involved in the chemical reaction in a commercially simulator, but affects the gelation time because of the exchange of ions. The formation is of course pre – flushed, but regardless of the volume KCl injected, it is not possible to fully avoid precipitation (D. Hatzignatiou et al. 2014).

Regarding the temperature simulations, the temperature profile from the injector to the producer is not fully understood. In field operations the temperature is only measured near the injection well and the production well, which gives limited information of the temperature profile in between the wells. Since in – depth gel plugging is relatively newly developed method, detailed simulated temperature profile has not been this essential before, therefore has not been sufficiently researched. In Figure 40, with both narrow and wide thief zone it can be seen that the temperature cool down extends to the producer, which in reality does not happen. The wide thief zone gave the best history match with regards to temperature, while other parameters, such as watercut, were better matched with a narrow thief zone. All in all, the narrow thief zone was preferred as the base case.

Other limitations:

The durability of the sodium silicate gel is something that should have been more discussed, since the silicate gel is expected to withstand over a prolonged period. As reported by D. Hatzignatiou et al. 2014, the disadvantages of silicate gels are the blocking effect and the gelation mechanisms. More specifically, the silicate gel tends to shrink over time, thus reducing the blocking effect of the gel. And since this method is still quite newly developed, it is not entirely known what will happen in the future, and what the consequences of this could be.

Regarding the volume pre – flush of KCl used in both the test pilot and the large scale interwell pilot were possible not enough, in order to reach the desirable minimum precipitation occurring near the injection wellbore.

As reported by Hunt et al. (2013), the study concluded that silica gel has limited applications at high temperatures because of fast gelation time and lack of long stability, but it is suitable for applications at lower – temperature geothermal fields.

Suggestions:

Simulation: There is a need to improve the mechanism (temperature/chemical reaction) for dynamic placement of in – depth plug (permeability reduction)(quote K. Skrettingland).

More calculations regarding the pre – flush volume should also be made. For instance conducting some simple calculations with PHREEQC in 1 dimensional flow, focusing especially on the effects from the ion Ca^{2+}. Since this ion not only creates precipitations but also initiates the gelation. By doing this, it is possible to establish which type of minerals creates the most precipitation during an injection. Since the main objective is to avoid near – well precipitation, one can use about 20 cells for instance which would represent the near – well area (quote Dag C. Standnes).

For the temperature simulations it can for instance be experimented on using smaller grid cells, in order to get a better resolution of the temperature profile. To get an improved understand on how the temperature profile increases towards the producer. Because in this work it was unknown whether or not the slope increases in a steep or a lean way. Also, the exact placement of the silica is not fully known due to the lack of knowledge concerning the temperature profile.

The technology pilot was costly due to the fact that the vessel had to be constructed/modified in order to execute the operation. In order to secure that the response was measureable, the injected volume was dimensioned in such a way that one could trust the response and conclude on whether or not a deep restriction in a large segment was established.

Future operations will be significantly cheaper since the vessel that executes these operations has been built. Not only that, but the volume/operational time will be reduced and optimized.

4 References

Hatzignatiou, D. G., Helleren, J., & Stavland, A. (2014, May 1). Numerical Evaluation of Dynamic Core-Scale Experiments of Silicate Gels for Fluid Diversion and Flow-Zone Isolation. Society of Petroleum Engineers. doi:10.2118/170240-PA

Skrettingland, K., Giske, N. H., Johnsen, J.-H., & Stavland, A. (2012, January 1). Snorre In-depth Water Diversion Using Sodium Silicate - Single Well Injection Pilot. Society of Petroleum Engineers. doi:10.2118/154004-MS

Skrettingland, K., Dale, E. I., Stenerud, V. R., Lambertsen, A. M., Nordaas Kulkarni, K., Fevang, O., & Stavland, A. (2014, March 31). Snorre In-depth Water Diversion Using Sodium Silicate - Large Scale Interwell Field Pilot. Society of Petroleum Engineers. doi:10.2118/169727-MS

Lund, T. and Kristensen, R. 1993. Qualification Program for Deep Penetration Gels: From laboratory to Field. Paper presented at the IEA Workshop and Symposium on EOR, Salzburg, Austria, October 17-21.

Rolfsvag, T.A., Jakobsen, S.R., Lund, T.A.T and Strømsvik, G. (1996) Thin Gel Treatment of an Oil producer at the Gullfaks Field: Results and Evaluation. Paper SPE 35548 presented at the European Production Operation Conference and Exhibition, Stavanger, Norway, 16-17 April. doi:10.2118/35548-MS.

Krumrine, P.H. and Boyce, S.D. 1985. Profile Modification and Water Control With Silica Gel-based Systems. SPE 13578 presented at the International Symposium on Oilfield and Geothermal Chemistry, Phoenix, Arizona, U.S.A., 9-11 March doi:10.2118/13578-MS.

Stavland, A., Jonsbraten, H. C., Vikane, O., Skrettingland, K., & Fischer, H. (2011, January 1). In-Depth Water Diversion Using Sodium Silicate on Snorre - Factors Controlling In-Depth Placement. Society of Petroleum Engineers. doi:10.2118/143836-MS

Skrettingland, K., Holt, T., Tweheyo, M.T. and Skjevrak, I. 2011. Snorre Low-Salinity-Water Injection – Coreflooding Experiments and Single-Well Field Pilot. SPEREE 14 (2) 182-192. SPE 129877-PA. doi:10.2118/129877-PA.

Stavland, A., Jonsbråten, H.C., Vikane, O., Skrettingland, K. and Fischer, H. 2011a. In-depth water diversion using sodium silicate – Preparation for single well field pilot on Snorre. Paper presented at the 16th European Symposium on Improved Oil Recovery, Cambridge, UK. 12-14 April.

Stavland, A., Jonsbråten, H.C., Vikane, O., Skrettingland, K. and Fischer, H. 2011b. In-Depth Water Diversion Using Sodium Silicate on Snorre - Factors Controlling In-Depth Placement. Paper SPE 143839 presented at the SPE European Formation Damage Conference, Noordwijk, The Netherlands. 7-10 June. doi:10.2118/143839-MS.

Bak, Tang and Wiesenfeld, Department of physics, Brooklyn National Library, Upton, New York, “Self-organized criticality”, 1987. Doi: 10.1103/PhysRevA.38.364.

Iler, R.K. 1979. The Chemistry of Silica, Solubility, Polymerization, Colloid and Surface Properties and Biochemistry. John Wiley & Sons.

International Standardization Organization, 1999. “ISO 7027, Water Quality – Determination of Turbidity,” International Standardization Organization, Geneva, Switzerland.

The dictionary of modern medicine, 1992. ISBN: 1850703213. Carnforth, Lancs, UK : Park Ridge, N.J., USA : Parthenon Pub. Group.

Galter, J. 1998 “The early history of reverse osmosis membrane development”. Department of Civil and Environmental Engineering, University of California at Los Angeles, Los Angeles, CA 90095, USA. doi:10.1016/S0011-9164(98)00122-2.

Zumdahl, Steven S. (2005). Chemical Principles (5th ed.). New York: Houghton Mifflin

Green, D.W. and Willhite, G.P. 1998. *Enhanced Oil Recovery*. SPE Textbook Series Vol 6. SPE, Richardson, Texas, USA.

Ramey, H.J. Jr. 1973. Correlations of Surface and Interfacial Tensions of Reservoir Fluids. Paper SPE-4429-MS available from SPE, Richardson, Texas

Brown, et al. Chemistry:The Central Science. 11th ed. Upper Saddle River, New Jersey: Pearson/Prentice Hall, 2008.

The Schlumberger Oilfield Glossary launched in 1998 (last update 2015).

Sheng, J.J. 2011. Modern Chemical Enhanced Oil Recovery Theory and Practice. Gulf professional Publishing, Burlington, MA, USA.

C.A.J. Appelo, D. Postma 2005. Geochemistry, Groundwater and Pollution, Second Edition. ISBN 9780415364287.

Blaker, T., Aarra, M.G., Skauge, A., Rasmussen, L., Celius, H.K., Martinsen, H.A. and Vassenden, F. 2002. Foam for gas Mobility Control in the Snorre Field: The FAWAG project. SPEREE, 5 (4) 317-323. SPE 78824-PA. doi:10.2118/78824-PA.

Nicolas P. Badertscher and Martin Burkhard 2000. “Brittle ductile deformation in the Glarus thrust Lochseiten (LK) calc-mylonite”. Volume 12, Issue 6. DOI: 10.1046/j.1365-3121.2000.00310.x

B. B. He 2006. “Residual Stress and Microstructure Analysis with X-ray Diffraction”. International Offshore and Polar Engineering Conference San Francisco, California, USA. ISBN 1-880653-66-4

Green, D.W. and Willhite, G.P. 1998. Enhanced Oil Recovery. SPE Textbook Series Vol 6. SPE, Richardson, Texas, USA.

M. Huysmans and A. Dassargues 2004. “Review of the use of Péclet numbers to determine the relative importance of advection and diffusion in low permeability environments”. DOI: 10.1007/s10040-004-0387-4.

B. Lovelock and S. K. Merz 2006. “FLOW TESTING IN INDONESIA USING ALCOHOL TRACERS”. Thirty-First Workshop on Geothermal Reservoir Engineering Stanford University, Stanford, California, USA.

Brigham, W. E., & Abbaszadeh-Dehghani, M. (1987, May 1). Tracer Testing for Reservoir Description. Society of Petroleum Engineers. doi:10.2118/14102-PA

Romero, C., Agenet, N., Lesage, A., & Cassou, G. (2011, January 1). Single-Well Chemical Tracer Test Experience in the Gulf of Guinea to Determine Remaining Oil Saturation. International Petroleum Technology Conference. doi:10.2523/14560-MS

Sabet, M.A.: Well Test Analysis, Gulf Publishing Company, Houston, TX (1991).

Merrill, L.S. Jr., Kazemi, H., and Gogarthy, W.B.: "Pressure Fall off Analysis in reservoirs with Fluid Banks," JPT (July 1974) 809-818.

Sloan, E. 1990. Clathrate Hydrates of Natural Gases. New York City: Marcel Dekker Inc.

Samandarli, O., Valbuena, E., & Economides, C. (2012, January 1). Production Data Analysis in Unconventional Reservoirs with Rate- Normalized Pressure (RNP): Theory, Methodology, and Applications. Society of Petroleum Engineers. doi:10.2118/155614-MS

D. G. Avery and R. Witty (1947). "Diffusion pumps: a critical discussion of existing theories"

Aulisa, E., Ibragimov, A., & Walton, J. (2009, December 1). A New Method for Evaluating the Productivity Index of Nonlinear Flows. Society of Petroleum Engineers. doi:10.2118/108984-PA

Makogon, Y.: Hydrates of Hydrocarbons, PennWell Books, Tulsa (1997) 262.

Nabzar, L., Chauveteau, G. and Rocque, C. 1996. “A New Model for Formation Damage by Particle Retention”. Paper SPE 31119, presented at the International Symposium on Formation Damage Control, Lafayette, Louisiana, U.S.A., 14-15 February. doi:10.2118/31119-MS.

Maharaja phD. Thesis June 2007. “GLOBAL NET-TO-GROSS UNCERTAINTY ASSESSMENT AT RESERVOIR APPRAISAL STAGE”.

Young, L.C. 1999. Rigorous Treatment of Distorted Grids in 3D. Presented at the SPE Reservoir Simulation Symposium, Houston, Texas, 14-17 February 1999. SPE-51899-MS.

Ács, G., Doleschall, S., and Farkas, E. 1985. General Purpose Compositional Model. SPE J. 25 (4): 543–553. SPE-10515-PA

Galli, G., Morra, D., Ghaddab, F., Sitep, M.T., Manrique, E., and Freeman, G. 2012. Thermally Activated Treatment to Improve Sweep Efficiency: Pilot Test Results and Field Scale Application Design in El Borma Field (Tunisia). Paper SPE154042 presented at the SPE Improved Oil Recovery Symposium, Tulsa, Oklahoma, USA, 14-18 April. http://dx.doi.org/10.2118/154042-MS.

Garmeh, R., Izadi, M., Salehi, M., Romero, J.L., Thomas, C.P., and Manrique, E.J. 2011. Thermally Active Polymer to Improve Sweep Efficiency of Water Floods: Simulation and Pilot Design Approaches. Paper 144234 presented at SPE Enhanced Oil Recovery Conference, Kuala Lumpur, Malaysia, 19-21 July. http://dx.doi.org/10.2118/144234-MS.

Matthews, C.S. and Russell, D.G. 1967. Pressure Buildup and Flow Tests in Wells, 1. Richardson, Texas: Monograph Series, SPE.

Hunt, J. D., Ezzedine, S. M., Bourcier, W. et al. 2013. Kinetics of the Gelation of Colloidal Silica at Geothermal Conditions, and Implications for Modifications and Management. Presented at the 38th Workshop on Geothermal Reservoir Engineering, Standford, California, USA, 11 – 13 February, SGP – TR – 198.